VOLUME LVI NUMBER 4

THE ASTROPHYSICAL JOURNAL

AN INTERNATIONAL REVIEW OF SPECTROSCOPY AND ASTRONOMICAL PHYSICS

EDITED BY

GEORGE E. HALE
Mount Wilson Observatory of the Carnegie Institution of Washington

EDWIN B. FROST
Yerkes Observatory of the University of Chicago

HENRY G. GALE
Ryerson Physical Laboratory of the University of Chicago

NOVEMBER 1922

THE CEPHEID VARIABLE η AQUILAE - - - - - - - - - - - - *Charles Clayton Wylie* 217

THE ECLIPSING BINARY ε AQUILAE - - - - - - - - - - - - *Charles Clayton Wylie* 232

A SPECTROSCOPIC METHOD OF DETERMINING THE ABSOLUTE MAGNITUDES OF A-TYPE STARS AND THE PARALLAXES OF 544 STARS - - - - - - *Walter S. Adams and Alfred H. Joy* 242

THE DISTRIBUTION OF THE VELOCITIES OF STARS OF SPECTRAL TYPES F TO M *Gustaf Strömberg* 265

THE APPLICATION OF VACUUM THERMOCOUPLES TO PROBLEMS IN ASTROPHYSICS *Edison Pettit and Seth B. Nicholson* 295

THE ELECTRIC FURNACE SPECTRUM OF IRON IN THE ULTRA-VIOLET, WITH SUPPLEMENTARY DATA FOR THE BLUE AND VIOLET - - - - - - - - - - - - *Arthur S. King* 318

CHANGES IN THE SPECTROGRAPHIC ELEMENTS OF Y SAGITTARII - - - - - *John C. Duncan* 340

PREPARATION OF ABSTRACTS - - - - - - - - - - - - - - - - - - 344

THE UNIVERSITY OF CHICAGO PRESS
CHICAGO, ILLINOIS, U.S.A.

THE CAMBRIDGE UNIVERSITY PRESS, London
THE MARUZEN-KABUSHIKI-KAISHA, Tokyo, Osaka, Kyoto, Fukuoka, Sendai
THE MISSION BOOK COMPANY, Shanghai

November 1922 Vol. LVI, No. 4

THE ASTROPHYSICAL JOURNAL

AN INTERNATIONAL REVIEW OF SPECTROSCOPY AND ASTRONOMICAL PHYSICS

EDITED BY

GEORGE E. HALE
Mount Wilson Observatory of the Carnegie Institution of Washington

EDWIN B. FROST
Yerkes Observatory of the University of Chicago

HENRY G. GALE
Ryerson Physical Laboratory of the University of Chicago

WITH THE COLLABORATION OF

JOSEPH S. AMES, Johns Hopkins University
ARISTARCH BELOPOLSKY, Observatoire de Poulkova
WILLIAM W. CAMPBELL, Lick Observatory
HENRY CREW, Northwestern University
CHARLES FABRY, Université de Paris
ALFRED FOWLER, Imperial College, London
CHARLES S. HASTINGS, Yale University
HEINRICH KAYSER, Universität Bonn
ALBERT A. MICHELSON, University of Chicago
HUGH F. NEWALL, Cambridge University
ERNEST F. NICHOLS, Nela Laboratory, Cleveland
ALFRED PEROT, Paris
CARL RUNGE, Universität Göttingen
HENRY N. RUSSELL, Princeton University
SIR ARTHUR SCHUSTER, Twyford
FRANK SCHLESINGER, Yale Observatory

The Astrophysical Journal is published by the University of Chicago at the University of Chicago Press, 5750 Ellis Avenue, Chicago, Illinois, during each month except February and August. ¶The subscription price is $6.00 a year; the price of single copies is 75 cents. Orders for service of less than a half-year will be charged at the single-copy rate. ¶Postage is prepaid by the publishers on all orders from the United States, Mexico, Cuba, Porto Rico, Panama Canal Zone, Republic of Panama, Dominican Republic, El Salvador, Bolivia, Colombia, Honduras, Nicaragua, Peru, Hawaiian Islands, Philippine Islands, Guam, Samoan Islands, Shanghai. ¶Postage is charged extra as follows: for Canada, 30 cents on annual subscriptions (total $6.30); on single copies, 3 cents (total 78 cents); for all other countries in the Postal Union, 50 cents on annual subscriptions (total $6.50), on single copies 5 cents (total 80 cents). ¶Patrons are requested to make all remittances payable to The University of Chicago Press in postal or express money orders or bank drafts.

The following are authorized to quote the prices indicated:

For the British Empire: The Cambridge University Press, Fetter Lane, London, E.C. 4. Yearly subscriptions, including postage, £1 16*s*. each; single copies, including postage, 4*s*. 6*d*. each.

For Japan and Korea: The Maruzen-Kabushiki-Kaisha, 11 to 16 Nihonbashi Tori Sanchome, Tokyo, Japan. Yearly subscriptions, including postage, Yen 13.65 each; single copies, including postage, Yen 1.68 each.

For China: The Mission Book Company, 13 North Szechuen Road, Shanghai. Yearly subscriptions, $6.00; single copies, 75 cents, or their equivalents in Chinese money. Postage extra, if mailed direct outside of Shanghai, on yearly subscriptions 50 cents on single copies 5 cents.

Claims for missing numbers should be made within the month following the regular month of publication. The publishers expect to supply missing numbers free only when losses have been sustained in transit, and when the reserve stock will permit.

Business correspondence should be addressed to The University of Chicago Press, Chicago, Illinois.

Communications for the editors and manuscripts should be addressed to the Editors of THE ASTROPHYSICAL JOURNAL, Ryerson Laboratory, University of Chicago, Chicago, Illinois.

The cable address is "University, Chicago."

The articles in this Journal are indexed in the *International Index to Periodicals*, New York, N.Y.

Entered as second-class matter, January 17, 1895, at the Post-office at Chicago, Ill., under the act of March 3, 1879.

Acceptance for mailing at special rate of postage provided for in Section 1103, Act of October 3, 1917, authorized on July 15, 1918.

PRINTED IN THE U.S.A.

THE
ASTROPHYSICAL JOURNAL
AN INTERNATIONAL REVIEW OF SPECTROSCOPY
AND ASTRONOMICAL PHYSICS

VOLUME LVI NOVEMBER 1922 NUMBER 4

THE CEPHEID VARIABLE η AQUILAE

By CHARLES CLAYTON WYLIE

ABSTRACT

Cepheid variable η Aquilae; photometric study.—A series of 111 observations made with a photo-electric photometer during 1920, gives an accurate *light-curve* of this 4th magnitude star (Fig. 2 and Table IV). The range of variation is $1^{M}12$; the period is $7^{d}176$. The "secondary maximum" is confirmed as a pronounced halt in the decrease of light, from phase $1^{d}8$ to $2^{d}4$. Another fluctuation was indicated with maximum about phase $4^{d}3$. *Comparison with previous observations* suggests a shortening of the interval from minimum to maximum since 1900 and a gradually increasing period. Luizet's tabulation of residuals from a constant period is brought up to date (Fig. 3). There is no evidence of any decrease of period since observations began in 1784.

Change of period of Cepheid variables.—The increasing period of η Aquilae, which is contrary to the requirement of the *pulsation theory*, and the decreasing period of δ Cephei can perhaps be reconciled on the basis of the *binary theory* by assuming that η Aquilae rotates relatively faster than δ Cephei.

New variables.—*β Aquilae* seems to be a variable with a long or irregular period, for a progressive decrease of $0^{M}05$ was observed over an interval of three months (Fig. 1). The spectroscopic *binary δ Aquilae* is suspected of being an eclipsing variable with a range of about $0^{M}1$ but no period has been found.

A photo-electric study of η Aquilae, one of the best-known Cepheid variables, was undertaken at the University of Illinois in the hope that something of value might be contributed to the discussion of this type of variation. In particular, irregularities and secondary oscillations might be too small for certain detection by visual observers and yet be conspicuous in a photo-electric light-curve.

Observations were begun in July 1920 and carried through to November of that year. In all 111 observations were secured,

one-third by Professor Stebbins and the remainder by myself. The variable and comparison stars are, in the Harvard system,

H.R. 7570, η Aquilae, magnitude 3.66–4.45, spectrum G.
H.R. 7377, δ Aquilae, magnitude 3.44, spectrum F.
H.R. 7602, β Aquilae, magnitude 3.90, spectrum K.

The Mt. Wilson spectral types are: η Aquilae, F9; δ Aquilae, A9; and β Aquilae, G7. An observation normally consisted of thirty-six measures taken in the following order: δ 3, η 3, β 6, η 3, δ 6, η 3, β 6, η 3, δ 3, one measure being a timing of the rate of motion of the electrometer thread between two scale divisions. Since δ Aquilae is brighter than β Aquilae, a neutral-tinted shade glass was used to reduce the light to approximate equality. Throughout this paper comparisons of other stars with δ Aquilae should be interpreted as comparisons with δ Aquilae observed through the shade glass, which reduced its light about $0^{M}.82$.

The differential correction for atmospheric extinction between η Aquilae and the comparison stars was taken from tables based on those in Müller's *Photometrie der Gestirne*. Nearly all observations were within the limits $19^{h}.0$ and $22^{h}.5$ sidereal time, during which interval the maximum tabular differential correction was for δ Aquilae, $0^{M}.018$, and for β Aquilae, $0^{M}.043$. The quantity from the table was multiplied by a factor depending on the transparency of the sky, which was obtained as in the work on σ Aquilae. The residuals from the preliminary curve were examined for a systematic hour angle correction; first, by plotting them for nights on which observations were carried on throughout nearly the entire three and a half hours during which the star could be observed; and second, by comparing residuals at different hour angles on different nights, using only the best nights. There was no indication of any appreciable systematic error remaining after the computed correction for differential extinction had been applied, although these corrections were larger than is usual in the work here.

The times were reduced to the sun, and the preliminary phases computed from the elements

$$\text{Maximum} = \text{J.D. } 2422606.562 + 7^{d}.176382 \cdot E$$

The period is that of Luizet,[1] without his harmonic term. A plot of the observations indicated that both comparison stars are probably variable. At certain times δ Aquilae was distinctly faint, in one case as much as one-tenth of a magnitude, and toward the end of the series β Aquilae was fainter than at the beginning.

In 1918 Messrs. Stebbins and Dershem used δ Aquilae as a comparison star for Nova Aquilae No. 3, and at that time it was suspected of variation.[2] It has been announced as a spectroscopic binary[3] of unknown period, and may be an eclipsing variable of small range. The other comparison star, β Aquilae, being of spectral type K, may be expected, if it varies at all, to be irregular.

As a first step toward unraveling the variations of the three stars, the observations where δ Aquilae was noticeably faint were marked. Then using only nights on which the transparency of the sky was good, and including no nights on which δ Aquilae had been marked faint at any time, the observed values of $\beta > \delta$ were plotted and a freehand curve drawn. The plotted values were compared with the curve, and one or two more rejections made on the ground that δ Aquilae was perhaps faint that night. The remainder were grouped into normal magnitudes which are given in Table II and plotted in Figure 1. From a freehand curve drawn through these normal magnitudes, the photo-electric reduction of β Aquilae to δ Aquilae could be obtained for the time of any observation.

The observed values of $\beta > \delta$ were compared with this curve, and from the residuals an unsuccessful attempt was made to get the period of variation of δ Aquilae. Phases were computed and the residuals plotted, at least around the supposed minima, for several different periods, but none was considered satisfactory. The range of variation is so small that it is probably better to await the determination of the period from spectroscopic observations.

Not knowing the variation of δ Aquilae, the following arbitrary rule was adopted. If any observed $\beta > \delta$ differed by more than $0^{M}040$ from the curve value, all comparisons with δ Aquilae were

[1] *Astronomische Nachrichten*, **163**, 361, 1903.

[2] *Astrophysical Journal*, **49**, 354, 1919.

[3] *Lick Observatory Bulletin*, **2**, 126, 1903; *Astrophysical Journal*, **39**, 265, 1914.

rejected on that night. If no residual exceeded $0^{M}.040$, but some exceeded $0^{M}.030$, the observations on that night were given half-weight. A few other observations had already been marked half-weight because of poor observing conditions.

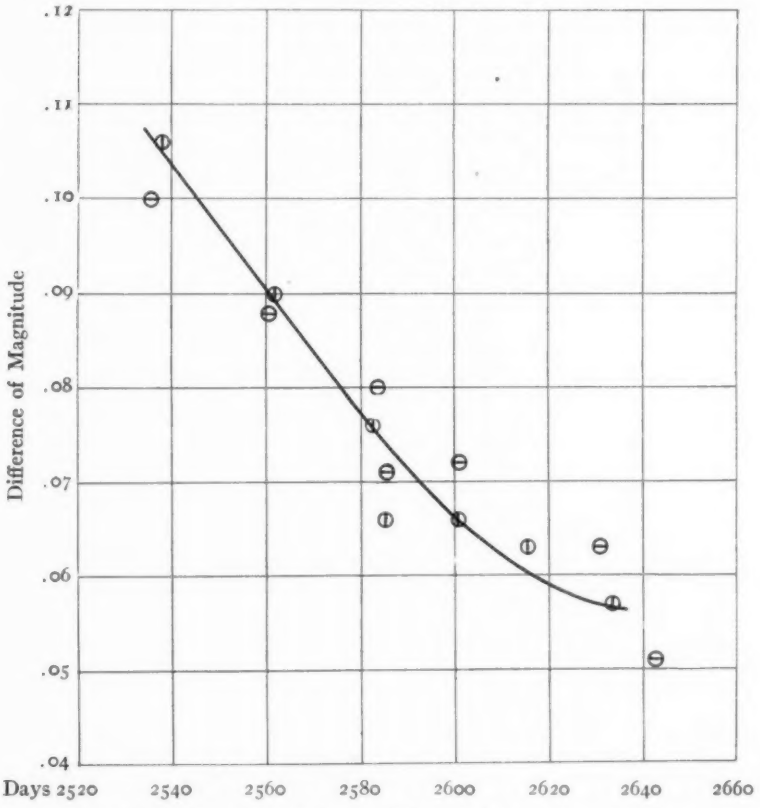

FIG. 1.—Variation of β Aquilae. Circles marked with vertical bars represent normal points from comparisons with δ Aquilae. Those marked with horizontal bars are from comparisons with η Aquilae.

Observations of $\beta > \eta$ were reduced to $\delta > \eta$ by applying the corrections scaled from Figure 1. Normal magnitudes for η were then formed, keeping the work on the two comparison stars separate, and a freehand curve drawn. As a check, the variation of β Aquilae was then determined by combining observed values of $\beta > \eta$ with the light-curve of η as based on δ, using only good nights. These

computed values of $\beta > \delta$ as derived through η were assembled into normal magnitudes, which are plotted in Figure 1 for comparison with the values of direct observation. The satisfactory agreement shows that the progressive change between β and δ during the time of observation must be due to a variation of β, and that the light variation of η repeats itself from period to period within the limits of the present measures.

The times of maximum and minimum, and the amplitude of variation for η Aquilae were derived graphically from the normal magnitudes as follows:

Maximum, phase	$0^d.09$,	magnitude $-0^M.501$
Minimum, phase	$5^d.17$,	magnitude $+0^M.616$
Maximum–minimum	$2^d.10$,	amplitude $1^M.12$

The correction to the time of maximum from the preliminary ephemeris is then $+0^d.09$. This was applied, giving the following elements which were adopted as final:

$$\text{Maxiumm} = \text{J.D. } 2422606.652 + 7^d.176382 \cdot E$$

Table I gives the photo-electric observations of η Aquilae. The first column gives the Greenwich mean time of observation, and the second the phase computed from the final elements; the third column gives the difference between η Aquilae direct and δ Aquilae measured through the shade glass, and the fourth is the measured difference between η Aquilae and β Aquilae. A positive sign means in each case that the comparison star was brighter than η. Rejected observations are in parentheses, and half-weight observations are noted under remarks. Since the average time of observation is the same for each star, the differences β brighter than δ are obtained by subtracting the third column from the fourth.

The normal magnitudes, with phases from the final elements, are given in Table III, and plotted in Figure 2, where points from the two comparison stars are kept separate, and the rejected δ Aquilae observations are plotted as crosses. No β Aquilae observations considered satisfactory at the time of making have been rejected, so all comparisons with that star are incorporated in the normal points.

TABLE I

OBSERVATIONS OF η AQUILAE

DATE, G.M.T.	PHASE	DIFFERENCE OF MAGNITUDE		REMARKS
		δ	β	
2422523.712	$3^d.182$	(+0^M.282)	.....	
.717	3.187	.....	+0^M.345	
.746	3.216	(+ .255)	.....	
.751	3.221	.....	+ .384	
2524.706	4.176	+ .448	+ .552	
.804	4.274	+ .455	+ .566	
2525.765	5.235	+ .588	+ .680	
2526.711	6.181	+ .138	+ .262	
2528.713	1.006	− .280	− .133	δ half-weight
.813	1.106	− .216	− .120	δ half-weight
2530.761	3.054	+ .211	+ .294	
2532.682	4.975	+ .606	+ .718	
2533.713	6.006	+ .270	+ .384	
.784	6.077	+ .189	+ .283	
2534.661	6.954	(− .566)	− .332	
.749	7.042	(− .536)	− .305	
.801	7.094	(− .500)	− .420	
2537.739	2.856	+ .116	+ .206	
2538.662	3.779	+ .366	+ .467	
.760	3.877	+ .377	+ .483	
2539.675	4.792	+ .566	+ .686	
.756	4.873	+ .591	+ .699	
2540.685	5.802	+ .404	+ .517	
.742	5.859	+ .364	+ .468	
2553.671	4.435	(+ .492)	+ .598	
.729	4.493	(+ .456)	+ .643	
2554.604	5.368	+ .563	+ .682	
.679	5.443	+ .559	+ .654	
2555.607	6.371	+ .005	+ .126	
2558.786	2.374	− .070	+ .036	
2559.717	3.305	+ .273	+ .370	
2561.731	5.319	+ .597	+ .681	
2566.622	3.032	+ .225	+ .296	
2567.599	4.009	+ .383	+ .506	δ half-weight
.738	4.148	+ .393	+ .496	δ half-weight
2570.594	7.004	− .443	− .381	
.659	7.069	− .470	− .427	
2573.709	2.943	+ .106	+ .220	δ half-weight
2580.585	2.642	− .008	+ .058	
.689	2.746	+ .053	+ .106	
2583.604	5.661	+ .499	+ .549	
.669	5.726	+ .471	+ .559	
.703	5.760	+ .424	+ .522	
2584.562	6.619	− .140	− .068	
.634	6.691	− .216	− .147	
.665	6.722	− .278	− .194	
.694	6.751	− .273	− .222	
2585.560	0.440	− .427	− .363	
.586	0.466	− .410	− .359	
.634	0.514	− .414	− .340	

TABLE I—*Continued*

Date, G.M.T.	Phase	Difference of Magnitude		Remarks
		δ	β	
2422585.649	$0^{d}.529$	$-0^{M}.389$	$-0^{M}.328$	
.664	0.544	− .377	− .315	
.679	0.559	− .390	− .322	
2586.552	1.432	(− .127)	− .045	
.599	1.479	(− .123)	− .014	
.643	1.523	(− .122)	− .008	
.685	1.565	(− .119)	− .044	
2587.560	2.440	− .029	+ .042	
2588.549	3.429	+ .302	+ .392	
.620	3.500	+ .291	+ .391	
2592.557	0.260	(− .472)	− .378	
.617	0.320	(− .491)	− .371	
.656	0.359	(− .511)	− .362	
.676	0.379	(− .430)	− .382	
2593.543	1.246	.....	− .082	β half-weight
.576	1.279	(− .158)	− .077	
.636	1.339	(− .194)	− .076	
.660	1.363	(− .151)	− .088	
2594.559	2.262	− .033	+ .048	Half-weight
2596.613	4.316	+ .465	+ .553	
2598.628	6.331	(+ .059)	+ .081	β half-weight
.648	6.351	(+ .040)	+ .094	
2599.615	0.141	− .469	− .417	δ half-weight
.662	0.188	− .500	− .398	δ half-weight
2600.545	1.071	− .208	− .144	
.599	1.125	− .188	− .131	
.644	1.170	− .203	− .135	
2601.569	2.095	− .074	+ .012	
.590	2.116	− .032	+ .029	
.636	2.162	− .068	+ .002	
.655	2.181	− .051	− .011	
2603.604	4.130	+ .433	+ .498	
2604.633	5.159	+ .616	+ .690	
2605.526	6.051	+ .250	+ .342	
.598	6.123	+ .191	+ .254	
2606.537	7.062	− .487	− .396	
.577	7.102	− .495	− .415	
2607.547	0.896	(− .304)	− .220	
.572	0.921	(− .337)	− .206	
.589	0.938	(− .315)	− .178	
2608.544	1.893	− .042	+ .018	
.587	1.936	− .054	+ .015	
.632	1.981	− .084	− .006	Half-weight
2609.581	2.930	+ .120	+ .215	
2614.545	0.718	− .346	− .286	
2615.535	1.707	(− .055)	+ .011	
.558	1.730	(− .107)	+ .009	β half-weight
2618.547	4.719	+ .566	+ .637	
.587	4.759	+ .558	+ .624	
2619.515	5.687	+ .481	+ .558	δ half-weight
.558	5.730	+ .437	+ .537	δ half-weight
2626.553	5.547	+ .542	+ .609	

TABLE I—*Continued*

Date, G.M.T.	Phase	Difference of Magnitude		Remarks
		δ	β	
2422627.540	$6^d.534$	$-0^M.073$	$-0^M.026$	
.558	6.552	− .074	− .032	
2628.542	0.360	− .450	− .367	
.565	0.383	− .476	− .392	
2632.561	4.379	+ .505	+ .558	
2633.515	5.333	+ .588	+ .648	
2641.535	6.175	+ .170	+ .210	
2642.531	7.171	− .485	− .449	
2649.494	6.958	− .422	− .387	

The adopted light-curve of η Aquilae is given in Table IV. It has not been drawn on Figure 2, as the observations themselves mark the course of the curve satisfactorily. Further, anyone examining suspected fluctuations will probably prefer a plot of the observations free from any evidence as to the judgment of others.

TABLE II

Normal Magnitudes of β Aquilae

Date, G.M.T.	Difference of Magnitude $\beta > \delta$	Number of Observations
2422537.7	$0^M.106$	7
2561.7	.090	4
2582.2	.076	4
2585.2	.066	10
2600.7	.066	8
2615.5	.063	1
2633.0	.057	2

A glance at the figure shows that the reality of a considerable "hump" cannot be questioned. Since absolutely all of the observations are represented in Figure 2, it is evident that the variations of β and δ do not affect the establishment of this secondary fluctuation. Luizet's[1] description of the irregularity, "comme un arrêt dans la diminution d'éclat de la variable," or the German "Stillstand," fits the photo-electric curve. The observations indicate a

[1] *Astronomische Nachrichten*, **163**, 364, 1903.

practically constant magnitude for about $0^d.6$ beginning at phase $1^d.8$. Some of the older curves from visual observations show a pronounced increase in brightness at this point. It was considered a real "secondary maximum," but most of the more recent light-curves have been drawn with no irregularity in the downward slope.[1] The modern tendency is to regard with suspicion permanent irregularities in curves by any but the most accurate photometric

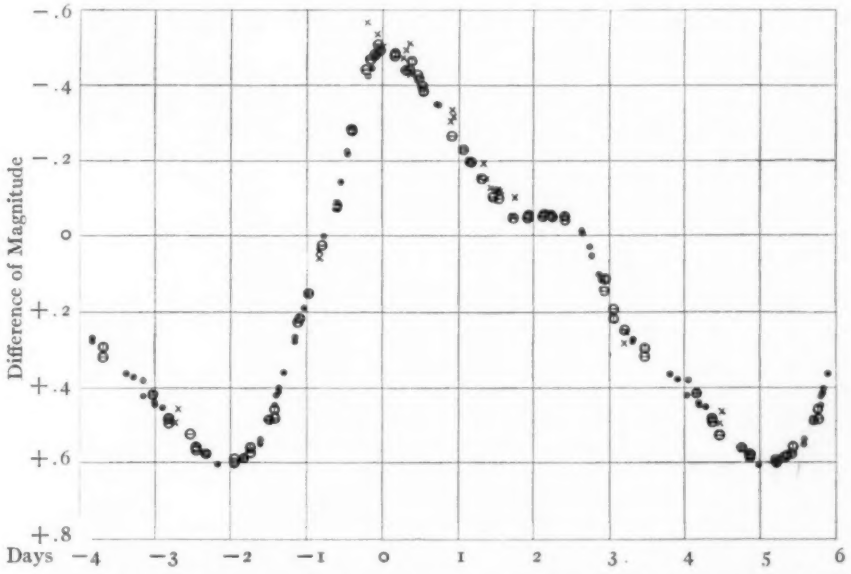

FIG. 2.—Normal magnitudes of η Aquilae. The smaller circles represent single observations and the larger circles normals of two or more observations. Comparisons with δ Aquilae are marked with vertical bars and those with β Aquilae with horizontal bars. Rejected observations are plotted as crosses.

methods.[2] Photo-electric work has in general justified this skepticism, but in this particular instance we find confirmation of a secondary oscillation in Cepheid variation, while in addition to the pronounced secondary, there is indication of another fluctuation with maximum about phase four days. Lockyer believed the irregularities due to a secondary oscillation with period $1^d.8$, one-

[1] *Ibid.*, **183**, 265–278, 1909; **214**, 195, 1921; *Mt. Wilson Contr.*, **7**, 14, 1916.

[2] *Publications American Astronomical Society*, **4**, 265, 1921.

fourth that of the principal light variation. But it is evident they cannot be represented by superposing a simple sine curve of any period on the principal variation. Using Lockyer's subperiod we

TABLE III

NORMAL MAGNITUDES OF η AQUILAE

PHASE	DIFFERENCE OF MAGNITUDE		NO. OBS.	PHASE	DIFFERENCE OF MAGNITUDE		NO. OBS.
	δ	β (reduced)			δ	β (reduced)	
$0^d.164$	$-0^M.484$	$-0^M.474$	2	$4^d.274$	$+0^M.455$	$+0^M.451$	1
0.313		− .440	3	4.348	+ .485	+ .494	2
0.372	− .463		2	4.464		+ .526	2
0.374		− .442	3	4.739	+ .562	+ .570	2
0.473	− .417	− .428	3	4.832	+ .578	+ .588	2
0.544	− .385	− .396	3	4.975	+ .606	+ .609	1
0.718	− .346	− .347	1	5.197	+ .602	+ .596	2
0.918		− .264	3	5.320	+ .592	+ .592	2
1.061		− .229	3	5.406	+ .561	+ .574	2
1.064	− .228		3	5.547	+ .542	+ .551	1
1.148	− .196	− .199	2	5.674	+ .490	+ .486	2
1.315		− .151	4	5.727	+ .460		2
1.456		− .104	2	5.728		+ .481	2
1.544		− .100	2	5.760	+ .424	+ .447	1
1.715		− .050	2	5.802	+ .404	+ .413	1
1.928	− .055	− .051	3	5.859	+ .364	+ .364	1
2.124	− .058	− .052	3	6.006	+ .270	+ .276	1
2.208	− .045	− .058	2	6.064	+ .220	+ .226	2
2.407	− .050	− .044	2	6.123	+ .191	+ .190	1
2.642	− .008	− .019	1	6.178	+ .154	+ .152	2
2.746	+ .053	+ .029	1	6.355		+ .026	3
2.856	+ .116	+ .100	1	6.371	+ .005		1
2.934	+ .115		2	6.543	− .074	− .086	2
2.936		+ .146	2	6.619	− .140	− .143	1
3.043	+ .218	+ .197	2	6.691	− .216	− .222	1
3.204		+ .250	2	6.736	− .276	− .283	2
3.305	+ .273	+ .279	1	6.956		− .440	2
3.464	+ .296	+ .320	2	6.958	− .422		1
3.779	+ .366	+ .362	1	7.004	− .443		1
3.877	+ .377	+ .378	1	7.023		− .468	2
4.009	+ .383	+ .421	1	7.064	− .481	− .477	2
4.136	+ .420		2	7.123		− .503	3
4.139		+ .422	2	7.136	− .490		2
4.176	+ .448	+ .437	1				

might assume that the secondary oscillation rises to its strongest maximum about phase $2^d.5$. A weaker maximum is reached at phase $4^d.3$, the following minimum being coincident with the principal minimum. The two succeeding secondary fluctuations are negligible.

As a matter of some interest, the light-curve was compared with the velocity curve as determined by Wright.[1] This shows that the pronounced halt in decreasing light is at apastron on the binary hypothesis, and just before the star reaches maximum volume on the pulsation hypothesis, following Eddington.

Possible variation from epoch to epoch of the light-curves of this and other Cepheids has been discussed by previous workers.[2] The photo-electric observations give evidence that there was no appreciable change in the form while the observations were in

TABLE IV

LIGHT-CURVE OF η AQUILAE

Phase	Difference of Magnitude	Phase	Difference of Magnitude
−2d.50	+0M.56	1d.50	−0M.11
−2.25	+ .60	1.75	− .06
−2.00	+ .61	2.00	− .05
−1.75	+ .57	2.25	− .05
−1.50	+ .49	2.50	− .03
−1.25	+ .33	2.75	+ .03
−1.00	+ .16	3.00	+ .21
−0.75	.00	3.25	+ .27
−0.50	− .20	3.50	+ .31
−0.25	− .41	3.75	+ .36
0.00	− .50	4.00	+ .40
+0.25	− .47	4.25	+ .45
0.50	− .40	4.50	+ .52
0.75	− .33	4.75	+ .57
1.00	− .24	5.00	+ .61
1.25	− .17	5.25	+ .60

progress, and the curve is not greatly different from others published for this star. The maximum, however, is somewhat sharper, and the interval from minimum to maximum light is less than in recent curves. From those previously referred to, the values of this interval were found to be: in 1900, 2d.38; 1906–1907, 2d.38; 1917, 2d.20; and 1920, 2d.10. A decrease for the more recent series is noticeable, but in all strictness comparison should be made between curves determined with the same type of photometer.

[1] *Astrophysical Journal*, **9**, 62, 1899.

[2] Lockyer, *Dissertation*, pp. 78–86 (Göttingen, 1897); Luizet, *Astronomische Nachrichten*, **193**, 83, 1912; Shapley, *Mt. Wilson Contr.*, **6**, 179, 1915; Jordan, *Publications American Astronomical Society*, **4**, 265, 1921.

The variation of the period of η Aquilae has also been discussed. Lockyer,[1] from his discussion of observations of the past century, concluded it was variable. Luizet[2] also found a variation, and included a harmonic term in his value for the period, the value which has been used by most observers of η Aquilae in recent years. On the other hand[3] some have rejected the harmonic term. The elements are

$$\text{Maximum} = \text{J.D. } 2396168.732 + 7^{d}.176382 \cdot E + 0.14 \sin (0^{\circ}.044 \cdot E + 304^{\circ})$$

$$\text{Maximum} - \text{minimum} = 2^{d}.373$$

Including the harmonic term the epoch of maximum derived from the photo-electric curve gives, as correction to the ephemeris, $-0^{d}.006$. This is good agreement, provided we go no farther, but for the minimum the correction is $+0^{d}.271$, which is not so satisfactory.

A more accurate determination of the length of the period in recent years was therefore made, using the photographic observations of Kohlschütter,[4] made in 1906–1907. The photographic and photo-electric amplitudes being practically the same, comparison of the curves is direct. Using Luizet's mean period between the two series normal magnitudes were formed from the photographic observations. Three observations were combined in a normal point except on the steep portion of the curve where two were used. This steep portion, between minimum and maximum, was used in the determination of the period, as the phase can be determined with more accuracy here than at the time of maximum or minimum.

A plot showed those points nearly a quarter of a day out of phase with the photo-electric curve, a graphical determination giving as a correction $0^{d}.22$. This gives as the correction to the period $+0^{d}.00032$, from which the value for the period between 1906 and 1920 is $7^{d}.17670$.

[1] *Op. cit.*, p. 91. [2] *Op. cit.*, **163**, 361, 1903.

[3] Hellerich, *Dissertation*, p. 6 (Bonn, 1913); Grouiller, *Bulletin Astronomique*, Deuxième Série, **1**, 356, 1922.

[4] *Astronomische Nachrichten*, **183**, 265, 1909.

This value for the length of the period is so much larger than the mean values of Lockyer and Luizet, obtained from a discussion of observations of the past century, that Luizet's tabulation of corrections to an ephemeris[1] from a constant period was brought up to date. Corrections computed from the light-curves of Kohlschütter and Lacchini,[2] and from the photo-electric light-curve, were added to the list. These residuals are plotted in Figure 3, points from

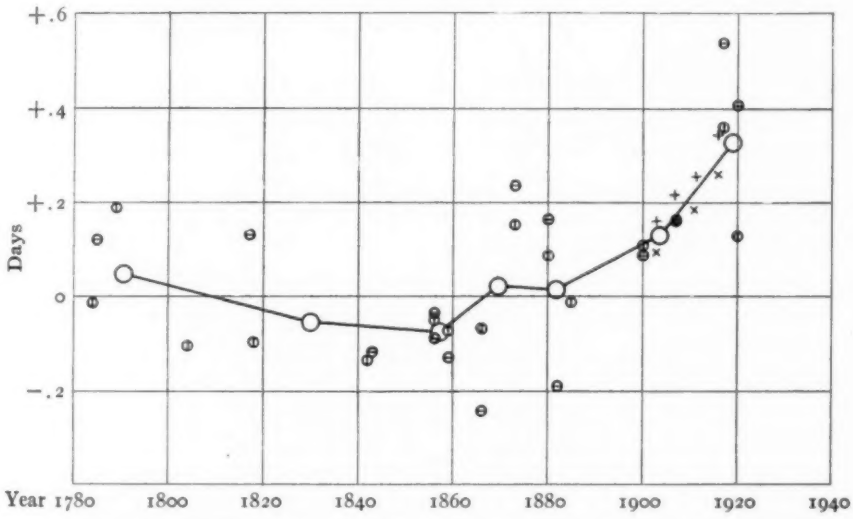

FIG. 3.—Variation in the period of η Aquilae. Points from maxima are marked with vertical bars and those from minima with horizontal bars. The large circles represent normal points. The results from Grouiller's recent values, which were not included in the normals, are plotted as plus signs and crosses, respectively.

maxima and minima being plotted separately. Normal points are formed, giving the determinations equal weight except that in the last point the photo-electric determination has been given double weight. The normal points are connected by a heavy line.

Grouiller's monograph[3] on η Aquilae was received after the investigations of this paper were completed. His normal points

[1] *Op. cit.*, **163**, 360, 1903.

[2] Lacchini, *Astronomische Nachrichten*, **214**, 195, 1921.

[3] *Bulletin Astronomique*, Deuxième Série, **1**, 331, 1922.

from observations after 1900 are plotted on the figure as plus signs and crosses.

This line is distinctly concave upward, hence observational evidence indicates an increasing period at least in recent years. Certainly there is no evidence of an appreciable decrease at any time in the last 140 years. If the variation is harmonic, the available portion of the curve is too little to determine either the amplitude or the period with any accuracy. However, both must be much greater than the values found by Luizet.

The question of variation of period is of importance in Cepheid theory. The pulsation hypothesis demands a shortening of the period,[1] about 40 seconds annually for δ Cephei on the contraction theory of a star's energy. Similar conclusions follow on the rotation hypothesis, while according to the binary theory the period may either increase or decrease.[2] Tidal action should in general lengthen the period, if it is equal to or greater than the rotation period of the principal star. But if the satellite revolves in less than the rotation period, the orbital period should decrease.

There is evidence that the period of δ Cephei is decreasing.[3] If these suspected variations of period are accepted as real and attributed to tidal action, the deduction that η Aquilae probably rotates faster than δ Cephei follows.

Since either a rotation or a pulsation should affect the appearance of the spectral lines, the fact that the lines of η Aquilae are broader than those of δ Cephei is worthy of mention. δ Cephei[4] has the narrow well-defined spectral lines typical of giant stars, while the lines of η Aquilae,[5] also classed with the giant stars, "have the general characteristics of breadth and haziness, which tend to make them objectionable for purposes of accurate measurement." In a footnote to this reference the statement is made that "There is undoubtedly a resemblance between the spectra of η Aquilae and δ Cephei, the lines of the latter being, however, better defined. . . . ."

[1] Eddington, *Observatory*, **41**, 379, 1918; **42**, 339, 1919.

[2] Plummer, *Monthly Notices*, **80**, 507–509, 1920.

[3] Eddington, *op. cit.*, **42**, 338, 1919; Ludendorff, *Astronomische Nachrichten*, **212**, 185, 1920.

[4] Adams, *Observatory*, **42**, 167–168, 1919.

[5] Wright, *Astrophysical Journal*, **9**, 60, 1899.

SUMMARY

1. A series of photo-electric observations made in 1920 gives an accurate light-curve for η Aquilae.

2. The observations indicate a long period or irregular variation for β Aquilae. A progressive decrease of $0^{M}.05$ is found for an interval of three months.

3. δ Aquilae, which has been announced as a spectroscopic binary of unknown period, is suspected of being an eclipsing variable with range about $0^{M}.1$, but no period has been found.

4. The "secondary maximum" in the light-curve of η Aquilae is confirmed as a pronounced halt, or pause, in the decrease of light. Another fluctuation, with maximum about phase four days, is indicated.

5. Within the accuracy of the measures the light-curve did not change between July and November 1920. There has perhaps been a shortening of the interval from minimum to maximum since 1900, but accurate curves determined with the same photometric equipment and at different epochs are needed for a thorough investigation of this point.

6. The period, between 1906 and 1920, is determined by comparison with Kohlschütter's photographic observations. Luizet's tabulation of residuals from the constant period $7^{d}.176382$ is brought up to date by including observations of 1906–1907, 1917, and 1920. Both methods of investigation favor an increasing period at present. The evidence is decidedly against a perceptible decrease in the period at any time since 1784.

7. The pulsation hypothesis demands a shortening of the period, while, according to the older binary theory, tidal action may increase or decrease the period. Other investigators have found evidence of a decrease in the period of δ Cephei.

Either pulsation or rotation should affect the spectral lines of a star. Attention is called to the evidence that the lines of η Aquilae are broader than those of δ Cephei, which have been examined for a pulsation effect.

UNIVERSITY OF ILLINOIS OBSERVATORY
May 1922

THE ECLIPSING BINARY σ AQUILAE

By CHARLES CLAYTON WYLIE

ABSTRACT

Eclipsing variable star, σ Aquilae; photometric study.—A series of 97 observations with a photo-electric photometer during 1920 gives an accurate *light-curve* of this fifth-magnitude star (Fig. 1). It is found to be a normal eclipsing system with two minima and continuous variation, due to ellipticity, between eclipses. The range of variation is $0^{M}.18$; the period is $1^{d}.95026$. *The precision of the measurements* is such that the probable error of each of the 37 normals is $\pm 0^{M}.006$. Because of the small range in partial eclipse, elements could not be determined from the light-curve alone; but since two spectra appear on the Allegheny plates of this binary, the spectroscopic orbit and estimates of relative intensity of the components enable the *elements and absolute dimensions for this system* to be given (Fig. 2 and Table VI).

Comparison star 22 Aquilae was constant within $0^{M}.01$ or $0^{M}.02$ from July to October 1920, but between 1918 and 1920 the observations indicate a change of $0^{M}.02$ for either 22 Aquilae or σ Aquilae.

The variable radial velocity of σ Aquilae (H.R. 7474, magnitude 5.17, spectrum B8) was discovered at Mount Wilson in 1912, and the spectroscopic orbit was published by Jordan in 1916.[1] Jordan pointed out that the large value of K suggested an eclipsing system.

The spectra of two components appear on the plates of this star. Eclipsing binaries showing both spectra are the rare and favorable cases, since by combining the spectroscopic data with that from a good light-curve the dimensions of the system and the masses of the bodies can be found.

A short series of photometric observations was made on this star by Dr. Elmer Dershem at the University of Illinois in the summer of 1918. The reduction of these showed variation in light, which was announced by Professor Stebbins at the twenty-third meeting of the American Astronomical Society.[2]

A second series of observations was begun in June 1920 by Professor Stebbins and myself. This was carried to the middle of October, at which time ninety-seven observations, about equally divided between the two observers, had been secured.

With two or three exceptions each of these observations is the mean of three complete sets of measures, a set consisting of two

[1] *Publications of the Allegheny Observatory*, **3**, 189, 1916.

[2] *Publications of the American Astronomical Society*, **4**, 115, 1919.

readings on the comparison star, four on the variable, and then two more on the comparison star. Throughout the series, 22 Aquilae (H.R. 7303, magnitude 5.40, spectrum Ao) was used as the comparison star.

The differential correction for atmospheric extinction between σ Aquilae and 22 Aquilae was taken from tables based on those in Müller's *Photometrie der Gestirne*. It was less than $0^{M}.015$ from sidereal time $17^{h}.4$ to $21^{h}.0$, and few measures were taken outside this limit. The correction to be applied was determined by multiplying the tabular value by a factor depending on the transparency of the sky, which was obtained in two ways: first, from the light effect of 22 Aquilae on the instrument, corrections for instrumental variation having been applied; and second, from the observer's estimate at the time of making the observation. The second method may seem somewhat crude, but the work at this observatory indicates that the estimate of an experienced observer deserves about the same weight as a result obtained by the first method. The factor for each observation was obtained by the two independent methods and the mean used. The two stars are of nearly the same spectral type, and as observations with large extinction have been rejected or given half-weight, errors due to uncertainty in this correction should be small.

The times were reduced to the sun, and the residuals from an approximate light-curve plotted using the total atmospheric extinction on σ Aquilae as abscissae. From this plot of the residuals it was decided to reject observations with an extinction greater than $0^{M}.25$. Those with an extinction between $0^{M}.18$ and $0^{M}.25$ were given half-weight, and a few which had been marked weak for some other reason, such as smoke, were given weight one-half or three-fourths.

The center of eclipse was determined graphically, and from the epoch of the spectroscopic observations and the 1920 photometric series a correction to the Allegheny period of $+0^{d}.00004$ was obtained. The available observations in 1918 were not sufficient for accurate determination of the epoch of eclipse, but a larger correction to the Allegheny period would bring them into better agreement with the 1920 series.

A plot of the residuals with the time as abscissa showed no evidence of variation in the comparison star throughout the 1920 series, but the 1918 observations were systematically high by two or three hundredths of a magnitude. Because of this, and the uncertainty in the period, the few observations of the earlier series were omitted in the formation of the normals.

By using the spectroscopic period, with the correction of $+0^d.00004$ derived above, and the photometric determination of epoch of eclipse the elements

$$\text{Minimum} = \text{J.D. } 2422486.797 + 1^d.95026 \cdot E$$

were obtained. These were adopted as final.

The photo-electric observations of σ Aquilae are given in Table I. The times were reduced to the sun, and the phases computed from the final elements given above. The difference of magnitude is the amount that σ was measured brighter than 22.

The observations of the 1920 series were then assembled according to phase and grouped into normal magnitudes. The rule was in general two observations to a normal during eclipse and three to a normal outside of eclipse. At one phase outside of eclipse two half-weight observations taken on the same night were rejected, as the others could be grouped into normals of approximately the same value. The thirty-seven resulting normal magnitudes and the residuals from the computed light-curve are given in Table II.

A plot of the normals showed a distinct ellipticity effect between minima. A periastron effect might also be suspected, but as the spectroscopic orbit is circular, this was considered error of observation. There is no appreciable reflection effect. The ellipticity factor z was obtained by Russell's graphical method, and the result used to determine the limits of the eclipses and check the definitive work which was as follows:

From normal magnitudes outside of eclipse the ellipticity effect was solved for, using the equation

$$m_0 - c \cos^2 \theta = m,$$

where m_0 denotes the maximum magnitude, m is the observed magnitude, θ is the phase from primary minimum, and c is a

TABLE I

OBSERVATIONS OF σ AQUILAE

Date, G.M.T.	Phase	Difference of Magnitude	Weight	Date, G.M.T.	Phase	Difference of Magnitude	Weight
1918 Series (not used)				2422533.615....	0.017	(0.267)	.....
2421783.765....	1.017	0.353	.....	.629....	0.031	(.274)	.....
1785.759....	1.061	.445	.....	.647....	0.049	.298	1/2
1786.764....	0.115	.459	.....	.661....	0.063	.328	3/4
1787.773....	1.124	.470	.....	.681....	0.083	.415	.....
1793.728....	1.229	.470	.....	.692....	0.094	.402	.....
1802.771....	0.520	.497	.....	.734....	0.136	.432	.....
1804.742....	0.541	.500	.....	.744....	0.146	.425	.....
1805.740....	1.539	.488	.....	2534.603....	1.005	.329	1/2
1806.751....	0.600	.457	.....	.619....	1.021	.342	1/2
1813.679....	1.677	.461	.....	.633....	1.035	.354	.....
1817.665....	1.762	.452	.....	.694....	1.096	.424	.....
1827.644....	0.040	.433	.....	.710....	1.112	.451	.....
1828.649....	1.045	.411	.....	.724....	1.126	.448	.....
1837.631....	0.275	.458	.....	2537.710....	0.211	.475	3/4
1845.611....	0.454	.468	.....	2539.609....	0.160	.430	.....
1920 Series				.624....	0.175	.433	.....
2422486.810....	0.017	.313	.....	2540.640....	1.191	.455	.....
2498.774....	0.279	.474	.....	.658....	1.209	.440	.....
.840....	0.345	.465	.....	.711....	1.262	.457	.....
2506.763....	0.468	.480	1/2	.722....	1.273	.449	.....
.797....	0.502	.481	.....	2553.690....	0.589	.485	1/2
2508.796....	0.551	.508	1/2	2554.647....	1.546	.457	.....
2509.826....	1.581	.496	1/2	.662....	1.561	.465	.....
2514.737....	c 641	.472	.....	2559.690....	0.738	.448	.....
2517.711....	1.665	.426	1/2	.699....	0.747	.447	.....
2521.768....	1.822	.423	.....	2561.694....	0.791	.424	3/4
.797....	1.851	.455	1/2	.706....	0.803	.417	3/4
2522.711....	0.814	.438	.....	2566.690....	1.887	.325	3/4
2523.646....	1.749	(.405)	.....	.708....	1.905	.349	3/4
.672....	1.775	.449	1/2	2567.680....	0.926	.377	.....
2524.679....	0.832	.454	.....	.697....	0.943	.328	1/2
.733....	0.886	.425	.....	2570.619....	1.915	.315	.....
.750....	0.903	.387	.....	.638....	1.934	.287	.....
.767....	0.920	.351	.....	2574.614....	0.059	.335	.....
.782....	0.935	.341	.....	.634....	0.079	.377	1/2
2525.697....	1.850	.409	.....	2583.630....	1.273	.440	.....
2526.651....	0.854	.430	.....	.645....	1.288	.452	.....
.668....	0.871	.426	.....	2584.600....	0.293	.453	.....
2528.750....	1.003	.349	.....	.614....	0.307	.455	.....
2529.681....	1.934	.302	.....	2585.606....	1.299	.452	.....
2530.615....	0.917	.377	1/2	.622....	1.315	.448	.....
.637....	0.939	.328	.....	2587.601....	1.344	.436	.....
2531.614....	1.916	.300	1/2	.615....	1.358	.431	.....
.672....	0.024	.298	.....	2588.592....	0.384	.451	.....
2532.642....	0.994	.315	.....	.605....	0.397	.461	.....
.701....	1.053	.383	.....	2589.574....	1.366	.475	.....
.734....	1.086	.438	.....	.594....	1.386	.446	.....
.751....	1.103	.442	.....	2593.594....	1.485	(.432)	.....
				.608....	1.499	(.424)	.....
				2595.595....	1.536	.473	.....

TABLE I—*Continued*

Date, G.M.T.	Phase	Difference of Magnitude	Weight	Date, G.M.T.	Phase	Difference of Magnitude	Weight
2422595.608....	1^d.549	0^M.455	.....	2422605.563....	1^d.751	0^M.441	.....
2596.554....	0.544	.462	.....	.574....	1.762	.435	.....
.566....	0.556	.460	.....	2606.514....	0.752	.440	.....
2600.581....	0.671	.441	.....	2609.542....	1.830	.422	.....
2603.577....	1.716	.430	.....	.553....	1.841	.420	1/2
.587....	1.726	.423	.....	.....	.....	.....	.....

constant. Twenty-one equations for the determination of m_0 and c gave

$$m_0 = \quad 0^M.467 \pm 0^M.0025,$$
$$c \quad = +0^M.042 \pm 0^M.0050,$$

from which $z = 0.075$. The ellipticity effect was removed from the observations by the formula

$$\text{Rectified magnitude} = m + 0^M.042 \cos^2 \theta.$$

From a plot of the rectified magnitudes at secondary minimum the center of that eclipse was determined as phase 0^d.980, from which

TABLE II

NORMAL MAGNITUDES

Phase	Difference of Magnitude	Residual O−C	No. Obs.	Phase	Difference of Magnitude	Residual O−C	No. Obs.
0^d.020.....	0^M.305	+0^M.012	2	1^d.013.....	0^M.336	−0^M.002	2
0.056.....	.323	− .019	2	1.044.....	.368	− .006	2
0.069.....	.348	− .017	2	1.091.....	.431	+ .003	2
0.088.....	.408	+ .010	2	1.114.....	.447	+ .012	3
0.147.....	.429	− .004	3	1.200.....	.448	+ .005	2
0.190.....	.451	+ .012	2	1.268.....	.453	+ .001	2
0.293.....	.461	+ .009	3	1.280.....	.446	− .008	2
0.375.....	.459	− .003	3	1.319.....	.445	− .013	3
0.512.....	.473	+ .006	3	1.370.....	.451	− .012	3
0.563.....	.478	+ .013	3	1.543.....	.462	− .002	3
0.656.....	.456	.000	2	1.568.....	.475	+ .013	2
0.742.....	.448	+ .004	2	1.710.....	.426	− .019	3
0.779.....	.428	− .011	3	1.760.....	.440	+ .001	3
0.833.....	.441	+ .008	3	1.826.....	.422	− .009	2
0.878.....	.426	+ .005	2	1.848.....	.424	+ .006	3
0.908.....	.384	.000	2	1.896.....	.337	− .001	2
0.923.....	.364	− .002	2	1.915.....	.310	.000	2
0.938.....	.337	− .010	2	1.934.....	.294	+ .004	2
0.998.....	.332	+ .005	2	.....	.....	.....	.....

$e \cos \omega = +0.004$. The photometric observations are too few to show with certainty that the orbit is not perfectly circular. But the eccentricity of the spectroscopic orbit is given to only one decimal, and this value of $e \cos \omega$ seems possible. The observations about secondary minimum were therefore reflected about phase $0^d.980$ for further work.

From the rectified normals at both primary and secondary, elements were derived by Russell's method. It was found, however, that, as Russell has pointed out,[1] the value of k can be determined from partial eclipses of such small range only with the addition of data other than that derived from the light-curve. The assumption that the eclipses were grazing total and annular, with k about 0.33, gave the best representation of the light-curve. But this means a difference of over two magnitudes in the light of the components, while from the spectroscopic plates it is known to be much less. The estimate published with the spectroscopic orbit is a difference of $0^M.5$. A second independent estimate made by Jordan in April 1921 is $0^M.3$.

The second estimate was used, and from this, with $1-\lambda_1$ and $1-\lambda_2$ the photometric depth of minima, k, a_0, and χ were obtained. After a few approximations the following elements were adopted as satisfactory:

$\chi = 1.70$	$C = 0.0799$	$D = 0.0470$
$k = 1.00$ (adopted)	$1-\lambda_1 = 0.121$	$1-\lambda_2 = 0.0905$.

Rectified primary minimum $= 0^M.327$.
Rectified secondary minimum $= 0^M.364$.

The adopted value for k corresponds to a difference of $0^M.31$ between the component stars, practically the second estimate. Using $k = 0.92$ the light-curve holds for the first estimate, $0^M.5$, so elements were computed for both values; but the masses of the component stars, and dimensions and inclination of the relative orbit, were found to be practically the same on the two assumptions, and only the results for $k = 1.00$ are given. An ephemeris was computed from the adopted elements, using Blazko's tables,[2] and

[1] *Astrophysical Journal*, **35**, 331, 1912.

[2] *Annales de l'observatoire astronomique de Moscou*, **5**, 104, 1911.

independently by Russell's method as a check. The computed light-curve, Tables III and IV, is shown in Figure 1. The residuals

TABLE III

CONSTANTS OF THE LIGHT-CURVE

	Magnitude	Range	Light	Loss
Maximum	$0^{M}.467$	.....	1.000	.....
Primary minimum	0.285	$0^{M}.182$	0.846	0.154
Secondary minimum	0.322	0.145	0.875	0.125
Rectified Curve				
Maximum	$0^{M}.467$	.....	1.000	.....
Primary minimum	0.327	$0^{M}.140$	0.879	0.121
Secondary minimum	0.364	0.103	0.910	0.090

TABLE IV

LIGHT-CURVE

Phase	Difference of Magnitude	Phase	Difference of Magnitude
$\pm 0^{d}.00$	$0^{M}.285$	$0^{d}.94$	$0^{M}.345$
±0.02	.293	0.96	.328
±0.04	.316	0.98	.322
±0.06	.349	1.00	.328
±0.08	.384	1.02	.345
±0.10	.415	1.04	.370
±0.116	.430	1.06	.396
+0.15	.434	1.08	.419
0.20	.440	1.096	.430
0.30	.453	1.20	.443
0.40	.464	1.30	.457
0.488	.467	1.40	.466
0.60	.462	1.463	.467
0.70	.450	1.50	.467
0.80	.437	1.60	.459
0.864	.430	1.70	.447
0.88	.418	1.80	.434
0.90	.395	1.834	.430
0.92	.369	.....	.....

from this curve are given in Table II, and from these we derive

$$\text{P.E. single normal} = \pm 0^{M}.006 .$$

The normal magnitudes are plotted as circles in Figure 1, the radius of each circle being equal to the computed probable error.

The data of the spectroscopic binary system,[1] are given in Table V. The value of sin i was known from the photometric elements. Combining this with the spectroscopic elements the absolute dimensions of the system and masses of the bodies were

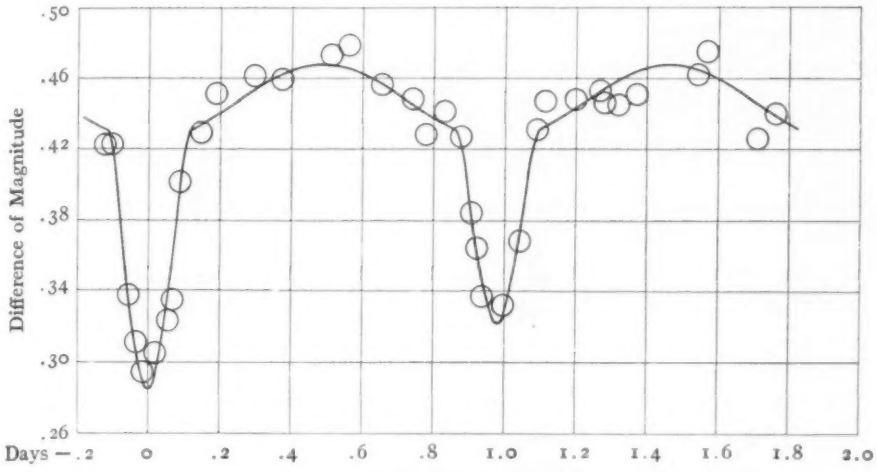

FIG. 1.—Light-Curve of σ Aquilae

TABLE V

SPECTROSCOPIC ELEMENTS OF σ AQUILAE (JORDAN)

P	$1^d.95022$	$\pm 0^d.0001$ (estimated)
μ	$184^\circ.595$	$\pm 0^\circ.0095$
e	0.0	±0.01
T (Max. vel.)	J.D. 2420054.331	$\pm 0^d.0031$
γ	−5.00 km/sec.	±1.04 km/sec.
K_1	163.52 km/sec.	±1.35 km/sec.
$a_1 \sin i$	4,380,000 km	±3600 km
$m_1 \sin^3 i$	5.3⊙	
K_2	199 km/sec.	±4.1 km/sec.
$a_2 \sin i$	5,340,000 km	±110,000 km
$m_2 \sin^3 i$	4.4⊙	

obtained. Following Russell,[2] the apparent diameter of the brighter star was computed from the magnitude and spectral type. From this and the actual diameter, the distance and parallax

[1] Jordan, *Allegheny Publications*, **3**, 192, 1916.

[2] *Publications of the Astronomical Society of the Pacific*, **32**, 315, 1920.

were obtained, the hypothetical parallax being 0".006 corresponding to a distance of about 550 light-years.

The light elements are assembled in Table VI, and Figure 2 is the system represented by them. The ellipticity of the star disks has been neglected in the figure.

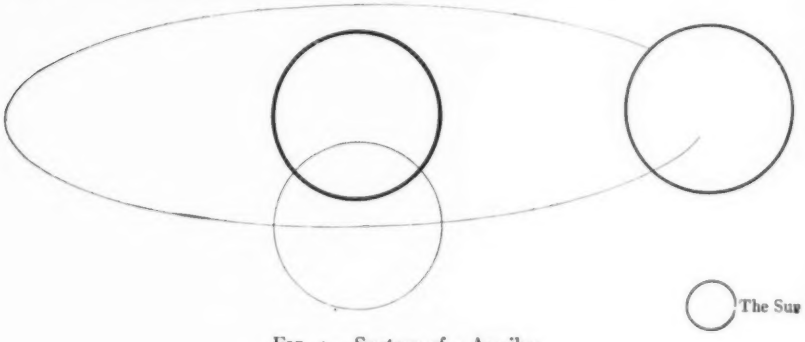

FIG. 2.—System of σ Aquilae

TABLE VI

ELEMENTS OF σ AQUILAE

Primary minimum, J.D. 242.....	.....	2486.797 G.M.T
Period of revolution (photometric).....	P	$1^d.95026$
Phase of secondary minimum.....	.....	$0^d.980$
Semi-duration of eclipse.....	.....	$0^d.116$
Component of eccentricity.....	$e \cos \omega$	+0.004
Cosine of inclination.....	$\cos i$	0.314
Ratio of radii.....	k	1.00
Ratio of axes.....	b/a	0.955
Major semi-axis.....	$a_1 = a_2$	0.242
Minor semi-axis.....	$b_1 = b_2$	0.231
Light of brighter star.....	L_1	0.572
Light of fainter star.....	L_2	0.428
Ratio of surface brightness.....	J_1/J_2	1.34
Magnitude of system.....	.....	$5^M.17$
Magnitude of brighter star.....	.....	$5^M.78$
Magnitude of fainter star.....	.....	$6^M.09$
From Allegheny spectroscopic elements	Sun = 1	
Major semi-axis.....	$a_1 = a_2$	3.56
Minor semi-axis.....	$b_1 = b_2$	3.40
Density of brighter star.....	ρ_1	0.150
Density of fainter star.....	ρ_2	0.125
Mean density of system.....	ρ_0	0.138
Mass of brighter star.....	m_1	6.19
Mass of fainter star.....	m_2	5.14
Parallax (from surface brightness).....	π	0".006

SUMMARY

1. A series of observations made with a photo-electric photometer during 1920 gives the light-curve of σ Aquilae.

2. Using residuals from the computed curve the thirty-seven normal magnitudes show a probable error of $\pm 0^{M}.006$.

3. The comparison star 22 Aquilae was constant within the limit of the measures from July to October 1920, but a change of $0^{M}.02$ between 1918 and 1920 is indicated for either 22 Aquilae or σ Aquilae.

4. Because of the small range in partial eclipse, elements of σ Aquilae from the light-curve alone would be indeterminate, but since two spectra appear on the Allegheny plates, the information on this eclipsing system is unusually complete. The elements and absolute dimensions derived are given in Table VI, and the system is shown in Figure 2.

I am indebted to Professor Joel Stebbins for supervision and direction throughout these investigations, and for part of the observational data, and to Mr. J. K. Willy for checking some of the reductions.

UNIVERSITY OF ILLINOIS OBSERVATORY
May 1922

A SPECTROSCOPIC METHOD OF DETERMINING THE ABSOLUTE MAGNITUDES OF A-TYPE STARS AND THE PARALLAXES OF 544 STARS

By WALTER S. ADAMS and ALFRED H. JOY[1]

ABSTRACT

Spectroscopic method of determining the absolute magnitudes of A-type stars.—In order to ascertain whether a spectroscopic method could be applied to these stars, spectrograms were obtained of nearly all the A-type stars in the Taurus and Ursa Major groups, fifty-six in all, whose absolute magnitudes are accurately known. The stars were then grouped (*a*) according to spectral type and (*b*) according to whether the lines were diffuse or sharp. A good correlation between magnitude and spectrum was found, the magnitude being brighter the earlier the spectral type and also brighter for spectra with sharp lines. The study was then extended to include all A-type stars for which both the spectral type and parallax were known, and the same correlation was found (see Fig. 1), the average difference being only $\pm 0''.0077$ for eighty-two parallaxes determined by group motion, and $0''.0131$ for 104 trigonometric parallaxes. The accuracy of parallax determinations by this method for A-type stars is thus of the same order as for stars of later types, and the method is evidently capable of considerable further refinement. A-type stars having "c" characteristics, such as α Cygni, require separate treatment, which may perhaps be based on the intensities of the well-known enhanced lines λ 4481 and λ 4233.

Spectroscopic parallaxes of 544 stars of type B7 to F2, determined on the basis of the foregoing results, are given in Table VI. When grouped according to their proper motions, the mean parallax of each group is found to increase from $0''.011$ for $\mu < 0''.010$ to $0''.037$ for μ about $0''.2$ (Fig. 2). This correlation is a very satisfactory confirmation of the accuracy of the method.

The spectroscopic methods used in the determination of the absolute magnitudes of stars of the later spectral types cannot in general be applied to those of the A-type of spectrum. With some notable exceptions, such as α Cygni and stars of similar spectra and those in which certain lines like λλ 4077, 4216, and 4481 are especially strong, the stars of this type do not show the large variations in the intensities of the lines which appear in the later types. They do, however, show very great differences in the appearance of the lines, in some stars such as Sirius the lines being sharp and well defined, and in others such as Altair very diffuse and vague. The importance of this characteristic will appear in the course of the discussion.

With a view to studying the nature of the spectra of stars of this type with known absolute magnitudes, spectrograms were

[1] *Contributions from the Mount Wilson Observatory*, No. 244.

obtained of nearly all the stars of type A which belong to the Taurus and the Ursa Major groups. The absolute magnitudes of these stars are known with a high degree of accuracy from the motions of the groups, and for many of the stars of the latter group trigonometric parallaxes are also available. A considerable range in absolute magnitude as well as in spectral type is found among these stars, and they afford, accordingly, excellent material for such an investigation.

The first step in the study of these spectra, and as it proved the most important one, was an accurate classification of spectral type. Since the H and K lines of calcium, which form an important criterion in the classification of A stars by Miss Cannon and the other Harvard observers, are far to one side of the region of best definition on our spectrograms and do not appear at all on those taken with high dispersion, we have based our classification upon the intensities of the metallic arc lines showing in the stellar spectra. In this we were aided greatly by the use of the spectra of standard stars chosen from among those classified by Dr. Kohlschütter at this Observatory in the years 1912 to 1914. Spectra in which the helium lines do not appear and such prominent arc lines as λλ 4326 and 4384 are not present or are extremely faint are called A0. With increasing intensity of the arc lines the stars are classified as A1, A2, A3, etc. When the helium lines λλ 4026 and 4471 are just visible, the spectrum is classed as B9, and when λ 4471 and λ 4481 are equal, as B8. This system appears to be in good agreement with that of the Harvard observers and of Kohlschütter, a result which would naturally follow from the use of the standard types of the latter to check the results. A comparison of the spectral types as determined by Miss Cannon and by Kohlschütter has already been published by the Harvard College Observatory.[1]

In addition to the symbols indicating the spectral type the letters "n" for nebulous and "s" for sharp have been appended to indicate the character of the spectral lines. Thus the spectrum of Sirius is A2s and that of Altair A2n. Stars like α Cygni have the "c" characteristics noted by the Harvard observers and are indicated by cA2s, for example. The lines are always exceptionally

[1] *Annals of the Harvard College Observatory*, **56**.

sharp and the letter "s" is scarcely necessary. These stars are few in number and do not enter into the present discussion, but a brief reference is made to them at a later point.

If we separate the stars of the Taurus and Ursa Major groups into the successive spectral subdivisions obtained in this way, we find the results given in Table I. The absolute magnitudes are

TABLE I

Boss	*M*	Boss	*M*	Boss	*M*
	A0n		A5n		A3s
3117	+0.6	919	+3.0	1029	+1.3
3190	1.7	1086	2.8	2930	0.8
3752	0.4				
3961	0.3		A6n		A4s
4009	0.6	1025	+3.2	553	+2.3
5573	1.7	1056	2.8	1046	0.7
				3506	0.6
	A1n		A7n		
1024	+1.2				A6s
1034	1.8	892	+3.2	1054	+2.1
1220	0.5	991	2.5		
3480	2.1	1022	2.1		A7s
		1058	3.2	1092	+2.3
	A2n	3360	2.8	1122	1.9
1033	+1.6			3475	2.3
1143	2.2		A8n		
2972	2.2	1004	+2.8		A8s
		1007	2.4	1114	+2.6
	A3n	1043	3.2	1226	2.7
1026	+1.3			2813	3.3
1047	2.3		F0n	5425	1.9
1051	2.8	935	+3.6		
1087	1.6	1040	2.9		F1s
1194	1.6			961	+3.2
			A2s	1013	3.0
	A4n	1732	+1.3	1055	2.7
1027	+2.8	3363	−0.2		
1067	1.9	3474	+0.6		F2s
1090	1.6			1018	+2.8
3382	2.7				

those given by Rasmuson in his valuable memoir on moving clusters,[1] but a constant correction of +1.57 magnitudes has been applied to reduce to the unit of 10 parsecs instead of that of one siriometer as used by him. Six of the stars of the Ursa Major group are of type A0n and thus supplement in an important way those of the Taurus group which are of a more advanced type on the average.

[1] *Meddelanden från Lunds Astronomiska Observatorium*, Serie II, No. 26.

If these results are collected, we obtain the following mean absolute magnitudes for the various spectral subdivisions.

TABLE II

	M	No.		*M*	No.
A0n	+0.9	6	A2s	+0.6	3
A1n	1.4	4	A3s	1.0	2
A2n	2.0	3	A4s	1.2	3
A3n	1.9	5	A6s	2.1	1
A4n	2.2	4	A7s	2.2	3
A5n	2.9	2	A8s	2.7	4
A6n	3.0	2	F1s	3.0	3
A7n	2.8	5	F2s	2.8	1
A8n	2.8	3			
F0n	3.2	2			

Two conclusions may be drawn from an inspection of these results.

1. A definite progression is shown between absolute magnitude and spectral type, the stars of the more advanced types being the fainter. The change of absolute magnitude with type is most rapid among the earlier A stars and becomes comparatively slight in the later types.

2. The average absolute magnitude of the stars with sharp lines is in the case of the earlier A stars considerably brighter than that of the stars of the same types with diffuse lines. This difference becomes small for the later types.

The first of these results is in agreement with that found for the stars of the Taurus group in the case of the larger spectral divisions by Hertzsprung[1] and Kohlschütter,[2] who showed that for the successive spectral types A, F, G, and K the apparent magnitudes, and hence the absolute magnitudes for stars at the same distance, become progressively fainter. Without a more accurate knowledge of spectral type, however, it has not been possible hitherto to establish such a relationship for the subdivisions within the A type.

The second conclusion, that stars with sharp lines are brighter than stars of the same type with diffuse lines, is in accord with our

[1] *Astronomische Nachrichten*, **209**, 119, 1919.

[2] *Ibid.*, **211**, 297, 1920.

knowledge of stars of the later types of spectrum. Thus the high luminosity of the Cepheid variables, the stars with the "c" characteristics of spectrum, and such objects as α Orionis and α Scorpii, is always found associated with narrow well-defined spectral lines. It is well known that the absorption spectrum of o Ceti changes from one with sharp lines at maximum of light to one with vague and diffuse lines near minimum. It seems altogether probable, as the measurement of stellar diameters has shown in a few cases, that the giant stars are large expanded bodies of gas of low density, a condition which favors the production of narrow lines, while the dwarf stars are smaller, more condensed bodies with atmospheres which show a much more rapid density gradient and so produce diffuse lines.

The results for the Taurus and Ursa Major groups proved to be of such interest that it seemed desirable to extend the investigation to include all the A-type stars for which reliable absolute magnitudes are available and for which photographs of spectra have been secured at Mount Wilson. The material used consists of 82 stars with absolute magnitudes derived from group motion and 104 stars with trigonometric parallaxes. Some of these are common to both lists so that the number of separate stars involved is 148. The absolute magnitudes of these stars have been taken from the lists of Rasmuson for the Taurus, Ursa Major, Perseus, Praesepe, and α Lyrae groups, and a few of his results have been included for other stars for which group motion seems to be clearly established. The trigonometric parallaxes are mainly from the Allegheny, McCormick, Mount Wilson, Sproul, Yale, and Yerkes observatories. These stars are all given in the general catalogue, Table VI of this article, with the corresponding trigonometric or group parallax, and so are not listed separately here. When an absolute magnitude has been derived both from group motion and from trigonometric parallax the arithmetical mean has been used.

All of these stars were classified independently by Adams and Joy, and in Table III are given the results for the two observers, collected according to spectral type and mean absolute magnitude.

TABLE III

	Adams		Joy			Adams		Joy	
	No.	*M*	No.	*M*		No.	*M*	No.	*M*
B9n.....	12	+0.6	5	+0.5	B9s.....	3	−0.1	4	0.0
A0n.....	16	0.9	28	1.0	A1s.....	4	+0.6	4	+0.6
A1n.....	15	1.3	5	0.7	A2s.....	10	0.9	9	0.7
A2n.....	12	2.0	11	1.9	A3s.....	8	1.4	4	1.6
A3n.....	11	1.9	3	1.6	A4s.....	2	1.7	4	2.1
A4n.....	13	2.1	7	2.2	A5s.....	4	2.0	3	1.4
A5n.....	7	2.3	14	2.3	A6s.....	4	2.0	3	0.5
A6n.....	6	2.6	10	2.3	A7s.....	2	2.9	2	2.3
A7n.....	3	3.0	4	2.2	A8s.....	4	2.3	3	2.8
A8n.....	2	2.8	9	2.6	A9s.....	1	3.8	1	3.0
A9n.....	3	2.7	1	3.6	F0s.....	.....	.....	6	2.5
F0n.....	.....	.....	2	2.9	F1s.....	4	2.0	1	3.0
F2n.....	1	3.6	.....	.....	F2s.....	2	3.4	2	2.4
F3n.....	.....	.....	2	3.0					

These results, although showing considerable variation in the number of stars of each subdivision as classified by the two observers, are in good agreement as regards the mean absolute magnitude for groups containing a fair number of stars. Most of the differences in classification represent variations of one or two subdivisions, as, for example, at A0n where several stars classified by Joy as of this type are called B9n by Adams.

TABLE IV

	Adams		Joy			Adams		Joy	
	No.	*M*	No.	*M*		No.	*M*	No.	*M*
B9n.....	12	+0.58	5	+0.5	B9s.....	3	−0.1	4	+0.1
A0n.....	16	0.87	33	0.92	A1s.....	4	+0.6	4	0.5
A1n.....	15	1.34	.....	.....	A2.5s...	18	1.15	13	0.99
A2.5n....	23	1.96	14	1.85	A4.5s ..	6	1.9	7	1.8
A4.5n....	20	2.14	21	2.29	A7s.....	10	2.29	8	1.8
A6.5n....	9	2.7	14	2.29	F1s.....	.....	.....	10	2.71
A8n.....	.....	.....	10	2.68	F2s.....	7	2.7	.....	.....
A9n.....	6	2.9	.....	.....					
F1n.....	.....	.....	4	2.9					

In order to facilitate the plotting of these quantities and partially to equalize the weights, the values have been further combined to form the mean results given in Table IV.

The curves plotted from these results are shown in Figure 1, and from these curves the values corresponding to each spectral subdivision have been determined as shown in Table V. Under O−C is given the difference between the values of the absolute

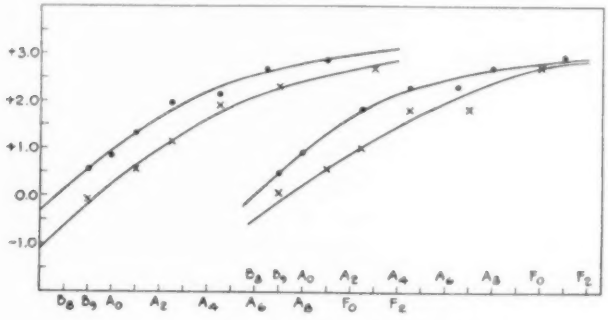

FIG. 1.—Curves showing the relationship between average absolute magnitude and spectral type for stars with parallaxes determined trigonometrically or from group motion. The points indicate groups of stars with diffuse (*n*) lines, the crosses sharp (*s*) lines. The curves on the left are for Adams, those on the right for Joy.

TABLE V

	Adams			Joy				Adams			Joy		
	M	O−C	No.	*M*	O−C	No.		*M*	O−C	No.	*M*	O−C	No.
B8n....	+0.2	.....	.....	0.0	.....	.....	B8s....	−0.7	.....	.....	−0.5	.....	.....
B9n....	0.6	0.0	12	+0.5	0.0	5	B9s....	−0.2	+0.1	3	−0.2	+0.2	4
A0n....	0.9	0.0	16	0.9	+0.1	28	A0s....	+0.2	.....	.....	+0.2	.....	.....
A1n....	1.3	0.0	15	1.3	−0.6	5	A1s....	0.6	0.0	4	0.5	+0.1	4
A2n....	1.7	+0.4	12	1.7	+0.2	11	A2s....	1.0	−0.1	10	0.8	−0.1	9
A3n....	2.0	−0.1	11	1.9	−0.3	3	A3s....	1.3	+0.1	8	1.2	+0.4	4
A4n....	2.2	−0.1	13	2.2	0.0	7	A4s....	1.7	0.0	2	1.5	+0.6	4
A5n....	2.3	0.0	7	2.3	0.0	14	A5s....	1.9	+0.1	4	1.7	−0.3	3
A6n....	2.5	+0.1	6	2.4	−0.1	10	A6s....	2.2	−0.2	4	2.0	−1.5	3
A7n....	2.7	+0.3	3	2.6	−0.4	4	A7s....	2.3	+0.6	2	2.2	+0.1	2
A8n....	2.8	0.0	2	2.7	−0.1	9	A8s....	2.4	−0.1	4	2.4	+0.4	3
A9n....	2.8	−0.1	3	2.7	+0.9	1	A9s....	2.5	+1.3	1	2.6	+0.4	1
F0n....	2.9	.....	.....	2.8	+0.1	2	F0s....	2.6	.....	.....	2.7	−0.2	6
F1n....	3.0	.....	.....	2.8	.....	.....	F1s....	2.7	−0.7	4	2.8	+0.2	1
F2n....	3.1	+0.5	1	2.9	+0.1	2	F2s....	2.8	+0.6	2	2.8	−0.4	2

magnitudes of Table III and those obtained from these curves. In other words, it shows to what extent the mean observed absolute magnitudes may be represented by a relationship based simply upon spectral type and the character of the spectral lines.

This comparison shows clearly that the relationship between absolute magnitude and spectral type may be used to determine the mean absolute magnitudes of these groups of stars with a very satisfactory degree of accuracy. Since a large amount of the material consists of absolute magnitudes derived from the trigonometric parallaxes of stars which do not belong to recognized clusters, we may draw the important conclusion that this same relationship may be applied to A-type stars in general, as well as to such groups as those of Taurus and Ursa Major.

The vital question as to the application of this method to the case of individual stars is the next to be considered. If it can be so applied, it involves the conclusion that there is no dispersion in absolute magnitude among A-type stars which have very closely the same spectral type and the same spectral characteristics. This conclusion is perhaps not so radical as it appears at first, since the definition of spectral type and line-characteristics, if carried to extreme limits, might well serve to define the absolute magnitude of a star uniquely. Among stars of the M type, for example, the absolute magnitudes are determined by the relative intensities of certain pairs of lines. If these lines were used to define the spectral type, the latter could be used equally well to determine the absolute magnitude. With a few striking exceptions, such as the A-type companion of o^2 Eridani and some other stars to which reference will be made later, the A-type stars in general appear to be giant stars with no very wide dispersion in absolute magnitude. Within these limits, accordingly, it is quite conceivable that an accurate determination of the spectral characteristics might define the absolute magnitude.

The investigation of this question has been made in three ways:

1. Direct comparison with individual group parallaxes.
2. Direct comparison with individual trigonometric parallaxes.
3. Comparison of the average parallaxes and the average proper motion of 544 stars.

Since the results for the individual stars are all given in the catalogue appearing as Table VI, it seems unnecessary to repeat them here. The absolute magnitudes have all been determined

by two independent observers and the parallaxes have then been combined. To illustrate: the spectral type of Boss 3474 (ζ^1 Ursae Majoris) as determined by Adams is A2s and by Joy A3s. Referring to Table V we find for these types the values +1.0 and +1.2 for the absolute magnitude. Combining with the apparent magnitude 2.4, we derive the parallaxes 0".052 and 0".057, or 0".054 in the mean. Summarizing the results obtained in this way for 82 stars in Table VI with parallaxes derived from group motion, and 104 stars with trigonometric parallaxes, we secure the following comparison:

Group parallaxes: 82 stars; systematic difference, −0".0014;
Average difference, ±0".0077.

Trigonometric parallaxes: 104 stars; systematic difference, 0".0000;
Average difference, +0".0131.

These results compare very favorably with those obtained in the case of the later-type stars where the average difference between spectroscopic and trigonometric parallaxes is ±0".015.

The agreement with the group parallaxes could, of course, be improved by a very slight readjustment of our reduction curves, but it has seemed preferable not to assign too great weight to these stars, both on account of the uncertainty still outstanding in the parallax of the Taurus group and because they represent a special selection of stars, while the trigonometric parallaxes are more representative of stars in general.

It is of interest to call attention to the results for the three most prominent stars in the list, Sirius (Boss 1732), Vega (Boss 4722), and Altair (Boss 5062). All three have well-determined trigonometric parallaxes, and in addition Sirius and Vega belong to recognized stellar groups and their parallaxes have been derived from group motion. The spectral types of these stars have been determined as A2s, A1s, and A2n, which give absolute magnitudes of +0.9, +0.55, and +1.7, and parallaxes of 0".316, 0".123, and 0".145, respectively. The trigonometric parallaxes are 0".374, 0".110, and 0".205, which correspond to absolute magnitudes of +1.3, +0.3, and +2.5. The group motion gives a parallax of 0".380 for Sirius and 0".104 for Vega. The correction of +0.4 to the spectroscopic

absolute magnitude of Sirius required to bring it into agreement with observation is not excessive, and a change of type from A2s to A3s would account for nearly the entire difference. In the case of Altair, the correction of +0.8 magnitude is larger than would be expected, but it may find its explanation in the well-known fact that the spectral lines in this star are extraordinarily diffuse. In such cases the absolute magnitude may prove to be fainter than that of stars with the usual "n" characteristics, and further refinement of the method may show that these stars require separate treatment.

This method of determining parallaxes has been applied to the 544 stars listed in Table VI. In order to condense the results the separate determinations of the absolute magnitudes and parallaxes by the two observers have been combined. As a result, this makes a slight apparent discrepancy in a few cases between the absolute magnitude and the corresponding parallax. Since all of the stars in Table VI are designated by their numbers in Boss's Catalogue, it has not seemed necessary to add their positions. The successive columns of Table VI, therefore, give the Boss number, the apparent visual magnitude on the Harvard system,[1] the proper motion according to Boss, the spectral types by Adams and Joy, respectively, the mean of the absolute magnitudes, and the mean of the corresponding parallaxes. The parallaxes as derived from group motion, the trigonometric parallaxes, and the sources for both are added in the last three columns. The following letters are used to indicate the principal authorities for the trigonometric parallaxes: A, Allegheny; F, Flint; M, McCormick; S, Sproul; W, Mount Wilson; Y, Yale; Ye, Yerkes.

The third test of the applicability of the method to A-type stars consists in a comparison between the average of the proper motions and the average of the parallaxes of the stars in Table VI. With the large number of stars available, this comparison should prove especially valuable. The stars have been divided into groups according to their proper motions, with the limits indicated. The

[1] In the case of visual binaries the values of *m* refer to the brighter component. In the case of spectroscopic binaries, however, owing to the uncertainty in the relative brightness of the components it has seemed to us preferable for the present to leave the magnitudes without correction.

TABLE VI

Boss	m	μ	Spectrum A.	Spectrum J.	M	Spect. π	Group π	Trig. π	Auth.
10	2.2	0".213	A1n	A0n	1.1	0".060	.....	.....	
43	4.4	0.052	A1n	A2n	1.5	0.026	.....	.....	
50	4.5	0.081	A0n	A1n	1.1	0.021	.....	0".017	A
52	6.0	0.028	B9s	B8n	−0.1	0.006	.....	.....	
66	6.6	0.015	B7n	B9n	0.2	0.005	.....	.....	
68	5.4	0.016	B9n	A0n	0.8	0.012	.....	.....	
91	5.2	0.039	A1n	A3n	1.5	0.020	.....	.....	
154	5.5	0.027	A2s	A3s	1.1	0.014	.....	.....	
159	5.4	0.022	B9s	A0n	0.4	0.010	.....	.....	
166	6.8	0.006	A2n	A1s	1.1	0.008	.....	.....	
169	5.4	0.014	B9s	A0s	0.0	0.008	.....	.....	
198	5.9	0.006	A3n	A1n	1.6	0.011	.....	.....	
223	5.9	0.024	A4s	A7s	2.0	0.016	.....	.....	
224	5.5	0.039	B9s	A0s	0.0	0.008	.....	.....	
247	5.7	0.018	B9n	B9n	0.6	0.010	.....	.....	
252	5.7	0.326	A8n	A8n	2.8	0.026	.....	.....	
257	4.5	0.010	B8s	B8s	−0.6	0.010	.....	0.010	Ye
263	5.5	0.038	B9s	B9s	−0.2	0.007	0".010	.....	Perseus
284	5.8	0.028	A2sp	B9s	0.4	0.008	.....	.....	
289	6.7	0.008	A0n	A0n	0.9	0.007	.....	.....	
295	5.3	0.056	A1n	A2n	1.5	0.018	.....	.....	
314	2.8	0.306	A3n	A3n	2.0	0.068	.....	.....	
340	5.8	0.025	B9n	A0n	0.8	0.010	.....	0.017	W
347	6.2	0.011	B9n	A0n	0.8	0.008	.....	.....	
379	5.4	0.053	B9s	B9s	−0.2	0.008	0.013	.....	Perseus
425	5.0	0.010	B8s	B8s	−0.6	0.008	.....	.....	
446	4.7	0.061	A4s	A5n	2.0	0.029	.....	0.020	S, Ye
449	4.1	0.045	A1n	A0n	1.1	0.025	.....	.....	
463 Ft.	5.2	0.042	A3n	A2n	1.8	0.022	.....	.....	
466	5.4	0.023	A2n	A1n	1.5	0.016	.....	.....	
469	5.4	0.072	B9n	A0n	0.8	0.012	.....	0.009	A, F, S, Y
490	6.7	0.035	A0n	A1n	1.1	0.008	.....	.....	
508	5.3	0.035	A0n	A0n	0.9	0.013	.....	.....	
521	5.7	0.015	A0n	A0n	0.9	0.011	.....	.....	
522	5.1	0.058	A1n	B9n	0.9	0.014	.....	.....	
526	5.3	0.012	A3s	A1s	0.9	0.014	.....	.....	
536	5.9	0.128	A9s	F0s	2.6	0.023	.....	.....	
550	4.8	0.015	A3s	A4s	1.4	0.021	.....	.....	
551	4.9	0.027	B9n	B9n	0.6	0.014	.....	.....	
553	5.8	0.076	A4s	A3sp	1.4	0.014	0.020	.....	Urs. Maj.
616	6.3	0.040	A2s	A3s	1.1	0.010	.....	.....	
622	3.7	0.210	A0n	A0n	0.9	0.027	.....	0.049	A, M, Y, Ye
644	4.3	0.213	A4n	A5n	2.2	0.039	.....	0.022	A
666	5.3	0.054	A0n	A1n	1.1	0.014	.....	.....	
674N	5.3	0.017	A3s	A2s	1.0	0.014	.....	0.018	S
674S	5.6	0.017	A3s	A2s	1.0	0.012	.....	.....	
682	5.5	0.017	B9n	B9n	0.6	0.010	.....	.....	
686	5.9	0.014	A5s	A4s	1.7	0.014	.....	.....	
696	4.2	0.150	A0n	A3n	1.4	0.028	.....	.....	
699	5.8	0.006	A1s	A0s	0.4	0.008	.....	.....	
715	5.6	0.038	B9n	B9n	0.6	0.010	0.009	.....	Perseus
719	5.6	0.019	B9n	A0n	0.8	0.010	.....	.....	
721	5.5	0.083	A3n	A6n	2.2	0.022	.....	.....	
727	6.8	0.018	A0n	A0n	0.9	0.007	.....	.....	
731	5.5	0.039	A2s	A2s	0.9	0.012	.....	.....	
757	5.0	0.058	A1n	A0n	1.1	0.016	.....	.....	
777	5.9	0.011	A1s	A0s	0.4	0.008	.....	.....	
791	5.0	0.033	A0n	A0n	0.9	0.015	.....	.....	
800	5.6	0.017	A1n	A2n	1.5	0.016	.....	.....	
801	5.1	0.021	B8n	B9n	0.4	0.011	.....	.....	
802	5.5	0.040	B8n	B9n	0.0	0.008	0.009	.....	Perseus
833	5.6	0.032	B9n	A0n	0.8	0.010	0.008	.....	Perseus
845	5.6	0.055	A4s	A5s	1.7	0.017	(0.013)	.....	Perseus
849	5.7	0.020	A4s	A5n	2.0	0.018	.....	.....	
878	5.1	0.042	A1n	A1n	1.3	0.017	.....	.....	
892	6.0	0.147	A7n	A7n	2.6	0.022	0.028	.....	Taurus
896	4.9	0.005	B9n	B9n	0.6	0.014	.....	.....	
898	5.3	0.039	B8n	B9n	0.4	0.010	0.009	.....	Perseus
901 Ft.	6.3	0.034	A0n	A0n	0.9	0.008	.....	0.005	M
919	5.8	0.141	A5n	A5n	2.3	0.020	0.028	.....	Taurus

TABLE VI—*Continued*

Boss	m	μ	Spectrum A.	Spectrum J.	M	Spect. π	Group π	Trig. π	Auth.
935	5.5	0".159	F2n	A0n	2.9	0".030	0".034	.....	Taurus
961	5.7	0.143	F1s	F1s	2.8	0.026	0.032	.....	Taurus
974	5.1	0.004	A1n	A0n	1.1	0.015	.....	.....	
989	4.8	0.066	A5s	A5s	1.8	0.025	.....	.....	
991	5.6	0.112	A8n	A6n	2.6	0.025	0.024	.....	Taurus
997	5.4	0.064	A1s	A0s	0.4	0.010	.....	.....	
1004	5.6	0.121	A6n	F0n	2.6	0.026	0.028	.....	Taurus
1007	5.3	0.116	A0n	A8n	2.8	0.031	0.027	.....	Taurus
1012	5.3	0.043	A1n	A0n	1.1	0.014	.....	.....	
1013	5.8	0.118	F1s	F1s	2.8	0.024	0.028	.....	Taurus
1018	5.7	0.114	F1s	F3s	2.8	0.026	0.027	.....	Taurus
1022	4.8	0.124	A6n	A8s	2.4	0.034	0.029	.....	Taurus
1023	5.8	0.029	A3n	A3n	2.0	0.017	.....	.....	
1024	5.2	0.072	A1n	A0n	1.1	0.016	0.019	0".015	Urs. Maj., M
1025	6.0	0.123	A5n	A6n	2.4	0.018	(0.029)	.....	Taurus
1026	4.4	0.112	A3s	A4n	1.8	0.030	0.025	.....	Taurus
1027	5.4	0.132	A3n	A5n	2.1	0.022	0.030	.....	Taurus
1029	4.2	0.109	A3s	A4s	1.4	0.028	0.026	.....	Taurus
1033	4.4	0.123	A2n	A3n	1.8	0.030	0.028	.....	Taurus
1034	4.6	0.118	A0n	A2n	1.3	0.022	0.028	.....	Taurus
1040	5.7	0.118	A0n	F0n	2.8	0.026	0.027	.....	Taurus
1043	6.0	0.111	A8n	A8n	2.8	0.022	0.027	.....	Taurus
1046	3.6	0.107	A3s	A6s	1.6	0.042	0.026	.....	Taurus
1047	5.1	0.111	A2n	A4n	2.0	0.024	0.028	.....	Taurus
1051	5.7	0.106	A3n	A4n	2.1	0.019	(0.026)	.....	Taurus
1054	4.8	0.116	A5s	A7s	2.0	0.028	0.029	.....	Taurus
1055	5.5	0.110	F1s	F0s	2.7	0.027	0.028	.....	Taurus
1056	5.5	0.110	A5n	A8n	2.5	0.025	0.028	.....	Taurus
1058	6.0	0.109	A5n	A8n	2.5	0.020	0.028	.....	Taurus
1061	6.1	0.007	A3s	A5s	1.5	0.012	.....	.....	
1064	5.9	0.029	A2s	B9s	0.4	0.008	.....	.....	
1067	4.8	0.104	A2n	A5n	2.0	0.028	0.027	.....	Taurus
1069	5.8	0.028	A3s	A4s	1.4	0.014	.....	.....	
1076	4.4	0.066	A3s	A0s	0.8	0.019	.....	.....	
1086	5.8	0.094	A4n	A6n	2.3	0.020	0.025	.....	Taurus
1087	4.3	0.104	A3n	A4n	2.1	0.036	0.028	.....	Taurus
1088	5.3	0.067	A4s	A6n	2.0	0.022	.....	.....	
1089	5.2	0.074	A4s	A6s	1.8	0.020	.....	.....	
1090	4.9	0.084	A3n	A5n	2.2	0.028	0.023	.....	Taurus
1092	5.6	0.082	A5s	A8s	2.2	0.020	0.023	.....	Taurus
1093	5.7	0.053	B0n	A0n	0.8	0.010	(0.012)	.....	Perseus
1095	5.0	0.046	A4s	A5s	1.7	0.022	.....	.....	
1097	5.4	0.027	B0n	A0n	0.8	0.012	.....	.....	
1099	5.7	0.061	A0n	A0n	0.9	0.011	0.016	.....	Perseus
1103	5.2	0.067	A0n	A0n	0.9	0.014	0.016	.....	Perseus
1106	7.2	0.047	A1n	A0n	1.1	0.006	.....	−0.014	S
1114	5.4	0.098	A8s	A8n	2.6	0.027	0.029	.....	Taurus
1118	5.7	0.052	A1n	A1n	1.3	0.013	.....	.....	
1122	5.4	0.066	A7s	A7s	2.2	0.024	(0.020)	.....	Taurus
1143	5.1	0.091	A2n	A2n	1.7	0.021	0.026	.....	Taurus
1146	5.6	0.013	A2n	A0s	1.0	0.012	.....	.....	
1150	5.6	0.007	A1n	A0n	1.1	0.012	.....	.....	
1155	5.8	0.010	A2s	A1s	0.8	0.010	.....	.....	
1161	4.4	0.012	A2s	A2s	0.9	0.020	.....	.....	
1163	4.7	0.145	A1n	A0n	1.1	0.019	.....	.....	
1165	5.7	0.024	B0n	B0s	0.2	0.008	.....	.....	
1177	5.6	0.067	A2s	A2n	1.4	0.014	.....	.....	
1182	6.0	0.013	F1s	F2s	2.8	0.022	.....	0.002	W
1194	4.7	0.082	A3n	A4n	2.1	0.030	(0.024)	.....	Taurus
1220	2.9	0.118	A1n	A2n	1.5	0.052	(0.033)	.....	Urs. Maj
1226	5.4	0.074	A7s	F0s	2.5	0.026	0.029	.....	Taurus
1248	6.2	0.016	A2s	A1s	0.8	0.008	.....	.....	
1272	6.5	0.019	A4n	A5s	2.0	0.012	.....	.....	
1275	5.7	0.003	A1n	A2s	1.0	0.011	.....	.....	
1281	4.7	0.020	B9s	B0n	0.2	0.012	.....	.....	
1293	5.9	0.015	B0n	B0s	0.2	0.008	.....	.....	
1310	5.7	0.019	B0s	B0s	−0.2	0.007	.....	.....	
1318	5.5	0.031	A0n	B0n	0.7	0.011	.....	.....	
1320	5.9	0.039	B0n	A0n	0.8	0.010	.....	.....	
1366 Ft	7.3	0.005	B0s	B0n	0.2	0.004	.....	.....	

TABLE VI—*Continued*

Boss	m	μ	Spectrum		M	Spect. π	Group π	Trig. π	Auth.
			A.	J.					
1378	5.6	0".016	A7s	Fon	2.6	0".025	.....	.....	
1411	5.5	0.009	A2s	A2s	0.9	0.012	.....	0".017	A
1423	5.7	0.059	A1n	Aon	1.1	0.012	.....	.....	
1424	5.5	0.010	Fos	Fos	2.6	0.026	.....	.....	
1427	6.4	0.007	A2n	A2n	1.7	0.011	.....	.....	
1433	6.0	0.024	A5s	A4s	1.7	0.014	.....	.....	
1453	4.9	0.014	A2s	A2n	1.4	0.020	.....	.....	
1478	2.8	0.047	Aonp	A2np	1.5	0.055	0".025	0.035	Urs. Maj., F, J, M
1482	2.7	0.105	A1s	A1s	0.6	0.037	.....	0.019	A
1568	5.3	0.021	B8n	Bos	0.0	0.009	.....	.....	
1572	5.4	0.017	Bos	Bos	−0.2	0.008	.....	.....	
1575	4.4	0.022	A2s	A4s	1.2	0.024	.....	0.026	M
1588	6.2	0.006	A1n	A1n	1.3	0.010	.....	.....	
1607	5.5	0.021	A7s	A6s	2.2	0.022	.....	.....	
1646	6.8	0.035	A2sp	A6sp	1.7	0.010	.....	.....	
1672	5.8	0.013	A1n	Aos	0.8	0.010	.....	.....	
1673	5.6	0.620	F2s	F3n	2.9	0.028	.....	0.039	G, Y
1690	1.9	0.065	A2s	A2s	0.9	0.063	.....	0.053	F, Ye
1716	5.3	0.015	A1n	Aon	1.1	0.014	.....	.....	
1732	−1.6	1.316	A2s	A2s	0.9	0.316	0.380	0.374	Urs. Maj., F, Gill, Ye
1751	5.7	0.023	Bos	Bos	−0.2	0.007	.....	.....	
1778	4.8	0.112	A4n	A5n	2.2	0.030	.....	0.049	A
1880	5.8	0.011	Bon	Aon	0.8	0.010	.....	.....	
1886	3.6	0.068	A2n	A1n	1.5	0.038	.....	0.038	A
1894	6.3	0.011	Aos	A8s	2.4	0.017	.....	.....	
1897	5.6	0.036	A6n	A6n	2.4	0.024	.....	.....	
1898	3.5	0.025	A3n	A6n	2.2	0.055	.....	0.062	A, M
1903	7.4	0.048	A3n	A8n	2.4	0.010	.....	0.009	A
1905	6.5	0.029	Aon	Aon	0.9	0.008	.....	0.006	A
1930	5.3	0.028	A1n	A3n	1.6	0.018	.....	.....	
1952	4.2	0.236	A5s	A4s	1.7	0.032	.....	0.055	A, Jo, M
1956	5.0	0.067	A1n	A3n	1.6	0.021	.....	.....	
1977	5.1	0.029	Aon	Aon	0.9	0.014	.....	.....	
1979 Br	2.0	0.203	A2s	A3s	1.1	0.066	.....	0.073	A, M, *et al.*
1984	5.8	0.016	Bon	Aon	0.8	0.010	.....	.....	
2045	5.3	0.027	Bon	Aon	0.8	0.012	.....	.....	
2051	5.1	0.017	A7n	A6n	2.6	0.031	.....	.....	
2054	6.2	0.020	A7n	A8n	2.7	0.020	.....	.....	
2078	5.0	0.047	Aon	A1n	1.1	0.016	.....	.....	
2121	6.2	0.017	A1n	A1n	1.3	0.010	.....	.....	
2122	5.9	0.011	Aon	Aon	0.9	0.010	.....	.....	
2178	6.4	0.017	A4s	A4n	2.0	0.012	.....	.....	
2185	5.5	0.005	A3n	A3n	2.0	0.019	.....	.....	
2237	4.0	0.071	Aon	Aon	0.9	0.024	.....	.....	
2240	6.3	0.011	A1n	A2n	1.5	0.011	.....	.....	
2241	6.3	0.011	A2n	A2n	1.7	0.012	.....	.....	
2246	5.4	0.070	A6s	A6s	2.1	0.022	.....	.....	
2287	5.6	0.027	A2s	A6s	1.5	0.016	.....	.....	
2295	4.2	0.074	Bon	Aon	0.8	0.020	.....	.....	
2305	6.7	0.036	A4n	A5n	2.2	0.013	0.011	.....	Praesepe
2309	6.5	0.036	A2s	A2n	1.4	0.010	0.011	.....	Praesepe
2311	6.3	0.036	A6n	A6n	2.4	0.017	0.011	.....	Praesepe
2313	6.7	0.021	A4n	A7n	2.4	0.014	.....	.....	
2314	6.8	0.041	A6s	A6s	2.1	0.012	0.011	.....	Praesepe
2328	5.7	0.011	A5s	A6n	2.2	0.020	.....	.....	
2343	6.0	0.005	A3n	A1n	1.6	0.016	.....	.....	
2353	5.7	0.098	Aon	Aon	0.9	0.011	.....	.....	
2357	5.2	0.046	Bon	Aon	0.8	0.013	.....	.....	
2381	5.7	0.045	A5n	A5s	2.0	0.018	.....	.....	
2400	5.2	0.062	A3s	A5n	1.8	0.022	.....	.....	
2404	3.1	0.502	A4n	A4n	2.2	0.066	.....	0.090	Ab, F, Y
2407	4.3	0.054	A4s	A5s	1.7	0.030	.....	.....	
2417	5.8	0.007	A2n	A2n	1.7	0.015	.....	.....	
2423	5.7	0.004	A2n	Aon	1.3	0.014	.....	.....	
2424	3.7	0.073	Bon	Aon	0.8	0.026	.....	.....	
2429	6.3	0.008	A1n	Aon	1.1	0.009	.....	.....	
2443	4.5	0.134	A8s	Fos	2.6	0.041	.....	.....	
2461	5.9	0.100	A3n	A4n	2.1	0.018	.....	.....	
2465	5.3	0.052	A1s	A2s	0.7	0.012	.....	.....	
2476	4.9	0.086	A1n	Aon	1.1	0.018	.....	.....	

TABLE VI—*Continued*

Boss	m	μ	Spectrum		M	Spect. π	Group π	Trig. π	Auth.
			A.	J.					
2479	3.8	0".338	A1n	A1n	1.3	0".032	.....	0".017	A
2484	5.7	0.022	A1s	A3s	0.9	0.012	.....	.....	
2492	5.5	0.040	B9n	A0s	0.4	0.010	.....	.....	
2494	6.4	0.058	A2n	A5n	2.0	0.013	.....	.....	
2495	4.0	0.137	B9n	B9n	0.6	0.021	.....	0.037	A, M
2540	3.8	0.117	A4n	A6n	2.3	0.050	.....	0.033	A
2565	4.6	0.073	B9n	B9n	0.6	0.016	.....	.....	
2576	6.2	0.042	A1n	A1n	1.3	0.010	(0".011)	.....	Praesepe
2584	5.2	0.020	A5n	A6n	2.4	0.026	.....	.....	
2598	6.1	0.029	A3n	A3n	2.0	0.014	.....	.....	
2632	3.9	0.330	A4n	A7n	2.4	0.050	.....	.....	
2634	6.0	0.049	F1s	F1s	2.8	0.022	(0.011)	.....	Praesepe
2637	5.0	0.009	A1s	A3s	0.9	0.015	.....	.....	
2641	6.0	0.033	A3n	A4n	2.1	0.016	.....	.....	
2642	5.3	0.194	A5n	A7s	2.2	0.024	.....	.....	
2647	5.9	0.204	A1s	A1s	0.6	0.008	.....	0.035	A, Ye
2650	5.8	0.076	A0n	B9n	0.8	0.010	.....	.....	
2692	4.5	0.054	A2n	A3n	1.8	0.028	.....	.....	
2698	1.3	0.247	B6n	B9n	0.4	0.064	.....	0.033	Y
2712	6.1	0.021	A1n	A0n	1.1	0.010	.....	.....	
2724	5.4	0.074	B9n	B9n	0.6	0.010	.....	.....	
2726	5.7	0.090	A3n	A3n	2.0	0.018	0.022	.....	*a* Lyrae
2737	5.8	0.065	A1n	A2n	1.5	0.014	.....	.....	
2744	6.7	0.001	A1n	A0n	1.1	0.008	.....	.....	
2745	5.6	0.130	A2n	A2n	1.7	0.017	.....	.....	
2756	5.8	0.027	A1n	A3n	1.6	0.015	.....	.....	
2768	4.8	0.107	F1s	A8s	2.6	0.036	.....	.....	
2773	5.8	0.102	A1n	A2n	1.5	0.014	.....	.....	
2777	5.9	0.014	A3s	A2s	1.0	0.011	.....	.....	
2787	5.9	0.011	A2s	A1s	0.8	0.009	.....	.....	
2788	5.2	0.052	A0n	A0n	0.9	0.014	.....	.....	
2797	5.5	0.048	B8n	B8n	0.1	0.008	.....	.....	
2798	5.8	0.015	A0n	A0n	0.9	0.010	.....	.....	
2802	4.8	0.141	A4n	A4n	2.2	0.030	.....	0.028	A
2808	5.6	0.040	B9n	A0n	0.8	0.010	.....	.....	
2813	5.2	0.074	A8s	A8s	2.4	0.027	0.043	0.034	Urs. Maj., A
2819	6.3	0.050	F0s	F3s	2.8	0.020	.....	.....	
2839	6.9	0.013	B9n	A0n	0.8	0.006	.....	.....	
2853	5.3	0.289	A0n	F0s	2.6	0.028	.....	0.023	A, Jo
2866	5.4	0.049	B9n	A0n	0.8	0.012	.....	.....	
2887	6.1	0.021	A3n	A3s	1.6	0.012	.....	.....	
2909	4.5	0.077	B9n	A0n	0.8	0.018	.....	.....	
2930	2.4	0.089	A3s	A2s	1.0	0.054	0.046	.....	Urs. Maj.
2940	6.1	0.071	A3n	A2n	1.8	0.014	.....	.....	
2951	6.4	0.004	A3s	A2s	1.0	0.009	.....	.....	
2956	5.6	0.004	A3s	A2n	1.5	0.016	.....	.....	
2972	2.6	0.207	A2n	A2n	1.7	0.066	(0.085)	.....	Urs. Maj.
2974	3.4	0.106	A2s	A2s	0.9	0.032	.....	0.021	A
2987	4.8	0.102	A0n	A1s	0.7	0.016	.....	.....	
2990	4.1	0.095	B9s	B9s	−0.2	0.014	.....	.....	
3023	5.3	0.052	B9n	A0n	0.8	0.012	.....	.....	
3052	6.4	0.035	A1n	A3n	1.6	0.011	.....	.....	
3055	4.8	0.061	B9n	A0n	0.8	0.016	0.015	.....	*a* Lyrae
3063	5.5	0.154	A4n	A3n	2.0	0.020	.....	.....	
3088	5.1	0.068	A1n	A2n	1.5	0.019	.....	.....	
3097	5.2	0.050	A1n	A0s	0.8	0.015	.....	.....	
3101	2.2	0.511	A2n	A2n	1.7	0.079	.....	0.114	F, S, Y
3117	2.5	0.094	A0n	A0n	0.9	0.048	0.041	0.011	Urs. Maj., F, M
3120	6.5	0.009	A1n	A0n	1.1	0.008	.....	.....	
3123	5.5	0.025	A3s	A3s	1.2	0.014	.....	.....	
3143	5.1	0.323	A0s	A0s	2.1	0.025	.....	0.013	A
3150	6.0	0.044	A7s	A7s	2.2	0.017	.....	.....	
3173	6.3	0.013	A1n	A1s	0.9	0.008	.....	.....	
3178	6.8	0.006	F1s	A8s	2.6	0.014	.....	.....	
3183	5.8	0.096	A7s	A8s	2.4	0.020	.....	.....	
3190	3.4	0.110	A0n	A0n	0.9	0.032	0.045	.....	Urs. Maj.
3202	5.9	0.030	A1n	A2n	1.5	0.013	.....	.....	
3206	6.2	0.038	A8s	A8s	2.4	0.017	.....	.....	
3208	6.3	0.067	F0n	A6n	2.6	0.019	.....	.....	
3229	6.0	0.084	A6n	A5n	2.4	0.019	.....	.....	

TABLE VI—*Continued*

Boss	m	μ	Spectrum A.	Spectrum J.	M	Spect. π	Group π	Trig. π	Auth.
3231	5.1	0".033	A3s	A2s	1.0	0".016	.....	.....	
3256	3.1	0.251	B9n	A0n	0.8	0.034	.....	0".026	Ye
3257	5.7	0.060	A1n	A1n	1.3	0.013	.....	.....	
3266	5.4	0.020	A3s	A2s	1.0	0.014	.....	.....	
3276	6.1	0.023	A4s	A3s	1.6	0.012	.....	.....	
3277	5.4	0.084	B9n	B9n	0.6	0.010	.....	.....	
3284	6.7	0.019	A5s	A4s	1.7	0.010	.....	.....	
3290	5.9	0.040	A0n	A1n	1.1	0.011	.....	.....	
3309	4.9	0.135	B9n	B9n	0.6	0.014	.....	.....	
3310	5.5	0.078	B9n	B9n	0.6	0.010	.....	.....	
3323	5.2	0.112	A6n	A4n	2.4	0.027	.....	.....	
3329	6.0	0.054	A0n	A1n	1.1	0.010	.....	.....	
3332	5.8	0.022	A3n	A4n	2.1	0.018	.....	.....	
3334	6.4	0.068	A0n	A0n	0.9	0.008	.....	.....	
3337	5.6	0.051	A0n	B9n	0.7	0.010	.....	.....	
3338	6.2	0.055	A8s	A9n	2.5	0.018	.....	.....	
3339	5.8	0.095	A0n	A0n	0.9	0.010	.....	.....	
3343	5.9	0.101	A0n	A0n	0.9	0.010	.....	.....	
3360	6.3	0.067	A7n	A7n	2.6	0.018	0".019	.....	Urs. Maj.
3363	1.7	0.115	A2s	A2s	0.9	0.069	0.042	.....	Urs. Maj.
3371	2.9	0.237	A1s	A1s	0.6	0.034	.....	0.044	Ye
3382	4.9	0.101	A4n	A5n	2.2	0.030	0.036	0.031	Urs. Maj., A
3392	5.1	0.027	B9n	B9n	0.6	0.012	.....	.....	
3409	4.4	0.057	A2s	A2s	0.9	0.020	.....	0.011	M
3428[1]	6.8	0.039	A1n	A1n	1.3	0.008	.....	.....	
3428[2]	7.2	0.039	A1n	A3n	1.6	0.008	.....	.....	
3462	5.9	0.080	A5s	A5s	1.8	0.015	.....	.....	
3474	2.4	0.130	A2s	A3s	1.1	0.054	0.044	0.049	Urs. Maj., F, M, Pe. Y
3475	4.0	0.136	A8s	A5s	2.0	0.052	0.046	0.022	Urs. Maj., M
3478	5.8	0.014	A3s	A2s	1.0	0.012	.....	.....	
3480	4.0	0.123	A1n	A0n	1.1	0.026	0.042	0.037	Urs. Maj., A, M
3506	4.9	0.052	A3s	A5s	1.5	0.021	0.014	0.028	Urs. Maj., M
3507	6.3	0.067	A1s	A2n	1.2	0.010	.....	.....	
3518	4.9	0.104	A1n	A2n	1.5	0.021	.....	0.052	S
3526	6.3	0.112	A7n	A5n	2.5	0.018	.....	0.015	A, M, S, Ye
3539	5.7	0.060	B9n	A0n	0.8	0.010	.....	.....	
3540	6.4	0.055	A0s	A1s	0.4	0.006	.....	.....	
3546	6.2	0.053	B9n	A0n	0.8	0.008	.....	.....	
3580	6.6	0.033	A2n	A2n	1.7	0.010	.....	.....	
3585	6.0	0.038	A1n	A3n	1.6	0.013	.....	.....	
3612	4.3	0.032	A1n	A0n	1.1	0.023	.....	.....	
3652	6.6	0.065	A9s	F2s	2.6	0.016	.....	0.025	A
3653	5.6	0.044	A0n	B9n	0.7	0.010	.....	.....	
3654	4.6	0.067	A4n	A5n	2.2	0.034	.....	0.025	A
3663	5.8	0.055	A5s	A5n	2.1	0.018	.....	.....	
3666	4.3	0.238	A1n	A0n	1.1	0.023	.....	0.041	A
3669	5.7	0.070	A3s	A3s	1.2	0.013	.....	.....	
3684	6.0	0.030	A0n	A0n	0.9	0.010	.....	.....	
3692 Br	5.1	0.072	B9n	A0n	0.8	0.014	.....	0.017	S, Ye
3692 Ft	7.4	0.072	F9s	F2n	2.8	0.012	.....	0.020	S, Ye
3706	6.2	0.098	A2n	A2n	1.7	0.013	.....	.....	
3719	6.6	0.088	A2n	A2n	1.7	0.010	.....	0.011	A
3722	3.0	0.182	A3n	A3n	2.0	0.062	.....	.....	
3729	4.5	0.228	F0s	F0s	2.6	0.043	.....	.....	
3743	5.5	0.027	A0n	A0n	0.9	0.012	.....	.....	
3752	4.4	0.061	A0n	A0n	0.9	0.020	(0.016)	.....	Urs. Maj.
3756	5.8	0.026	B9n	B9n	0.6	0.009	.....	.....	
3766 Br	5.2	0.238	A5n	A5n	2.3	0.026	.....	.....	
3771 Ft	5.1	0.049	A2n	A2n	1.7	0.021	.....	0.019	A
3787	2.9	0.131	F1n	F1n	2.9	0.100	.....	.....	
3788	5.7	0.024	B9n	B9n	0.6	0.010	.....	.....	
3814	4.6	0.192	A4n	A4n	2.2	0.033	.....	.....	
3820	6.4	0.029	A1n	A1n	1.3	0.010	.....	.....	
3866	4.7	0.061	B9n	B9n	0.6	0.014	.....	.....	
3868	6.0	0.068	A0n	A0n	0.9	0.010	.....	.....	
3875	6.3	0.029	B9s	B9s	−0.2	0.005	.....	.....	
3883	5.3	0.078	A0n	A0n	0.9	0.013	.....	.....	
3885	5.6	0.109	A1n	A3n	1.6	0.016	.....	.....	
3902	6.1	0.029	A5s	A4n	2.0	0.016	.....	.....	
3911	5.5	0.017	A2n	A1n	1.5	0.016	.....	.....	

TABLE VI—*Continued*

Boss	m	μ	Spectrum A.	Spectrum J.	M	Spect. π	Group π	Trig. π	Auth.
3915	5.4	0".051	A0n	B9n	0.7	0".012	.....	.....	
3918	6.1	0.077	A5n	A5n	2.3	0.017	.....	.....	
3940	3.7	0.190	F2s	F2s	2.8	0.066	.....	.....	
3946	6.1	0.016	B9n	B9n	0.6	0.008	.....	.....	
3960 Br.	4.2	0.068	A4n	A7n	2.4	0.044	.....	0".013	A, Ye
3960 Ft.	5.2	0.068	A5n	A6n	2.4	0.026	.....	0.019	A, Ye
3961	2.3	0.158	A0n	A0n	0.9	0.052	0".050	0.059	Urs. Maj., Corona, F, M
3985	5.8	0.162	A7n	A5n	2.5	0.022	.....	.....	
3993	5.3	0.044	A3np	A2s	1.4	0.018	.....	.....	
3998	4.0	0.105	A0n	A1n	1.1	0.026	.....	0.021	A, S, Ye
4007	5.6	0.033	A2s	A0n	1.0	0.012	.....	.....	
4009	3.7	0.091	A1n	A0n	1.1	0.030	0.023	0.035	Urs. Maj., A, M
4016	3.6	0.092	A0s	B9n	0.4	0.022	.....	.....	
4021	5.1	0.070	A1n	A3n	1.6	0.020	.....	.....	
4022	5.8	0.010	A6s	A8s	2.3	0.020	.....	.....	
4026	3.8	0.136	A6s	A4s	1.8	0.042	.....	0.035	A
4028	5.2	0.099	A0n	A0n	0.9	0.014	.....	.....	
4037	5.4	0.046	B7n	B6n	−0.6	0.007	(0.012)	.....	Scorpius
4041	5.9	0.034	B9n	A0n	0.8	0.010	0.009	.....	Scorpius
4070	5.6	0.034	A1s	A1s	0.6	0.010	.....	.....	
4072	5.0	0.193	A5n	A8n	2.5	0.032	.....	.....	
4080	4.9	0.045	A0s	A2n	1.0	0.017	.....	.....	
4097	5.6	0.065	B9n	A0n	0.8	0.010	.....	.....	
4119	4.9	0.027	A3s	A3s	1.2	0.018	.....	.....	
4120	5.5	0.041	A1n	A3n	1.6	0.016	.....	.....	
4122	5.9	0.014	A2s	A3s	1.1	0.010	.....	.....	
4146	5.7	0.028	A2n	A2n	1.7	0.016	.....	.....	
4155	4.8	0.042	A3s	A4s	1.4	0.021	0.011	.....	Scorpius
4163	4.8	0.172	A5n	A7n	2.4	0.034	.....	0.031	A
4165	3.8	0.062	A3n	A0n	1.4	0.035	.....	0.017	A
4176	6.2	0.022	A1n	B9n	0.9	0.008	.....	.....	
4181	5.0	0.261	A6n	A8n	2.6	0.034	.....	0.045	G
4182	4.5	0.079	A2s	A2s	0.9	0.019	.....	.....	
4184	5.5	0.026	A1n	A0n	1.1	0.013	.....	.....	
4203	4.0	0.097	A1n	A1n	1.3	0.029	.....	0.000	A, M, S, Ye
4206	4.6	0.033	A2s	A5s	1.4	0.022	.....	.....	
4210	5.6	0.023	A1s	A1s	0.6	0.010	.....	.....	
4213	5.0	0.042	B9n	A0n	0.8	0.014	.....	.....	
4221	5.8	0.021	A1n	A2n	1.5	0.014	.....	.....	
4229	5.6	0.024	B9s	A0n	0.4	0.009	.....	.....	
4260	6.0	0.003	B9n	A0n	0.8	0.009	.....	.....	
4285	5.6	0.029	A2s	A0n	1.0	0.012	.....	.....	
4291	6.4	0.011	A0n	A1s	0.7	0.008	.....	.....	
4300	5.4	0.098	A5s	A6n	2.2	0.022	.....	.....	
4332	5.3	0.012	A3s	A3s	1.2	0.016	.....	.....	
4338	6.2	0.038	B9n	B9n	0.6	0.009	.....	.....	
4348 Br.	6.3	0.055	A1n	A3n	1.6	0.012	.....	.....	
4353	6.0	0.032	A0n	A2n	1.3	0.012	.....	.....	
4360	3.3	0.093	A3s	A1s	0.9	0.033	.....	.....	
4376	3.2	0.165	A0n	A0n	0.9	0.035	.....	0.028	A, M
4391	4.8	0.066	A0n	A0n	0.9	0.017	.....	.....	
4395	4.4	0.036	A0n	A1n	1.1	0.022	.....	.....	
4402	5.1	0.018	B9n	B9s	0.2	0.011	.....	.....	
4418	5.7	0.044	A4s	A3s	1.4	0.014	.....	.....	
4419	4.5	0.038	B9n	B9s	0.2	0.014	.....	−0.004	A
4420	4.3	0.132	A6s	A7s	2.2	0.038	.....	.....	
4430	5.8	0.015	A1n	A0n	1.1	0.012	.....	0.014	Ye
4442	5.7	0.108	A0n	A3n	1.4	0.014	.....	.....	
4449	6.6	0.015	B9s	A1s	0.2	0.005	.....	.....	
4458	5.0	0.158	A5n	A6s	2.2	0.027	.....	0.019	A, F
4459	2.1	0.262	A0n	B9n	0.7	0.052	0.046	0.062	Corona, F, M, Y, Ye
4461	5.8	0.028	A5s	A8s	2.2	0.019	.....	.....	
4468	5.7	0.023	B9n	A0n	0.8	0.010	.....	.....	
4494	5.7	0.043	B9n	A0n	0.8	0.010	.....	.....	
4511	5.2	0.208	A1n	A0n	1.1	0.016	.....	−0.001	A, Y
4514	6.4	0.009	A1sp	B9s	0.2	0.006	.....	.....	
4521	6.4	0.026	A0n	A2n	1.3	0.010	.....	.....	
4552	4.4	0.026	B9n	A0n	0.8	0.018	.....	.....	
4554	5.5	0.009	A0s	F2s	2.6	0.027	.....	.....	
4557	5.1	0.030	A1n	B9n	0.9	0.014	.....	.....	

TABLE VI—*Continued*

Boss	m	μ	Spectrum A.	Spectrum J.	M	Spect. π	Group π	Trig. π	Auth.
4581	3.7	0".103	A5s	A5s	1.8	0".042	.....	0".037	A
4592	5.2	0.027	A4s	A4s	1.6	0.019	.....	.....	
4640	6.5	0.010	B9n	A0n	0.8	0.008	.....	.....	
4643	5.5	0.057	A4s	A3s	1.4	0.016	.....	.....	
4669	5.7	0.034	A3s	A3s	1.2	0.013	.....	.....	
4685	5.2	0.035	B9n	A0n	0.8	0.013	.....	.....	
4702	5.4	0.007	B9s	B9s	−0.2	0.008	.....	.....	
4713	5.4	0.146	A5n	A8n	2.5	0.026	.....	0.024	A
4719	5.8	0.026	A2s	A2s	0.9	0.010	.....	.....	
4722	0.1	0.346	A1s	A1s	0.6	0.123	0".104	0.110	α Lyrae, F, J, Y, Ye
4748	6.0	0.057	A3n	A6n	2.2	0.018	.....	0.000	Ye
4751 Br	5.7	0.031	A3s	A6s	1.6	0.016	.....	.....	
4752	4.3	0.031	A5s	A8s	2.2	0.037	.....	0.026	A
4754	5.9	0.022	A1n	A2n	1.5	0.013	.....	0.030	A
4761	4.4	0.123	A2n	A5n	2.0	0.034	.....	0.056	A
4777 Ft	7.8	0.020	B8n	B8n	0.1	0.003	.....	(−0.006)	Ye
4779	5.3	0.019	A0s	A1s	0.4	0.010	.....	.....	
4820	5.7	0.120	F2s	F2s	2.8	0.026	.....	0.040	A, S
4821	5.8	0.002	B8n	B8n	0.1	0.007	.....	.....	
4824	3.3	0.008	B9sp	B9s	−0.2	0.020	.....	0.012	M
4846	5.1	0.091	A2n	A4n	2.0	0.024	.....	.....	
4856	5.9	0.016	B9n	A0n	0.8	0.010	.....	.....	
4858	3.0	0.102	B9n	A0n	0.8	0.036	.....	0.037	A, M
4866	5.7	0.056	A3s	A7s	1.8	0.016	.....	.....	
4867	5.5	0.098	A2n	A5n	2.0	0.020	.....	.....	
4899	5.6	0.044	A1n	A0n	1.1	0.012	.....	.....	
4914	5.1	0.011	A3n	A3s	1.6	0.020	.....	0.011	A
4928	5.5	0.002	B9s	A0n	0.4	0.010	.....	.....	
4932	4.0	0.031	A4n	A7s	2.2	0.044	.....	0.049	M
4947	6.0	0.019	A3s	A6s	1.6	0.014	.....	.....	
4953	3.4	0.265	A3n	A6n	2.2	0.058	.....	0.057	A, M
4965	5.6	0.040	B9n	B9n	0.6	0.010	.....	.....	
4974	5.8	0.037	A0n	A0n	0.9	0.010	.....	.....	
4979	6.0	0.017	A0n	A0n	0.9	0.010	.....	.....	
4980	5.7	0.041	A0s	A0s	0.2	0.008	.....	.....	
4988	3.9	0.126	A1n	A0n	1.1	0.028	.....	0.018	A, Ab
4998	4.9	0.004	B9n	B8n	0.3	0.012	.....	.....	
5007	5.9	0.006	B9np	A0n	0.8	0.009	.....	.....	
5024	5.4	0.032	A0s	A0s	0.2	0.009	.....	.....	
5042	6.1	0.017	A0s	B9s	0.0	0.006	.....	.....	
5048	3.0	0.065	A1n	A0n	1.1	0.042	.....	0.055	S
5062	0.9	0.655	A2n	A2n	1.7	0.145	.....	0.205	M, Y, Ye, *et al.*
5092	5.5	0.024	B9n	A2n	1.2	0.014	.....	.....	
5105	4.8	0.051	B9n	A0n	0.8	0.016	.....	.....	
5117	6.3	0.005	A1n	A0n	1.1	0.009	.....	.....	
5130	6.0	0.020	B9s	B9n	0.2	0.007	.....	.....	
5134	5.3	0.099	A6n	A6n	2.4	0.026	.....	.....	
5160	6.2	0.038	A0sp	A1n	0.8	0.008	.....	.....	
5171	3.4	0.032	B9s	B9s	−0.2	0.019	.....	.....	
5173	5.5	0.007	A1np	A0n	1.1	0.013	.....	.....	
5186	5.0	0.017	A0n	A0n	0.9	0.015	.....	0.010	A, M
5188	5.0	0.094	A2n	A1n	1.5	0.020	.....	.....	
5211	5.5	0.046	A1n	A1n	1.3	0.014	.....	.....	
5220	6.1	0.022	A0n	A0n	0.9	0.009	.....	.....	
5224	5.4	0.018	B7n	B8n	−0.1	0.008	.....	.....	
5233	6.1	0.008	A0n	A0n	0.9	0.009	.....	.....	
5236	5.7	0.004	B7n	B8n	−0.1	0.007	.....	.....	
5244	5.0	0.026	A4n	A8n	2.4	0.031	.....	0.024	M
5249	5.4	0.073	A1n	A0n	1.1	0.014	.....	.....	
5269	6.5	0.005	A1n	A0n	1.1	0.008	.....	.....	
5282	4.7	0.038	A1n	A4n	1.8	0.026	.....	.....	
5292	5.4	0.048	A2s	A2s	0.9	0.013	.....	.....	
5295	6.2	0.009	A0n	A0n	0.9	0.009	.....	.....	
5296	6.4	0.069	A3n	A5n	2.2	0.014	.....	.....	
5301	4.8	0.058	B9s	A1n	0.6	0.015	.....	.....	
5322	5.6	0.017	B8s	B9s	−0.4	0.006	.....	.....	
5337	3.8	0.044	A1n	A3n	1.6	0.037	.....	0.023	M
5366	5.5	0.011	B9s	B9s	−0.2	0.007	.....	.....	
5371	4.8	0.051	A7n	F0s	2.7	0.038	.....	0.010	M
5393	4.9	0.025	B9n	B9n	0.6	0.014	.....	0.000	A

TABLE VI—*Continued*

Boss	m	μ	Spectrum A.	Spectrum J.	M	Spect. π	Group π	Trig. π	Auth.
5417	4.9	0".060	A4s	A5s	1.7	0".023	.....	.....	
5425	6.3	0.051	A8s	A8n	2.6	0.018	0".013	.....	Urs. Maj.
5443	4.8	0.169	A7s	A0s	2.4	0.034	.....	0".044	M
5465	5.4	0.015	B9s	B9s	−0.2	0.008	.....	.....	
5480	2.6	0.160	A2n	A0n	1.3	0.056	.....	0.084	A, F, M
5491	5.1	0.054	A1s	A4s	1.0	0.016	.....	.....	
5498	5.7	0.124	A3n	A6n	2.2	0.020	.....	.....	
5511	5.5	0.206	A4n	A4n	2.2	0.022	0.052	0.037	α Lyrae, A, Jo
5525	5.4	0.018	B9n	B8n	0.3	0.010	.....	.....	
5532 Ft	8.0	0.012	A2n	A2n	1.7	0.005	.....	(−0.011)	Ye
5548	6.0	0.008	B9n	A0n	0.8	0.009	.....	.....	
5550	6.3	0.026	A0n	A0n	0.9	0.008	.....	.....	
5555	5.3	0.100	A3n	A0n	1.4	0.018	.....	.....	
5558	5.8	0.117	A2n	A5n	2.0	0.018	.....	.....	
5573	6.0	0.052	A0n	A0n	0.9	0.010	0.013	0.010	Urs. Maj., M
5581	5.9	0.030	A2n	A4n	2.0	0.016	.....	.....	
5585	5.6	0.038	B9n	A2n	1.2	0.014	.....	.....	
5591	6.9	0.061	A5n	A8n	2.5	0.013	.....	.....	
5600	3.0	0.392	A3n	A5n	2.2	0.068	.....	0.115	M
5626	6.5	0.001	B9n	A0s	0.4	0.006	.....	.....	
5639	6.0	0.009	B8s	B8n	−0.4	0.006	.....	.....	
5641	5.6	0.036	A0n	A0n	0.9	0.011	.....	.....	
5664	5.7	0.004	B7s	B6s	−1.2	0.004	.....	.....	
5667	5.5	0.007	B8n	B9n	0.4	0.010	.....	.....	
5669	5.6	0.039	B9n	A1n	1.0	0.012	.....	.....	
5709	4.4	0.026	A4n	F2n	2.6	0.043	.....	0.005	A, M
5738	6.2	0.028	B8n	B9n	0.4	0.006	.....	.....	
5742	4.2	0.452	A6n	A6n	2.4	0.045	0.108	0.055	α Lyrae, A, M, S, Y, Ye
5780	6.2	0.004	A1n	A0n	1.1	0.009	.....	.....	
5803	4.9	0.030	A1s	B9s	0.2	0.012	.....	.....	
5818	5.5	0.014	A1n	A2n	1.5	0.016	.....	.....	
5847	6.1	0.019	A2s	A1s	0.8	0.009	.....	.....	
5848	5.2	0.019	A0n	A2n	1.3	0.017	.....	.....	
5858	4.8	0.036	A2s	A3s	1.1	0.018	.....	.....	
5879	5.7	0.037	A1n	A0s	0.8	0.010	.....	.....	
5904	3.5	0.052	A1n	A1n	1.3	0.036	.....	.....	
5967	5.3	0.024	B9n	B9n	0.6	0.011	.....	.....	
5969	5.6	0.015	A4s	A3s	1.6	0.015	.....	.....	
5973	5.2	0.017	A1n	A0n	1.1	0.016	.....	.....	
5996	5.9	0.012	A6s	A8s	2.3	0.019	.....	.....	
6011	6.2	0.017	A2s	A1s	0.8	0.008	.....	.....	
6020	6.5	0.233	A0n	F0s	2.8	0.018	.....	0.016	W
6023	5.5	0.005	A2n	B9s	0.8	0.012	.....	.....	
6031	4.9	0.124	A3s	A3s	1.2	0.018	.....	0.043	A
6063	5.5	0.042	A1n	B9n	0.9	0.012	.....	.....	
6075	5.3	0.016	B9n	B9n	0.6	0.011	.....	.....	
6113	5.8	0.027	A3n	A4s	1.8	0.016	.....	.....	
6128	5.4	0.033	A1n	A3n	1.6	0.018	.....	.....	
6133	6.2	0.013	A2s	A1s	0.8	0.008	.....	.....	
6139	6.1	0.014	A1s	A0s	0.4	0.008	.....	.....	
6166	5.7	0.007	A5s	A8s	2.2	0.016	.....	.....	
6168	6.1	0.013	B9s	B9s	−0.2	0.005	.....	.....	
6174	6.3	0.004	A4s	A3n	1.8	0.012	.....	.....	
6180	6.0	0.008	A2s	A1s	0.8	0.009	.....	.....	

results are given in Table VII and a curve drawn from them is shown in Figure 2.

Two results are given for the last group according as Boss 1732 (Sirius) is included or not. For statistical purposes it is, no doubt, better to omit it.

These values show an excellent degree of correlation between proper motion and parallax. The influence of occasional stars

of small proper motion and large parallax, or large proper motion and small parallax, is not serious, because of the considerable number

TABLE VII

Limits of μ	No.	Av. μ	Av. π
$<0''.010$	49	$0''.006$	$0''.011$
$0''.010$ to $0''.019$	83	0.015	0.012
0.020 to 0.029	72	0.025	0.014
0.030 to 0.039	56	0.035	0.014
0.040 to 0.049	39	0.044	0.016
0.050 to 0.069	74	0.059	0.019
0.070 to 0.099	55	0.084	0.020
0.100 to 0.149	68	0.118	0.029
0.150 to 0.250	30	0.196	0.037
$>0''.250$	18	0.430	0.071
	17	0.378	0.057

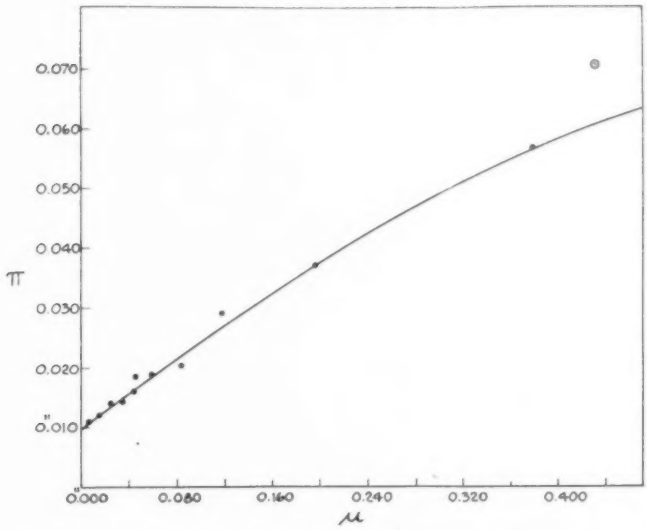

FIG. 2.—This curve shows the relationship between the average value of the proper motion and the average value of the spectroscopic parallax for the 544 stars of Table VI. The stars have been grouped according to the limits of proper motion given in Table VII. The point surrounded by a circle represents the value for the group of largest proper motion when Sirius is included; the neighboring point on the curve represents the same group when Sirius is omitted.

of stars in each group, the only important exception being that of Sirius. It is of interest to note that the curve would give an average parallax of $0''.009$ for stars of zero proper motion, a result almost

identical with that found by Strömberg[1] for stars of the later types of spectrum. Reference may also be made to the fact that the eighth group of stars, with proper motions between 0".100 and 0".149, while it includes most of the members of the Taurus moving cluster, also includes a large number of other stars. The parallax of 0".029 is in good agreement with that of Rasmuson for the Taurus cluster, thus indicating that the latter stars do not differ materially in distance from other A stars having the same amount of proper motion.

We have referred previously to α Cygni (Boss 5320) and some other stars with similar spectral characteristics. Most of these are listed as "c" stars by Miss Cannon and have sharp narrow lines with the enhanced lines remarkably strong and prominent.

TABLE VIII

Boss	Spectrum	μ	b
478	A2s	0".009	−3°
533	A1s	0.011	−3
534	A2s	0.005	−5
724	A2s	0.004	0
1268	A4s	0.016	−1
4503	A4s	0.015	−7
5320	A2s	0.001	+1
6111	A2s	0.010	0

Those at λλ 4233 and 4481 are especially striking, and it seems probable from a brief examination already made that these lines vary definitely with absolute magnitude. At present, however, we have no results based upon trigonometric measures or other data from which to determine absolute magnitudes which may serve as standards of reduction for the spectroscopic intensities. There can be little question that α Cygni is extremely bright, its absolute magnitude probably being of the order of −4 or −5. In spectral characteristics, great luminosity, small proper motion, and low galactic latitude these stars are associated with the Cepheid variables and stars of similar spectra and appear to form a continuation of the Cepheid chain of giant stars. Table VIII gives the stars

[1] *Mt. Wilson Contr.*, No. 170.

of this type which we have found in our list. The galactic latitude is indicated by b.

The A-type companion of o^2 Eridani and probably the companion of Sirius appear to be cases of the rare phenomenon of A-type stars of very low luminosity. Three other stars of which we have spectrograms are much fainter than the vast majority of those of the A type. These are:

	m	Spectrum	μ	Trig. π	M
Lal. 5761	8.0	A2s	0".90	0".039	6.0
Lal. 28607	7.3	A2s	1.17	0.033	4.9
W. B. 23^h175	8.4	A2s	1.31	0.028	5.6

The last star is a double and the value of M refers to the combined magnitude.

The spectra of these stars are peculiar. The hydrogen lines are narrow and sharp, the metallic lines are very faint, and λ 4481 and λ 4233 are hardly visible. These latter lines, accordingly, show a behavior just the reverse of that in "c" stars like α Cygni. It is of interest to note that λ 4481 and λ 4233 are also very faint in the spectrum of the companion of o^2 Eridani.

Forty-five of the stars which appear in Table VI have been included in the list of 1646 stars[1] of the later spectral types for which absolute magnitudes derived by the spectroscopic method have been published. The latter values were obtained by an extrapolation of the reduction-curves for stars of the F type and have always been considered by us as subject to considerable uncertainty. A comparison of the results given in Table VI with those in the list of 1646 stars shows a mean difference of $0^M.5$, the absolute magnitudes in Table VI being the fainter. The difference is systematic although much of it is due to a small number of stars. We consider the parallaxes given in Table VI as superior to the earlier values and hope by means of these results to form a connection between the two systems which will render them consistent with one another.

[1] *Mt. Wilson Contr.*, No. 199; *Astrophysical Journal*, **53**, 13, 1921.

In conclusion, we may call attention to the agreement of the results of this investigation with those obtained by Lindblad[1] through a spectrophotometric study of the intensity of the continuous spectrum. Lindblad found that the region λ 3889–λ 3907, when compared with the adjacent region λ 3907–λ 3935, was relatively less intense in the spectrum of the intrinsically fainter stars. This effect he ascribed to the expansion of the wings of Hζ in such stars, as well as to the widening of certain of the arc lines of iron and silicon. In other words, the spectra of such stars are diffuse, and we obtain the same differentiation between the absolute magnitudes of stars with sharp and diffuse lines that has been found by other methods in the course of this investigation.

It is hardly necessary to state that the methods described in this communication can no doubt be greatly improved and refined. They appear capable, however, of yielding results of considerable value for the stars belonging to the largest of the spectral types. In addition, it seems probable that similar methods may be applied to the stars of the B type. It is well known from the work of several investigators that the stars of types B8 and B9 are considerably fainter intrinsically than those of the earlier divisions like Bo and B1. There is a strong probability, therefore, that a relationship between spectral type and absolute magnitude similar to that found for the A stars exists among those of type B.

SUMMARY

The principal results of this study may be summarized briefly.

1. A considerable number of A-type stars belonging to the Taurus and Ursa Major groups have been classified as accurately as possible into the subdivisions of this type and the spectra designated as nebulous or sharp according to the character of the lines.

2. From a comparison of the results a definite relationship between absolute magnitude and spectral type, as well as between absolute magnitude and the sharp or diffuse character of the lines, has been established.

[1] *Mt. Wilson Contr.*, No. 228; *Astrophysical Journal*, **55**, 85, 1922.

3. Through an extension to stars with parallaxes determined by trigonometric methods, it is found that the same relationships are valid for stars outside of the moving clusters.

4. When this method for the determination of absolute magnitudes is applied to individual stars, a degree of accuracy is found quite comparable with that for stars of the later spectral types.

5. A catalogue of the parallaxes of 544 stars derived in this way is given.

6. A comparison between the average of the proper motions and the average of the parallaxes of these stars shows a satisfactory degree of correlation between the two.

7. The stars such as α Cygni having the so-called "c" characteristics require separate treatment. It seems probable that the intensities of the well-known enhanced lines λ 4481 and λ 4233 may be used as criteria for the determination of the absolute magnitudes of such stars. The same lines may perhaps be used for intrinsically faint A-type stars, in which these lines are very weak.

MOUNT WILSON OBSERVATORY
May 1922

THE DISTRIBUTION OF THE VELOCITIES OF STARS OF SPECTRAL TYPES F TO M[1]

By GUSTAF STRÖMBERG

ABSTRACT

Frequency-distribution of the velocity-vectors of stars of types F to M.—The three components of the velocities of about 1300 stars were computed from available data and referred to the galactic system of co-ordinates, assuming a solar motion of 20 km toward the apex $\alpha = 270°$, $\delta = +30°$. The frequency-distribution of the velocity-vectors in each of six groups, including, respectively, types A6–F9, F0–G5, G6–K1, K2–K9, Ma–Md, G0–M, and magnitudes 0–6, <3, <4, <4, <3, >3, was represented by a three-dimensional cosine-series with a large number of terms determined by harmonic analysis. From these results curves of equal frequency were drawn in the *xy*- and *yz*-planes (Figs. 1–6). It is evident from these that *giant stars* of types F2M form a single group or stream with an approximately ellipsoidal distribution, the shortest axis being nearly in the direction of the galactic pole. The elongation of the ellipsoid is greatest for the bright F stars and least for the late K and M stars, for which the distribution is nearly spherical. Among stars of spectral type F and magnitude 0 to 6 an additional stream was found moving nearly parallel with the Taurus group and including about one-fifth of the stars of this type. There is a marked asymmetry in the distribution of velocities, especially for the higher velocities. As a result, the most frequent velocity coincides neither with the mean velocity nor with the center of the velocity-ellipsoid, but has the values given in Table VII, being 13.4 km in the direction $\alpha = 86°.2$, $\delta = -30°.8$ (relative to the sun) for the giant stars. Another consequence of the asymmetry is that the constants of the ellipsoidal frequency-function depend somewhat on the method of computation on account of the difference in weighting the high velocities. The results of two methods are given (Tables IV, V, and VI). The *dwarf stars* also form a single group and show an ellipsoidal distribution of velocities, the most frequent velocity being 37.7 km in the direction $\alpha = 98°.8$, $\delta = -17°.4$ (relative to the sun).

Solar motion derived from the algebraic means of velocities of stars of types F to M is found to be dependent on the spectral types and absolute magnitudes of the group of stars used. Giant stars of later types give a somewhat higher declination of the apex (+44°) than stars of earlier types (+27°), while dwarf stars give +30°. The velocity from giants comes out 18.8 km while dwarfs give 31.7 km; in fact, stars of high velocity give, in general, a higher solar motion than slower stars, which indicates that the high-velocity stars have a systematic motion in a direction opposite to the sun's motion.

The large number of spectroscopic parallaxes recently determined by Mr. Adams and his collaborators[2] has made it possible to compute the absolute motions in space of about 1300 stars for which the proper motions and radial velocities are determined. The fact that the errors of the spectroscopic parallaxes are proportional to the parallaxes themselves makes them in general better adapted

[1] *Contributions from the Mount Wilson Observatory*, No. 245.

[2] *Ibid.*, No. 199; *Astrophysical Journal*, **53**, 13, 1921.

to this purpose than the trigonometric parallaxes. A large number of radial velocities have been determined at the Mount Wilson Observatory during recent years, and I am greatly indebted to my colleagues engaged in this work for permission to use these, as well as the spectroscopic parallaxes, in advance of publication.

The result of a study of the space-velocities, irrespective of their directions, was published in *Mount Wilson Contribution* No. 210; *Astrophysical Journal*, **54**, 9, 1921. Since it is well known that the frequency of velocity-vectors of a given size is quite different in different directions, a detailed study has been made of the general distribution of the three-dimensional velocities. In order to obtain the general character of this distribution, the possible dependency of the velocity-distribution upon position in space was neglected. The known dependency of velocity upon absolute magnitude and spectral type has been taken into account to some extent by grouping the stars according to spectral type and for each type dividing them into two groups of different absolute magnitudes.

COMPUTATION OF THE VELOCITY-COMPONENTS

The three co-ordinates of a star relative to the sun and referred to the equatorial system are

$$\Xi = D \cos\alpha \cos\delta\,; \quad \mathrm{H} = D \sin\alpha \cos\delta\,; \quad \mathrm{Z} = D \sin\delta\,,$$

where α and δ are the right ascension and declination of the star and D its distance from the sun in kilometers. Differentiating these equations with respect to the time, we obtain the three velocity-components in the equatorial system relative to the sun:

$$\left.\begin{aligned} \xi &= \frac{d\Xi}{dt} = V\cos\alpha\cos\delta - \frac{k}{\pi}(\mu_\alpha \sin\alpha\cos\delta + \mu_\delta \cos\alpha\sin\delta) \\ \eta &= \frac{d\mathrm{H}}{dt} = V\sin\alpha\cos\delta + \frac{k}{\pi}(\mu_\alpha \cos\alpha\cos\delta - \mu_\delta \sin\alpha\sin\delta) \\ \zeta &= \frac{d\mathrm{Z}}{dt} = V\sin\delta + \frac{k}{\pi}\mu_\delta\cos\delta \end{aligned}\right\} \qquad (1)$$

where V is the radial velocity relative to the sun, μ_α and μ_δ are the proper motions in right ascension and declination expressed in

seconds of arc per year, π is the parallax, and k is the mean distance earth–sun in kilometers divided by the number of seconds in a year. We have thus $k = 4.737$ km year/sec.

The proper motions have been taken from Boss's *Catalogue* and corrected according to the formula:[1]

$$\Delta\mu_\alpha^s = +0^s.00021 - 0^s.00015 \sin\alpha \tan\delta$$
$$\Delta\mu_\delta'' = -0''.0023 \cos\alpha$$

For stars not in the Boss *Catalogue* the proper motions have in most cases been taken from the *Publications of the Cincinnati Observatory*, No. 18, Part IV, and in some cases, proper motions determined at Greenwich, and by Kapteyn, Roy, and others have been used. The radial velocities are from the lists published by the Lick, Mount Wilson, Yerkes, Cape, and other observatories, and in addition to these, use has been made of a large number of unpublished radial velocities determined at the Mount Wilson Observatory. The spectroscopic parallaxes have been used except in a few cases where the trigonometric parallaxes are large and well determined.

From this list of stars of known parallax, proper motion, and radial velocity, the following stars have been omitted: (1) the fainter components of binaries, the absolute magnitude used being that of the brighter component; (2) stars selected for observation on account of small proper motion, ninety-nine such stars being omitted; (3) spectroscopic binaries with large variation of the radial velocity for which the orbits are not determined. Many of the stars were of course selected for observation originally on account of large proper motion, but as this selection is mainly a selection of near and thus absolutely faint stars which have been treated separately, no omission is made for this reason. The inclusion of a large number of stars of large proper motion produces, however, an excess of stars of high speed among the giant stars.

SOLAR MOTION

If we form the means of the three velocity-components ξ, η, and ζ for a group of stars, we obtain the velocity of the "centroid" of

[1] *Op. cit.*, p. xxviii.

this group of stars relative to the sun. The opposite vector is the velocity of the sun relative to this centroid. The polar coordinates of this vector are given by the equations:

$$\left.\begin{aligned} V_0 \cos A_0 \cos D_0 &= -\bar{\xi} \\ V_0 \sin A_0 \cos D_0 &= -\bar{\eta} \\ V_0 \sin D_0 &= -\bar{\zeta} \end{aligned}\right\} \qquad (2)$$

where A_0 and D_0 are the right ascension and declination of the sun's apex and V_0 is the solar velocity. Table I gives the results of this computation for different spectral types and absolute magnitudes. In this case all stars with a space-velocity higher than 100 km have been omitted.

TABLE I

Spectral Type	Absolute Magnitude	Number	A_0	D_0	V_0
A6 to F9	≤ 3.0	153	269°	+27°	21.2
	≥ 3.1	133	274	+35	23.4
G0 to G9	≤ 3.0	224	266	+32	19.9
	≥ 3.1	154	279	+23	40.2
K0 to K9	≤ 4.0	325	282	+43	18.3
	≥ 4.1	112	286	+31	33.1
M	< 4.0	98	271	+44	16.2
	> 6.0	16	354:	+68:	26.6:
A6 to M	Giants	800	272.7	+36.9	18.8
A6 to M	Dwarfs	415	280.8	+29.5	31.7

From Table I we see that for the giant stars the declination of the sun's apex shows a steady increase from +27° to +44°, which is in agreement with the results of several investigators who have determined its value from proper motions. This increase of the declination of the sun's apex with advancing spectral type was found by Dyson and Thackeray[1] to be especially pronounced among the faint stars in the zone +24° to +32°, and was attributed by them to an increase in the proportion of stars belonging to the second stream among stars of later types. That this explanation

[1] *Monthly Notices of the Royal Astronomical Society*, **79**, 201, 1919.

is in agreement with the results obtained in the present investigation will be seen later.

Another conclusion to be drawn from Table I is that the dwarf stars apparently show a higher velocity for the sun than the giant stars. This result seems to explain the peculiar fact that the velocity of the sun as determined from the Mount Wilson radial velocities is somewhat larger than the original values of Campbell. The proportion of faint stars of large proper motion measured for radial velocity, most of which are dwarf stars, is fairly large among the stars observed at the Mount Wilson Observatory.

This increase in the velocity of the sun is especially marked if we group the stars according to space-velocity. This velocity, v, corrected for a standard solar motion of 20 km toward the point $\alpha = 270^\circ$, $\delta = +30^\circ$, has been computed for each star according to the formula

$$v^2 = \xi^2 + (\eta - 17.3)^2 + (\zeta + 10.0)^2.$$

Grouping the stars according to this space-velocity, v, and computing the solar motion for each group, we find a very great increase of the sun's motion with increasing space-velocity of the stars (Table II). This indicates that the stars of high velocity have a systematic motion opposite to the sun's motion, a result which was found by Adams and Joy[1] from a study of the space motion of thirty-seven stars of large radial velocity.

TABLE II

v	No.	$A_\odot$	$D_\odot$	$V_\odot$
km				km
0 to 60	1026	272°.1	+29°.5	20.6
60 to 100	210	295.4	+43.4	36.3
100 to 150	50	288.9	+38.6	75.7
>150	37	313.1	+53.8	209.1

DISTRIBUTION OF VELOCITIES

The solar motion is only one of a large number of characteristics which determine the general distribution of the velocities. To

[1] *Mt. Wilson Contr.*, No. 163; *Astrophysical Journal*, **49**, 179, 1919.

describe this distribution we may think of a certain number of stars starting at the same moment from a common origin with velocities equal and parallel to their velocities in space. After one second they will have spread out into a cluster, the mean density of which at a certain point is proportional to the probability that a star of this group has the velocity corresponding to the point in question. In studying this distribution two different types of frequency-functions have been used, viz., those based upon the two-drift theory of Kapteyn and the ellipsoidal theory of Schwarzschild. In order to make an inductive study of the distribution of the velocity-vectors without restricting ourselves to a special frequency-function, a more general type of function has to be used. One such function has been introduced by Charlier[1] for a "unitary statistical population" with three variables. The practical application of this function, however, requires the use of moments of high order, and this necessarily gives the stars of high velocity a much higher weight in the determination of the constants of the function than stars of low velocity. In the present case we are dealing with fairly small groups of stars and, on account of the selection of stars of large proper motion, too great a proportion of stars of high speed has probably been included. Hence it is especially important, at least when dealing with linear velocities, to use a function, the constants of which can be determined *directly* from the *numbers* of stars whose velocity-vectors lie between certain limits. To obtain the general character of the distribution of the velocities, we need, therefore, a general interpolation formula in three dimensions which can easily be integrated and whose constants can be determined simply from the integrated function. For this purpose use has been made of a three-dimensional cosine-series with the origin in the center of the limiting planes. Such a series can be written

$$\left.\begin{aligned} F(xyz) = a_0 &+ a_{100}\sin\alpha + a_{010}\sin\beta + a_{001}\sin\gamma + a_{200}\cos 2\alpha + a_{110}\sin\alpha\sin\beta \\ &+ a_{101}\sin\alpha\sin\gamma + a_{020}\cos 2\beta + a_{011}\sin\beta\sin\gamma + a_{002}\cos 2\gamma \\ &+ a_{300}\sin 3\alpha + a_{210}\cos 2\alpha\sin\beta + a_{201}\cos 2\alpha\sin\gamma + a_{120}\sin\alpha\cos 2\beta \\ &+ a_{111}\sin\alpha\sin\beta\sin\gamma + \ldots\ldots \end{aligned}\right\} \quad (3)$$

[1] *Meddelanden från Lunds Observatorium*, Serie II, No. 9, p. 79, 1913.

where

$$\alpha=\frac{x\pi}{2c_1}, \qquad \beta=\frac{y\pi}{2c_2}, \qquad \gamma=\frac{z\pi}{2c_3}.$$

The six limiting planes are $x=\pm c_1$, $y=\pm c_2$, $z=\pm c_3$. The three angles α, β, and γ vary between the limits $-\pi/2$ and $+\pi/2$. The only assumptions made in using this frequency-function are that the number of velocity-vectors terminating in a cube $dx\,dy\,dz$ varies continuously with x, y, and z, and that

$$\frac{dF}{dx}=0, \quad \frac{dF}{dy}=0, \quad \text{and} \quad \frac{dF}{dz}=0 \quad \text{for} \quad x=\pm c_1, \quad y=\pm c_2, \quad z=\pm c_3,$$

respectively.

The disadvantages of this function are that we must use a very large number of terms, and even then it may not be possible to represent the more rapid changes of the mean density of the velocity-cluster. The function is characterized by a large number of coefficients, and it is necessary to plot it graphically in order to gain an idea of its general character. It is, however, a convenient means for obtaining some information about the *actual* distribution of velocities, from which we can afterward decide what type of theoretical frequency-function can best be adopted.

The number of velocity-vectors of a group of stars terminating in a cube $dx\,dy\,dz$ is expressed by

$$F(xyz)\,dx\,dy\,dz\,.$$

Integrating this function between the limits x_1, x_2; y_1, y_2; z_1, z_2, we find

$$\left.\begin{aligned}\int_{x_1}^{x_2}\int_{y_1}^{y_2}\int_{z_1}^{z_2} F(xyz)\,dx\,dy\,dz = A(A_0 &+A_{100}\sin\bar{\alpha}+A_{010}\sin\bar{\beta}+A_{001}\sin\bar{\gamma}\\ &+A_{200}\cos 2\bar{\alpha}+A_{110}\sin\bar{\alpha}\sin\bar{\beta}+A_{101}\sin\bar{\alpha}\sin\bar{\gamma}\\ &+A_{020}\cos 2\bar{\beta}+A_{011}\sin\bar{\beta}\sin\bar{\gamma}+A_{002}\cos 2\bar{\gamma}+A_{300}\sin 3\bar{\alpha}\\ &+A_{210}\cos 2\bar{\alpha}\sin\bar{\beta}+\ldots.)\end{aligned}\right\}(4)$$

where

$$A=(x_2-x_1)(y_2-y_1)(z_2-z_1).$$

$$\bar{\alpha}=\tfrac{1}{2}(\alpha_1+\alpha_2)=\frac{\pi}{4c_1}(x_1+x_2)$$

$$\bar{\beta}=\tfrac{1}{2}(\beta_1+\beta_2)=\frac{\pi}{4c_2}(y_1+y_2)$$

$$\bar{\gamma}=\tfrac{1}{2}(\gamma_1+\gamma_2)=\frac{\pi}{4c_3}(z_1+z_2)$$

$$A_{lmn}=k_l k_m k_n a_{lmn}$$

$$k_l=\frac{\sin\dfrac{l\Delta\alpha}{2}}{\dfrac{l\Delta\alpha}{2}}\;;\quad \Delta\alpha=\alpha_2-\alpha_1=\frac{\pi}{2c_1}(x_2-x_1)$$

$$k_m=\frac{\sin\dfrac{m\Delta\beta}{2}}{\dfrac{m\Delta\beta}{2}}\;;\quad \Delta\beta=\beta_2-\beta_1=\frac{\pi}{2c_2}(y_2-y_1)$$

$$k_n=\frac{\sin\dfrac{n\Delta\gamma}{2}}{\dfrac{n\Delta\gamma}{2}}\;;\quad \Delta\gamma=\gamma_2-\gamma_1=\frac{\pi}{2c_3}(z_2-z_1)\,.$$

As the unit of volume, we have for convenience used 1000 km^3; thus we have to replace the A just given by

$$0.001(x_2-x_1)(y_2-y_1)(z_2-z_1).$$

Starting with a group of N stars of a certain range in spectral type and absolute magnitude, we can compute how many rectilinear velocity-components fall inside a parallelopiped inclosed by the planes $x=x_1$; $x=x_2$; $y=y_1$; $y=y_2$; $z=z_1$; $z=z_2$. If N is the total number of stars in the group and n is the number of velocity-vectors terminating inside this parallelopiped, we have equations of condition of the form

$$N\int_{x_1}^{x_2}\int_{y_1}^{y_2}\int_{z_1}^{z_2}F(xyz)\,dx\,dy\,dz=NA(A_0+A_{100}\sin\bar{\alpha}+A_{010}\sin\bar{\beta}+\ldots.)=n. \quad (5)$$

The computation of the constants of the series is very much facilitated by dividing the distances $-c_1$ to $+c_1$, $-c_2$ to $+c_2$, $-c_3$ to $+c_3$ into p_1, p_2, and p_3 equal parts, respectively, the p's being even numbers.

The solution of the equations of condition (5) is then simplified by the relationships

$$\left.\begin{aligned} \Sigma \sin^2 \bar{\alpha} = \Sigma \cos^2 2\bar{\alpha} = \Sigma \sin^2 3\bar{\alpha} = \Sigma \cos^2 4\bar{\alpha}, \text{ etc.} = \frac{p_1}{2} \\ \Sigma \sin^2 \bar{\beta} = \Sigma \cos^2 2\bar{\beta} = \Sigma \sin^2 3\bar{\beta} = \Sigma \cos^2 4\bar{\beta}, \text{ etc.} = \frac{p_2}{2} \\ \Sigma \sin^2 \bar{\gamma} = \Sigma \cos^2 2\bar{\gamma} = \Sigma \sin^2 3\bar{\gamma} = \Sigma \cos^2 4\bar{\gamma}, \text{ etc.} = \frac{p_3}{2} \end{aligned}\right\} \qquad (6)$$

All the products in the least-squares solution vanish, and we have, for example,

$$NAA_0 = \frac{\Sigma n}{p_1 p_2 p_3}, \quad NAA_{100} = \frac{2\Sigma n \sin \bar{\alpha}}{p_1 p_2 p_3}, \quad NAA_{020} = \frac{2\Sigma n \cos 2\bar{\alpha}}{p_1 p_2 p_3},$$

$$NAA_{111} = \frac{8\Sigma n \sin \bar{\alpha} \sin \bar{\beta} \sin \bar{\gamma}}{p_1 p_2 p_3}, \quad NAA_{231} = \frac{8\Sigma n \cos 2\bar{\alpha} \sin 3\bar{\beta} \sin \bar{\gamma}}{p_1 p_2 p_3}.$$

When the coefficients A_{lmn} have been determined, the coefficients a_{lmn} are found from the equation

$$a_{lmn} = \frac{1}{k_l k_m k_n} A_{lmn}.$$

The total number of stars in the group has been reduced to 1000, and the series $F = a_0 + a_{100} \sin \alpha + a_{010} \sin \beta \ldots$, gives us then the number of velocity-vectors terminating in a cube of 10 km on the edge, the center of which is in the point x, y, z.

The fact that the motions of the stars are related to the plane of the galaxy makes it convenient to use galactic co-ordinates instead of equatorial. In order to have the origin near the center of the distribution, we have corrected all velocities for a standard solar motion of 20 km toward the point $A_0 = 270°$, $D_0 = +30°$. The pole of the galaxy is supposed to have the position $\alpha = 190°.6$, $\delta = +27°.2$ (Kapteyn).

If x, y, and z denote the galactic co-ordinates, we have the following equations of transformation:

$$\left.\begin{aligned} x &= +0.185\,\xi - 0.983\,\eta + 17.0 \\ y &= +0.449\,\xi + 0.084\,\eta + 0.889\,\zeta + 7.4 \\ z &= -0.874\,\xi - 0.164\,\eta + 0.457\,\zeta + 7.4 \end{aligned}\right\} \tag{7}$$

All constants derived from the frequency-functions are given in this system of co-ordinates. They can readily be converted into equatorial co-ordinates relative to the sun by aid of the equations

$$\left.\begin{aligned} \xi &= v\cos\alpha\cos\delta = +0.185x + 0.449y - 0.874z \\ \eta &= v\sin\alpha\cos\delta = -0.983x + 0.084y - 0.164z + 17.3 \\ \zeta &= v\sin\delta \quad = \quad +0.889y + 0.457z - 10.0 \end{aligned}\right\} \tag{8}$$

In Table III are given some data for the six different groups for which the coefficients in the series have been computed. The first two of these groups are overlapping. All terms up to the sixth order have been computed and in some cases terms of an even higher order. The total number of stars is in all cases reduced to

TABLE III

	Group					
	I	II	III	IV	V	VI
Spectrum	A6 to F9	F0 to G5	G6 to K1	K2 to K9	Ma to Md	G0 to M
Absolute magnitude	0.0 to 5.5	≤ 2.9	≤ 3.9	≤ 3.9	<3	≥ 3.0
c_1	40	40	60	60	60	160
c_2	30	30	60	60	60	160
c_3	30	30	60	60	60	160
Number of stars	278	197	252	220	115	343
Number within limits	174	148	231	205	108	340
Taurus stars omitted	9	4	5	0	0	0

1000, and the unit of volume is 1000 km^3. The most frequent velocity corresponds to the point of highest density in the velocity-cluster, and such a point is inclosed by non-intersecting surfaces of equal density. The intersections of these equi-frequential surfaces with any plane are closed curves surrounding the point or points of highest density.

In Figures 1 to 6 are shown the intersections of the surfaces of equal frequency with the xy-plane (galactic plane) and the xz-plane. The x-axis is directed toward the intersection of the galactic plane with the equator (in Aquila). The velocity of the sun in this system of co-ordinates has the components +17.0, +7.4, and

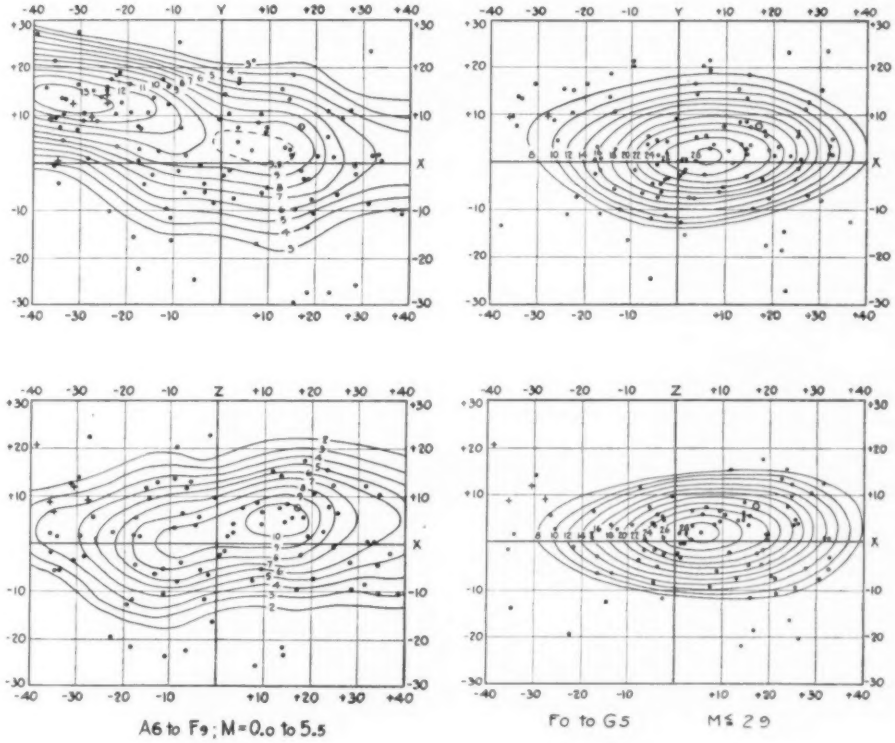

FIG. 1

FIG. 2

+7.4 km, and is denoted by the symbol ⊙. The recognized members of the Taurus stream were omitted in the computation but are marked in the diagram by crosses. The dots in the diagrams represent the velocities of those stars whose velocity-components perpendicular to the plane of projection are small, the limits in Figures 1 and 2 being ± 10 km and in Figures 3 to 5, ± 20 km. For the dwarf stars in Figure 6 the projections in the xy- and xz-planes of the velocities of all the stars are given.

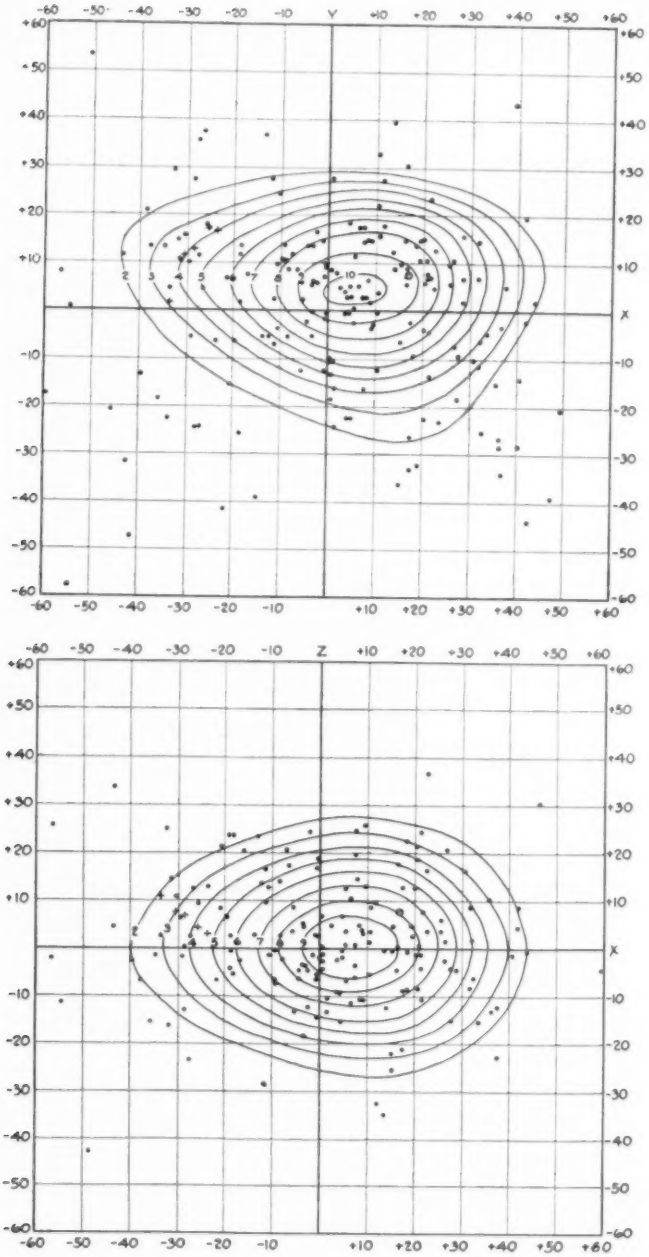

G6 to K1, M≦3.9

FIG. 3

A study of the diagrams in Figures 1 to 6 and the series upon which they are based leads to the following conclusions:

1. The giant stars of all types form a single "group" with an approximately ellipsoidal distribution, the longest and the intermediate axes in all cases lying very nearly in the galactic plane and coinciding approximately with the x- and y-axes. The shortest axis is nearly perpendicular to the galactic plane. The elongation of the ellipsoids is largest for the bright F stars and decreases for later types, the distribution being nearly spherical for the later K and the M stars.

2. The spread of the velocity-cluster increases with advancing spectral type and is much larger for the dwarf stars than for the giant stars.

3. The most frequent velocity does not coincide with the origin but lies for all the groups of giant stars in the first quadrant of the xy-plane and has the approximate values, $x=+5.8$, $y=+2.7$, $z=+1.7$ km. Relative to the sun this velocity is 13.4 km toward the point $\alpha=86°$, $\delta=-31°$.

4. If we exclude the very brightest F stars, many of which are Cepheid variables and stars of similar spectra, and take together stars of types A6 to F9, absolute magnitude 0 to 5.5, we find that these stars divide themselves into two streams. One of these coincides with the general group of giant stars, as can be seen from the agreement of its condensation point with that of the giant stars of other spectral types, while the other stream moves nearly parallel to the Taurus group. This latter stream comprises about 20 per cent of the ordinary stars of F type and its existence seems to indicate that a large number of stars of this spectral type in all regions of the sky are traveling with a velocity nearly identical with that of the Taurus group. Even among the brighter F stars, as well as among the G-type giants, the presence of members of this group is indicated by the protruding form of the equi-frequential surfaces in this region. This stream might be identified with Kapteyn's first drift, although the galactic latitude is not quite zero.

5. The dwarf stars, among which have been included stars of spectral types G0 to M of absolute magnitude fainter than 3.0, seem to form a group of their own as regards their motions. The

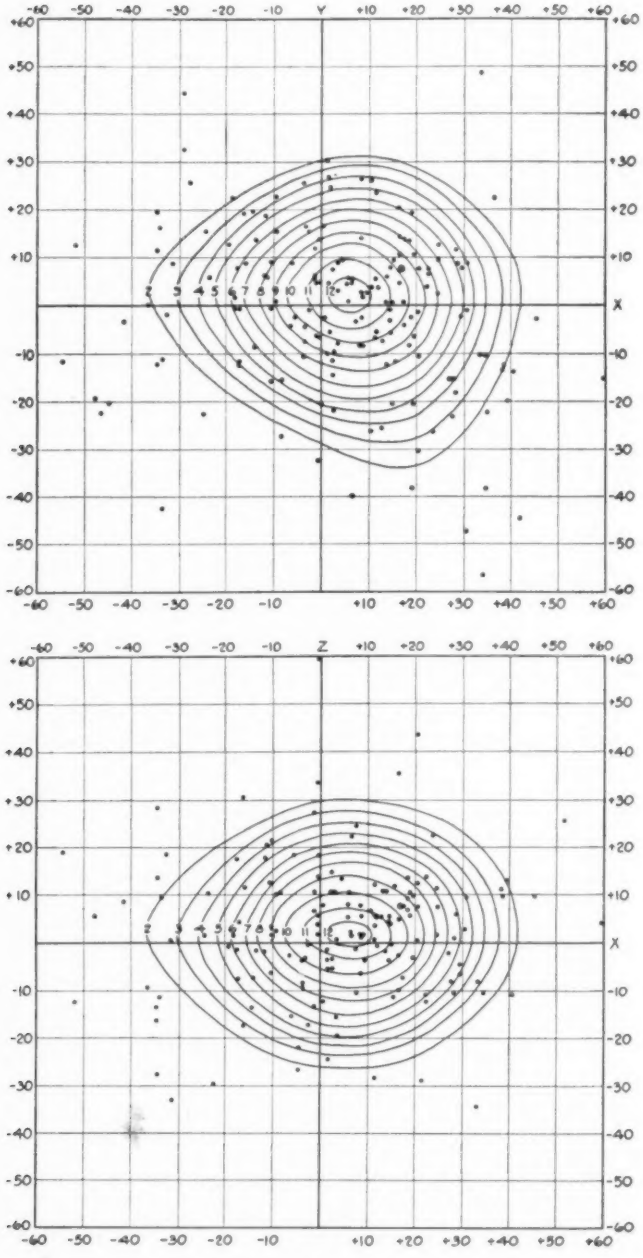

K2 to K9 ; M ≦ 3.9

FIG. 4

distribution of the velocities is ellipsoidal, with the major axis forming an angle of about 160° with the x-axis. The most frequent velocity is approximately $x=-19$, $y=-2$, $z=+1$ km, which nearly coincides with Kapteyn's first drift, while his second drift has been swallowed up by the ellipsoidal stream of giant stars.

6. There is a very marked asymmetry in the distribution of the velocities around the most frequent velocity-vector. The stars of high velocity show a tendency to avoid the first quadrant of the xy-plane. This produces a difference between the most frequent velocity and the mean velocity. The latter nearly coincides with the origin if the stars of very high speed are omitted, as was shown in the values for the solar motion given before. That this asymmetry is not due to any selection of stars of large proper motion moving opposite to the sun is shown by a study of the velocity-distribution of stars having very high speeds. In the diagram in Figure 7 are plotted the projections in the xy-plane of the velocities of the stars having space motions larger than 100 km relative to the origin. The effect of the selection of large proper motions relative to the sun instead of to our adopted origin is then insignificant, and we find that, whatever the spectral type or the absolute magnitude, if the velocity of a star is great there is an avoidance of the first quadrant of the xy-plane.[1] No star of speed higher than 100 km is moving in this direction, a result in agreement with that found by Adams and Joy[2] for stars of high radial velocity.

Different methods can be employed to obtain the constants of the frequency-functions. For all groups of stars except Group I we may use the ellipsoidal theory to represent approximately the distribution. We then disregard the asymmetry already alluded to and the excess of stars of high velocity which has been found to exist when a comparison is made with the distribution of velocities as given by Maxwell's law.[3] The first method was to use the

[1] Dr. Merrill has called my attention to the fact that this asymmetry in the motion of stars of high velocity is also indicated by the high value of the solar motion as derived from Md stars and bright-line nebulae. The former have a residual radial velocity of 31 km and give a velocity of the sun of 56 km (P. W. Merrill, *Popular Astronomy*, **29**, 637, 1921). The latter have a residual radial velocity of 30 km and give a velocity of the sun of 29 km (*Lick Observatory Publication*, **13**).

[2] *Loc. cit.* [3] *Mt. Wilson Contr.*, No. 210; *Astrophysical Journal*, **54**, 9, 1921.

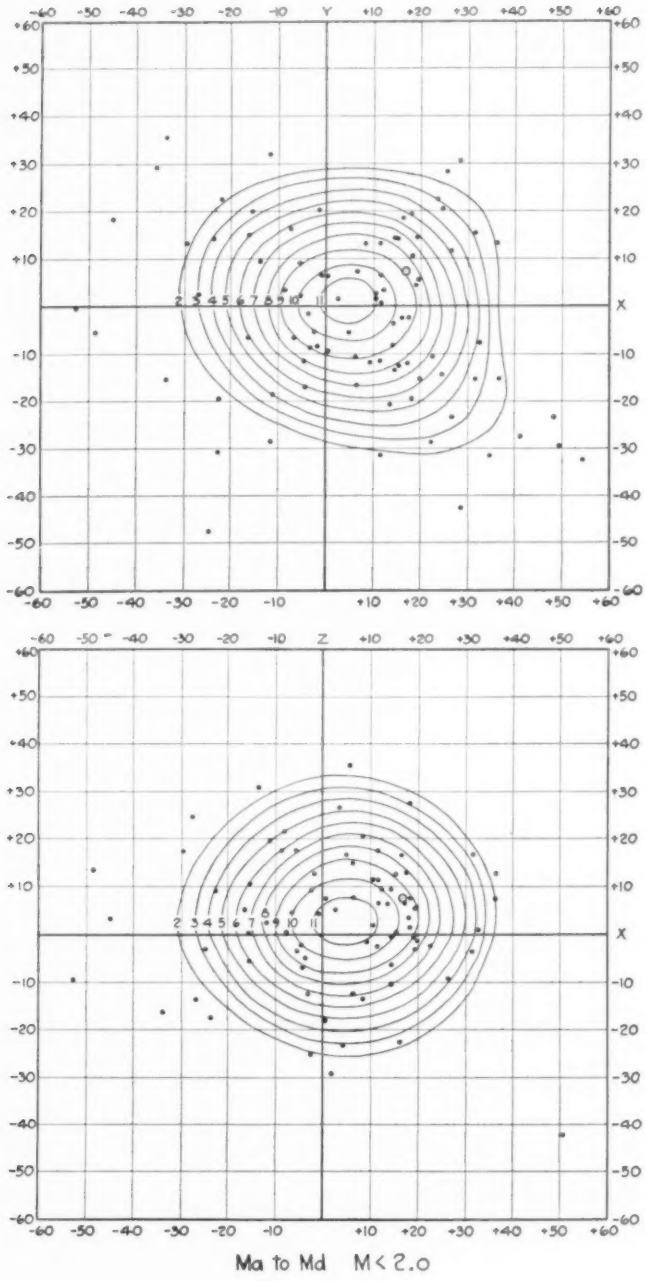

FIG. 5

trigonometric series already determined, and from the coefficients to derive the moments of first and second order. We thus diminish to a large extent the effect of the higher velocities, although in a somewhat arbitrary way.

The values of $\bar{x}$, $\bar{y}$, $\bar{z}$, $\bar{x}^2$, $\overline{yx}$, etc., can be found from the relations

$$\left.\begin{aligned} k\overline{x^l y^m z^n} &= \int_{-c_1}^{c_1}\int_{-c_2}^{c_2}\int_{-c_3}^{c_3} x^l y^m z^n F(xyz)\,dx\,dy\,dz \\ k &= \int_{-c_1}^{c_1}\int_{-c_2}^{c_2}\int_{-c_3}^{c_3} F(xyz)\,dx\,dz\,dy \end{aligned}\right\} \tag{9}$$

From the trigonometric series we find

$$\left.\begin{aligned}
a_{000}\frac{\pi^2}{4c_1}\bar{x} &= a_{100}-\frac{a_{300}}{9}+\frac{a_{500}}{25}+\ldots+(-1)^{\frac{n-1}{2}}\frac{a_{n00}}{n^2} \\
a_{000}\frac{\pi^2}{4c_2}\bar{y} &= a_{010}-\frac{a_{030}}{9}+\frac{a_{050}}{25}-\ldots+(-1)^{\frac{n-1}{2}}\frac{a_{0n0}}{n^2} \\
a_{000}\frac{\pi^2}{4c_3}\bar{z} &= a_{001}-\frac{a_{003}}{9}+\frac{a_{005}}{25}-\ldots+(-1)^{\frac{n-1}{2}}\frac{a_{00n}}{n^2} \\
\bar{x^2} &= \frac{c_1^2}{3}-\frac{8c_1^2}{a_{000}\pi^2}\left[\frac{a_{200}}{2^2}-\frac{a_{400}}{4^2}+\ldots+(-1)^{\frac{n}{2}+1}\frac{a_{n00}}{n^2}\right] \\
\bar{y^2} &= \frac{c_2^2}{3}-\frac{8c_2^2}{a_{000}\pi^2}\left[\frac{a_{020}}{2^2}-\frac{a_{040}}{4^2}+\ldots+(-1)^{\frac{n}{2}+1}\frac{a_{0n0}}{n^2}\right] \\
\bar{z^2} &= \frac{c_3^2}{3}-\frac{8c_3^2}{a_{000}\pi^2}\left[\frac{a_{002}}{2^2}-\frac{a_{004}}{4^2}+\ldots+(-1)^{\frac{n}{2}+1}\frac{a_{00n}}{n^2}\right] \\
\frac{a_{000}\pi^4}{16c_1c_2}\overline{xy} &= a_{110}-\frac{a_{310}}{9}-\frac{a_{130}}{9}+\frac{a_{510}}{25}+\frac{a_{330}}{81}+\frac{a_{150}}{25}+\ldots+(-1)^{\frac{m+n}{2}-1}\frac{a_{mn0}}{m^2n^2} \\
\frac{a_{000}\pi^4}{16c_1c_3}\overline{xz} &= a_{101}-\frac{a_{301}}{9}-\frac{a_{103}}{9}+\frac{a_{501}}{25}+\frac{a_{303}}{81}+\frac{a_{105}}{25}+\ldots+(-1)^{\frac{m+n}{2}-1}\frac{a_{m0n}}{m^2n^2} \\
\frac{a_{000}\pi^4}{16c_2c_3}\overline{yz} &= a_{011}-\frac{a_{031}}{9}-\frac{a_{033}}{9}+\frac{a_{051}}{25}+\frac{a_{033}}{81}+\frac{a_{015}}{25}+\ldots+(-1)^{\frac{m+n}{2}-1}\frac{a_{0mn}}{m^2n^2}
\end{aligned}\right\} \tag{10}$$

From these moments we can determine the axes upon which we have to project the velocity-components in order to make the sum

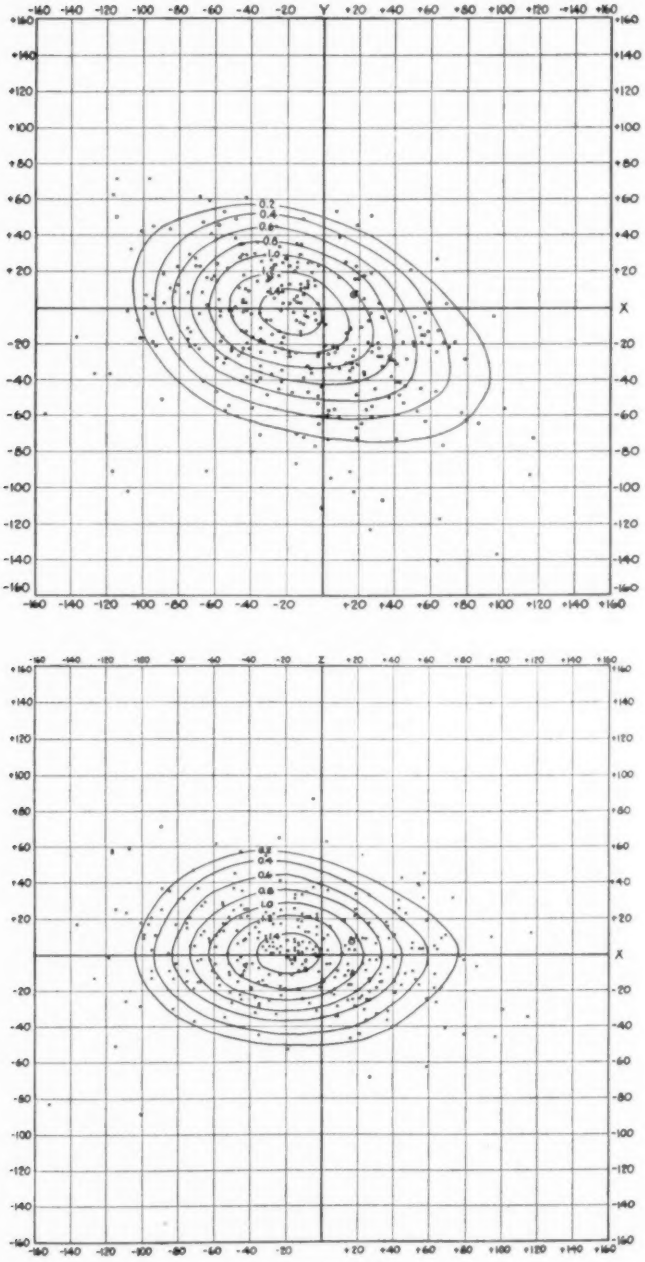

FIG. 6

of the squares of the projected velocities a maximum or a minimum. We thus obtain the principal axes of the velocity-ellipsoids, except for the effect of the stars outside the planes $\pm c_1$, $\pm c_2$, and $\pm c_3$, which have been omitted. We should expect in this case to find the length of the axes somewhat smaller than if they had been computed directly from all the velocity-components. On the other hand, the directions of the axes can be determined with

TABLE IV

CONSTANTS OF VELOCITY-ELLIPSOIDS AS COMPUTED FROM MOMENTS AND REFERRED TO THE GALACTIC CO-ORDINATE SYSTEM

GROUP	CENTROID FROM TRIG. SERIES			CENTROID FROM VELOCITY COMP. OF STARS WITHIN LIMITS			CENTROID FROM VELOCITY COMP. OF ALL STARS		
	$\bar{x}$	$\bar{y}$	$\bar{z}$	$\bar{x}$	$\bar{y}$	$\bar{z}$	$\bar{x}$	$\bar{y}$	$\bar{z}$
	km	km	km	km	km	km	km	km	km
I	− 2.9	+ 3.0	0.0	− 4.3	+ 3.6	+0.3	−11.9	−14.8	+1.3
II	+ 3.3	+ 2.0	+0.1	+ 2.0	+ 2.0	+0.3	+ 1.4	− 3.4	−2.2
III	+ 1.6	− 0.1	+1.3	+ 0.6	+ 0.2	+1.5	− 1.7	− 2.4	+0.8
IV	+ 3.8	− 2.5	+2.4	+ 4.2	− 1.9	+2.0	+ 1.8	− 5.4	0.0
V	+ 5.5	− 2.2	+0.3	+ 5.7	− 2.0	+0.5	+ 5.1	− 5.7	+0.3
VI	−16.1	−12.4	+1.3	−15.3	−13.3	+0.9	−15.9	−16.9	+0.2

GROUP	MAJOR AXIS OF ELLIPSOID			INTERMEDIATE AXIS OF ELLIPSOID			MINOR AXIS OF ELLIPSOID		
	L	B	a	L	B	b	L	B	c
			km			km			km
II	173°	− 3	18.9	83°	+ 6°	13.5	238°	+83°	8.9
III	181	− 2	25.2	92	+16	20.2	265	+74	15.6
IV	158	+10	21.8	65	+16	18.8	280	+71	11.1
V	147	+11	23.5	54	+14	19.1	275	+72	16.1
VI	153	+ 5	51.3	63	+ 5	32.3	285	+83	22.6

higher accuracy than if the high-velocity stars had been included. In Table IV are given the co-ordinates of the centroid as computed from the trigonometric series. For comparison the co-ordinates of the centroid computed directly from the velocity-components are added, as well as the co-ordinates of the axes of the velocity-ellipsoids. All of these results are in galactic co-ordinates.

The moments, however, are affected to an unequal extent by small changes in the larger and smaller velocities, and furthermore we have arbitrarily omitted stars of high velocity. This effect may be quite appreciable since we have reason to expect an excess

of stars of high velocity compared with ellipsoidal distribution, and the influence of the asymmetry of the distribution may not be eliminated properly. Accordingly another method has been used which gives the constants of the ellipsoidal distribution directly from the observed *number* of velocity-components of definite size. Starting from approximate values of the constants of the function, we can compute corrections to these values from the differences

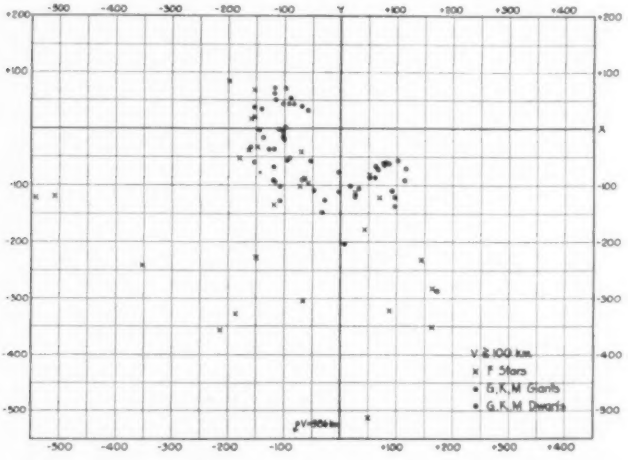

FIG. 7.—Projection on galactic plane of velocities of stars having speeds greater than 100 km per second.

between the observed and the computed number of velocity-vectors terminating in different regions of space. In order to simplify conditions we have to start from axes of co-ordinates which nearly coincide with the principal axes of the velocity-ellipsoids. We assume the following form for the frequency-function:

$$F(x)dx\,dy\,dz = Ke^{-S}\,dx\,dy\,dz; \quad S = h_1^2\xi^2 + h_2^2\eta^2 + h_3^2\zeta^2 .$$

Integrating between infinite limits, we have for a total of 1000 stars

$$\int_{-\infty}^{+\infty}\int\int F(x)dx\,dy\,dz = K\frac{\pi^{3/2}}{h_1h_2h_3} = 1000$$

Thus

$$K=\frac{1000\,h_1h_2h_3}{\pi^{3/2}}.$$

The equation of the velocity-ellipsoid of Schwarzschild is then

$$\frac{\xi^2}{a^2}+\frac{\eta^2}{b^2}+\frac{\zeta^2}{c^2}=1=2S$$

and for the axes of the ellipsoid, in other words, the dispersion (mean square deviation) along the principal axes, we have

$$a=\frac{1}{\sqrt{2}h_1},\qquad b=\frac{1}{\sqrt{2}h_2},\qquad c=\frac{1}{\sqrt{2}h_3}.$$

We shall assume that the axes of the system of co-ordinates are approximately parallel to the principal axes of the ellipsoids. This assumption can be made in all cases except for the dwarf stars. For these a recomputation of the distribution has been made relative to another co-ordinate system turned through an angle of -24° about the z-axis.

The co-ordinates ξ, η, ζ in the system of co-ordinates which corresponds to the principal axes of the ellipsoids and the center of which coincides with the center of the ellipsoids are connected with the co-ordinate system used previously by the equations

$$\left.\begin{aligned}\xi&=\alpha_1(x-x_0)+\alpha_2(y-y_0)+\alpha_3(z-z_0)\\ \eta&=\beta_1(x-x_0)+\beta_2(y-y_0)+\beta_3(z-z_0)\\ \gamma&=\gamma_1(x-x_0)+\gamma_2(y-y_0)+\gamma_3(z-z_0)\end{aligned}\right\}\qquad(11)$$

x_0, y_0, and z_0 here denote the co-ordinates of the center of the ellipsoid; α_1, α_2, and α_3, the direction cosines for the ξ-axis, etc.

Assuming approximate value of h_1, h_2, h_3, x_0, y_0, z_0 and $\alpha_1=\beta_2=\gamma_3=+1$; $\alpha_2=\alpha_3=\beta_1=\beta_3=\gamma_1=\gamma_2=0$, we can compute the number of velocity-vectors that terminate in a parallelopiped limited by the

six planes x_1, x_2; y_1, y_2; z_1, z_2, as well as its derivatives with regard to the constants of the frequency-function. If n_c is this number, we have

$$n_c = K \int_{\xi_1}^{\xi_2} e^{-h_1^2\xi^2} d\xi \int_{\eta_1}^{\eta_2} e^{-h_2^2\eta^2} d\eta \int_{\zeta_1}^{\zeta_2} e^{-h_3^2\zeta^2} d\zeta$$

$$= 125\, \Theta(\xi_1\xi_2)\, \Theta(\eta_1\eta_2)\, \Theta(\zeta_1\zeta_2) \quad (12)$$

where

$$\Theta(\xi_1\xi_2) = \frac{2}{\sqrt{\pi}} \int_{h_1\xi_1}^{h_1\xi_2} e^{-t^2} dt\,; \quad \Theta(\eta_1\eta_2) = \frac{2}{\sqrt{\pi}} \int_{h_2\eta_1}^{h_2\eta_2} e^{-t^2} dt\,;$$

$$\Theta(\zeta_1\zeta_2) = \frac{2}{\sqrt{\pi}} \int_{h_3\zeta_1}^{h_3\zeta_2} e^{-t^2} dt\,.$$

The orientation of the ellipsoid can be determined by three independent quantities L_1, B_1, and B_2, of which L_1 and B_1 are the galactic longitude and latitude of the ξ-axis and B_2 the galactic latitude of the η-axis. These are all supposed to be fairly small quantities and correspond to small rotations about the z-, y-, and x-axis, respectively.

The equations of conditions then take the form

$$\left.\begin{aligned} &\frac{dn}{dh_1}\Delta h_1 + \frac{dn}{dh_2}\Delta h_2 + \frac{dn}{dh_3}\Delta h_3 + \frac{dn}{dx_0}\Delta x_0 + \frac{dn}{dy_0}\Delta y_0 + \frac{dn}{dz_0}\Delta z_0 \\ &\qquad + \frac{dn}{dL_1} L_1 + \frac{dn}{dB_1} B_1 + \frac{dn}{dB_2} B_2 + n_c\kappa = n_0 - n_c\,. \end{aligned}\right\} \quad (13)$$

The observed number n_0 is reduced to a total of 1000 stars. Since we wish to determine the constants of the function from the distribution of velocities within a limited space, and do not wish to impose the condition that the number of stars of very high velocity is in exact agreement with the assumed distribution-law, we add the term $n_c\kappa$.

The expressions for the derivatives have been found to be the following:

$$
\left.
\begin{aligned}
\frac{dn}{dh_1} &= -\frac{250}{\sqrt{\pi}h_1}\Phi(\xi_1\xi_2)\Theta(\eta_1\eta_2)\Theta(\zeta_1\zeta_2)\\
\frac{dn}{dh_2} &= -\frac{250}{\sqrt{\pi}h_2}\Theta(\xi_1\xi_2)\Phi(\eta_1\eta_2)\Theta(\zeta_1\zeta_2)\\
\frac{dn}{dh_3} &= -\frac{250}{\sqrt{\pi}h_3}\Theta(\xi_1\xi_2)\Theta(\eta_1\eta_2)\Phi(\zeta_1\zeta_2)\\
\frac{dn}{dx_0} &= \frac{250h_1}{\sqrt{\pi}}\Psi(\xi_1\xi_2)\Theta(\eta_1\eta_2)\Theta(\zeta_1\zeta_2)\\
\frac{dn}{dy_0} &= \frac{250h_2}{\sqrt{\pi}}\Theta(\xi_1\xi_2)\Psi(\eta_1\eta_2)\Theta(\zeta_1\zeta_2)\\
\frac{dn}{dz_0} &= \frac{250h_3}{\sqrt{\pi}}\Theta(\xi_1\xi_2)\Theta(\eta_1\eta_2)\Psi(\zeta_1\zeta_2)\\
\frac{dn}{dL_1} &= \frac{250(h_2^2-h_1^2)}{\pi h_1h_2}\Psi(\xi_1\xi_2)\Psi(\eta_1\eta_2)\Theta(\zeta_1\zeta_2)\\
\frac{dn}{dB_1} &= \frac{250(h_3^2-h_1^2)}{\pi h_1h_3}\Psi(\xi_1\xi_2)\Theta(\eta_1\eta_2)\Psi(\zeta_1\zeta_2)\\
\frac{dn}{dB_2} &= \frac{250(h_3^2-h_2^2)}{\pi h_2h_3}\Theta(\xi_1\xi_2)\Psi(\eta_1\eta_2)\Psi(\zeta_1\zeta_2)
\end{aligned}
\right\} \qquad (14)
$$

$$
\begin{aligned}
\Phi(\xi_1\xi_2) &= h_1\xi_1e^{-h_1^2\xi_1^2} - h_1\xi_2e^{-h_1^2\xi_2^2}\\
\Phi(\eta_1\eta_2) &= h_2\eta_1e^{-h_2^2\eta_1^2} - h_2\eta_2e^{-h_2^2\eta_2^2}\\
\Phi(\zeta_1\zeta_2) &= h_3\zeta_1e^{-h_3^2\zeta_1^2} - h_3\zeta_2e^{-h_3^2\zeta_2^2}\\
\Psi(\xi_1\xi_2) &= e^{-h_1^2\xi_1^2} - e^{-h_1^2\xi_2^2}\\
\Psi(\eta_1\eta_2) &= e^{-h_2^2\eta_1^2} - e^{-h_2^2\eta_2^2}\\
\Psi(\zeta_1\zeta_2) &= e^{-h_3^2\zeta_1^2} - e^{-h_3^2\zeta_2^2}
\end{aligned}
$$

where ξ_1, ξ_2, η_1, etc., are determined by equation (11). Using the products of the functions Θ, Φ, and Ψ as coefficients, we secure a homogeneous set of equations of condition.

The distribution of velocities for Group I cannot be represented even approximately by an ellipsoidal frequency-function. In this

case the sum of one ellipsoidal and one spherical frequency-function has been used, viz.:

$$F(xyz)=\mu Ke^{-S}+(1-\mu)Ke^{-h^2[(x-x_0^1)^2+(y-y_0^1)^2+(z-z_0^1)^2]}$$

$\mu/(1-\mu)$ is the relative proportion of stars belonging to ellipsoidal and to the spherical stream.

The new derivatives in this case are

$$\frac{dN_2}{dh}=-\frac{2N_2}{\sqrt{\pi}h}\left[\frac{\Phi(x_1^1x_2^1)}{\Theta(x_1^1x_2^1)}+\frac{\Phi(y_1^1y_2^1)}{\Theta(y_1^1y_2^1)}+\frac{\Phi(z_1^1z_2^1)}{\Theta(z_1^1z_2^1)}\right]$$

$$x_1^1=x-x_0^1,\quad y_1^1=y-y_0^1,\quad \text{etc.}$$

$$\frac{dn}{d\mu}=N_1-N_2,\quad n=n_c=\mu N_1+(1-\mu)N_2$$

$$\frac{dN_2}{dx_0^1}=\frac{250\,h}{\sqrt{\pi}}\Psi(x_1^1x_2^1)\Theta(y_1^1y_2^1)\Theta(z_1^1z_2^1),\ \text{etc.}$$

We have then

$$\mu\left[\frac{dN_1}{dh_1}\Delta h_1+\frac{dN_1}{dh_2}\Delta h_2+\ \ldots\ .\ +\frac{dN_1}{dB_2}B_2\right]$$
$$+(1-\mu)\left[\frac{dN_2}{dh}\Delta h+\frac{dN_2}{dx_0^1}\Delta x_0^1+\frac{dN_2}{dy_0^1}\Delta y_0^1+\frac{dN_2}{dz_0^1}\Delta z_0^1\right]$$
$$+\frac{dn}{d\mu}\Delta\mu+\kappa n_c=n_0-n_c\,.$$

The results of this computation are given in Table V. The probable errors in each case are given below the corresponding numerical values. According to the usual convention, that direction of the major axis is given which most nearly corresponds to 180° of galactic longitude in order to be comparable with Kapteyn's first stream. The dispersion along the two shortest axes in several cases is so nearly the same that only the direction of the major axis can be well determined.

The elements of the spherical stream of Group I are found to be,

$$x_0 = -31.1 \pm 1.4 \text{ km}$$
$$y_0 = +14.5 \pm 1.1$$
$$z_0 = +\ 3.0 \pm 0.7$$
$$a = \frac{1}{\sqrt{2h}} = 8.1 \pm 0.5$$
$$1 - \mu = 0.185 \pm 0.028.$$

Relative to the sun and in the equatorial system of co-ordinates, this condensation-point has the co-ordinates

$$\alpha = 92^\circ.3, \qquad \delta = +4^\circ.9, \qquad v = 48.7 \text{ km}$$

Boss's value[1] for the convergent point of the Taurus group is

$$\alpha = 91^\circ.8, \qquad \delta = +6^\circ.9, \qquad v = 45.6 \text{ km}.$$

We can thus identify this stream, which is superimposed on the general ellipsoidal distribution, with the Taurus stream, although these stars are scattered all over the sky. The percentage of stars belonging to this general Taurus stream is, as appears from the value of $1-\mu$, 18.5 ± 2.8 per cent of the stars of spectral type A7 to F9 and absolute magnitude 0.0 to 5.5. If we include in this group the nine recognized members of the Taurus stream which were omitted in the analysis, we find that 22 per cent of the stars of this type and absolute magnitude belong to the general Taurus stream. The spread corresponding to a dispersion of 8.1 km is no doubt due in part to errors in the quantities involved, but may also be due in part to an inherent dispersion of the velocities. Attention may be called to the fact that the dispersion of the velocities of the members of the Taurus stream has necessarily been estimated too low hitherto because of the selection of stars whose velocities are very nearly parallel. Even among the stars of type G there are several which belong to this general Taurus stream. This may be

[1] L. Boss, *Astronomical Journal*, **26**, 31, No. 604, 1908.

TABLE V

CONSTANTS OF THE VELOCITY-ELLIPSOIDS AS COMPUTED FROM DISTRIBUTION OF VELOCITY-VECTORS AND REFERRED TO THE GALACTIC CO-ORDINATE SYSTEM

GROUP	CENTER			MAJOR AXIS			INTERMEDIATE AXIS			MINOR AXIS		
	x	y	z	L	B	a	L	B	b	L	B	c
	km	km	km			km			km			km
I	+ 5.39	+0.80	+0.06	173°.6	− 8°.5	22.86	.....	.....	12.25	.....	.....	11.68
	± 1.30	±0.35	±0.55	± 4.1	± 3.0	± 1.04	.....	.....	± 0.36	.....	.....	± 0.45
II	+ 5.49	+1.52	+1.45	177.6	− 0.1	18.47	87.6	+ 9.1	10.02	+267.1	+80.9	7.92
	± 0.83	±0.65	±0.34	± 3.4	± 2.0	± 1.13	± 3.4	± 7.7	± 0.43	± 3.4	± 7.7	± 0.32
III	+ 3.10	−0.82	+0.68	181.0	+ 4.1	23.19	.....	.....	16.49	.....	.....	16.13
	± 1.02	±0.98	±0.53	± 6.5	± 4.4	± 0.87	.....	.....	± 0.58	.....	.....	± 0.69
IV	+ 3.30	−1.03	+2.50	153	+ 2	19.86	.....	.....	15.93	.....	.....	14.55
	± 0.81	±0.87	±0.33	± 12	± 5	± 0.67	.....	.....	± 0.50	.....	.....	± 0.99
V	+ 1.3	−1.6	+5.5	142	+27	18.8	.....	.....	16.0	.....	.....	15.2
	± 2.1	±2.3	±1.3	± 25	±22	± 1.4	.....	.....	± 1.4	.....	.....	± 1.1
VI	−17.0	−6.8	+1.2	148.7	+ 7.3	48.97	58.7	+37.0	26.94	255.3	+52.4	21.80
	± 2.7	±2.2	±1.3	± 4.6	± 2.4	± 1.07	± 4.6	±11.5	± 0.86	± 4.6	±11.5	± 0.90

seen from the form of the equi-frequential surfaces as well as from an inspection of the points in the diagram.

In Table VI are given the same quantities as in Table V but referred to the equatorial system of co-ordinates, the center of the ellipsoids being referred to the sun.

TABLE VI

CONSTANTS OF THE VELOCITY-ELLIPSOIDS AS COMPUTED FROM THE DISTRIBUTION OF VELOCITY-VECTORS REFERRED TO THE SUN AND TO THE EQUATORIAL CO-ORDINATE SYSTEM

GROUP	CENTER			MAJOR AXIS		INTERMEDIATE AXIS		MINOR AXIS	
	α	δ	v	α	δ	α	δ	α	δ
			km						
I	84°0	−37°7	15.2	90°2	+ 1°7	.....	.....	.....	.....
II	88.0	−34.0	14.2	95.5	+ 2.1	3.0	+71.7	190.1	+18.1
III	91.7	−36.7	17.5	104.8	+ 1.0	.....	.....	.....	.....
IV	98.7	−35.7	16.8	89.4	+24.8	.....	.....	.....	.....
V	109.6	−29.5	18.2	105.7	+44.0	.....	.....	.....	.....
VI	102.4	−24.6	37.4	92.4	+31.1	252.4	+61.8	181.6	− 9.4

If we take the vectors opposite to those given in columns 2–4 of Table VI, we have the velocity of the sun referred to the center of the velocity-ellipsoid. For the giant stars this velocity is appreciably smaller than the velocity of the sun computed from the mean velocity. This result is due to the asymmetry of the distribution of the velocities taken in combination with the different weights given different stars in the use of quantities of zero order (numbers) and of first order (means). If the solar motion is used for the purpose of computing parallaxes from parallactic motion, the velocity based upon the means of the components should be employed.

Another consequence of this asymmetry is that the most frequent velocity does not correspond either to the mean velocity or to the center of the ellipsoidal distribution. From the diagrams we can easily estimate this most frequent velocity by determining the points of highest density of the general frequency-function. In Table VII these values are given both in galactic rectilinear co-ordinates relative to our adopted origin, and in equatorial polar co-ordinates relative to the sun.

TABLE VII

MOST FREQUENT VELOCITY-VECTORS

Group	x	y	z	a	δ	v
	km	km	km			km
I	+ 9	+3	+5	100°	−33°	9
II	+ 6.1	+1.1	+1.9	90.4	−36.6	13.7
III	+ 6.0	+4.9	+0.4	75.9	−24.6	13.2
IV	+ 5.8	+2.2	+2.0	88.6	−32.2	13.5
V	+ 4.7	+1.0	+3.4	97.9	−31.8	14.4
VI	−19.0	−2.0	+1.2	98.8	−17.4	37.7
Giants (II to V)	+ 5.8	+2.7	+1.7	86.2	−30.8	13.4

SUMMARY

The three components of the velocities of about 1300 stars of spectral types F to M have been computed from the proper motions, radial velocities, and parallaxes. The following are the principal results of the investigation:

1. The solar motion as derived from the algebraic means of the velocity-components is found to be dependent on the spectral types and absolute magnitudes of the stars to which it is referred. The giant stars of the later types give a somewhat higher declination of the sun's apex than the giant stars of earlier types. The dwarf stars give a much larger solar motion than the giant stars, and, in general, stars of high velocity give a larger motion than stars of low velocity.

The distribution of velocities of different groups of stars has been studied in different ways. The velocities are referred to the galactic system of stars and have been corrected for a standard solar velocity of 20 km toward the point $\alpha = 270°$, $\delta = +30°$.

In order to learn the nature of this distribution a very general type of frequency-function has been used, which in reality is an interpolation formula in three dimensions. The function is a three-dimensional cosine-series in which the coefficients are determined directly from the *number* of velocity-vectors within different limits. A very large number of terms has been determined by harmonic analysis, a synthesis has been made for the xy- and xz-planes, and curves of equal frequency have been drawn in these planes (Figs. 1–6 and Table III). From a study of these figures we can draw the following conclusions:

2. The giant stars of types F to M form a single group or "stream" with an approximately ellipsoidal distribution, the longest axis lying in the galactic plane and nearly coinciding with the x-axis, the line of intersection of the equator with the galactic plane. The shortest axis is nearly in the direction of the galactic pole. The elongation of the velocity-ellipsoid is largest for the bright F stars and smallest for the late K and M stars, for which the distribution is nearly spherical.

3. The most frequent velocity does not coincide with the origin, but for all groups of giant stars lies in the first quadrant of the xy-plane, and corresponds approximately to a velocity 13.4 km relative to the sun in the direction $\alpha = 86^\circ.2$, $\delta = -30^\circ.8$. For the dwarf stars the most frequent velocity relative to the sun is 37.7 km in the direction $\alpha = 98^\circ.8$, $\delta = -17^\circ.4$ (Table VII).

4. Among the stars of spectral types A7 to F9 and absolute magnitudes 0 to +6 there is in addition to the general group of giants another stream the motion of which coincides with that of the Taurus group. These stars are scattered all over the sky and comprise about 20 per cent of the stars of the above-mentioned spectral types and absolute magnitudes. Even among stars of somewhat later types there are stars belonging to this general Taurus group.

5. There is a marked asymmetry in the distribution of the velocities around the most frequent velocity-vector. Stars of high velocity show a tendency to avoid moving toward the first quadrant of the xy-plane. This asymmetry which is especially marked among the stars of very high velocity can be traced even among stars of ordinary velocity, thus producing a systematic difference between the most frequent velocity-vectors and the mean velocity.

6. Neglecting this asymmetry, the constants of the ellipsoidal frequency-function have been computed in two different ways: First, the method of moments was used, the moments being computed from the trigonometric series previously determined (Table IV). Second, the constants were determined from the distribution of velocities itself, approximate values for the constants being assumed and then corrected by values computed from the difference between the observed and the computed number of velocity-vectors

terminating in different parallelopipeds (Tables V and VI). The values computed in this way differ somewhat from those computed from the moments on account of the difference in weighting. The asymmetry in the distribution produces different values for the velocity of the sun, according as the latter is computed from the distribution of velocities itself, or from algebraic means. The first necessarily gives the smallest value for the sun's velocity, the latter the highest.

In the extensive computation involved in this investigation the author has received valuable help from the following members of the computing division: Mrs. Hannah M. Marsh, Miss Ada M. Brayton, and Miss Florence MacCreadie. Dr. Jean Paraskévopoulos of Athens and Professor D. T. Wilson of Cleveland also have taken part in the computations.

MOUNT WILSON OBSERVATORY
June 1922

THE APPLICATION OF VACUUM THERMOCOUPLES TO PROBLEMS IN ASTROPHYSICS[1]

By EDISON PETTIT and SETH B. NICHOLSON

ABSTRACT

Sensitive vacuum thermocouples.—*Construction* of the couple and cells is described. The couples were made of metal strips about 3 mm long, $\frac{1}{10}$ mm wide and $\frac{1}{250}$ mm thick, each overlapping junction being fused to a blackened tin disk receiver, $\frac{1}{2}$ mm in diameter and $\frac{1}{500}$ mm thick, each couple weighing only about $\frac{1}{30}$ mg. The sensitivity with a high vacuum (10^{-4} mm) was found to be from two to eleven times the value at atmospheric pressure, depending on the couple. To maintain the vacuum, metallic calcium was used. With a sensitive galvanometer (5×10^{-10} amp./mm) the *temperature sensitivity* obtained was 8×10^{-5} deg./mm, in one case. The *efficiency*, however, was very low, only about 10^{-6} of the incident energy being transformed into electrical energy. An ideal heat engine would be a hundred times more efficient.

Stellar radiation measurements.—*Method of application of the vacuum thermocouple* is described. The cell was mounted on a plate adapted to the Newtonian double-slide plate-holder of the 100-inch telescope, and connected by wires to a D'Arsonval galvanometer in the basement where the deflections were recorded on a moving plate. *Photographic records of the deflections for Vega, Arcturus, α Herculis, and R Hydrae,* with and without a water absorption cell, are reproduced (Plate VII).

Applications of thermocouple to solar energy measurements already made are the registration (1) of spectral energy distribution, (2) of drift curves across the disk in various wave-lengths, and (3) of total radiation curves across sun-spots and faculae.

Self-registering microphotometer is described in which the photo-electric cell is replaced by a vacuum thermopile. A suitable optical system enables the light through a slit 9 mm long and 0.1 mm wide to be integrated so as to eliminate the grain effect in the spectrograms measured.

Transmission curve for water, 1 cm thick, is reproduced.

Optical system for sensitive galvanometer.—By placing a spectacle lens of 6 m focus at the galvanometer and observing the image with cross-hair and eyepiece, a power of 350 could be used and the scale read accurately to 0.1 mm at 8 m.

In 1895 Lebedew[2] found that a thermocouple of iron-constantan was more sensitive in a vacuum than at atmospheric pressure. Since that time the thermocouple has been used both in vacuum and at atmospheric pressure by a number of physicists, for the study of radiation problems. The vacuum thermocouple has been applied to the study of stellar radiation with marked success by Pfund, and more recently by Coblentz. Pfund employed couples of 95Bi+5Sn against 97Bi+3Sb, and Coblentz employed Bi against 95Bi+5Sn and also Bi against Pt with success. The former[3] used

[1] *Contributions from the Mount Wilson Observatory,* No. 246.

[2] *Annalen der Physik,* **56,** 12, 1895.

[3] *Allegheny Observatory Publications,* **3,** 45, 1913.

charcoal heated by electric discharge, while the latter[1] employed metallic calcium, to maintain the vacuum.

FORM OF CELL EMPLOYED

In the present investigation we have used the three types of cell shown in Plate VI. After considerable experimenting type 3 was adopted. The cell body and connecting tubes are made of Pyrex glass, the calcium tube C is of clear quartz, and the plug P, containing the platinum wires carrying the thermocouples, is of soda glass. The cell body A has an inside diameter of 42 mm and a wall 1.5 mm thick. The quartz tube C (14 mm inside diameter) is attached to the Pyrex tube by a ground joint and stop-cock grease, and sealed with red sealing wax. The metallic calcium is held in place by a wad of glass wool. The plug P carries three platinum wires to which two thermocouples are attached, at T. It is attached with a ground joint, sealed with stop-cock grease, and may be removed or replaced without destroying the thermocouples.

The cell A is fitted with two windows, W_1, W_2, of 10 mm clear aperture. The window W_1, which admits the radiation to the thermocouple, is closed with a quartz window 1.5 mm thick, the junction with the ground surface of the lip being made with stop-cock grease and protected by a rim of red sealing wax. In type 2 the window W_1 is of microscope cover-glass 0.12 mm thick. W_2 is closed with a piece of microscope slide-glass 1.28 mm thick. On looking through W_2 the thermocouple junction may be seen projected against the star image or other radiation entering W_1.

The advantages of this design of cell are as follows: (1) large bearing surfaces at the ground junctions of the plug and calcium tube; (2) a minimum exposure of contact surfaces at the windows; (3) couples may be withdrawn or replaced within the cell without danger of damage; (4) the blackened surfaces of the couples may be exposed to either window by simply rotating the plug, thus enabling the cell to be adapted to various apparatus.

PREPARATION OF THE THERMOCOUPLES

The choice of metals for the couples is dependent on a number of physical properties, which may be briefly enumerated as follows:

[1] *Bulletin Bureau of Standards*, **11**, 185, 1915.

PLATE VI

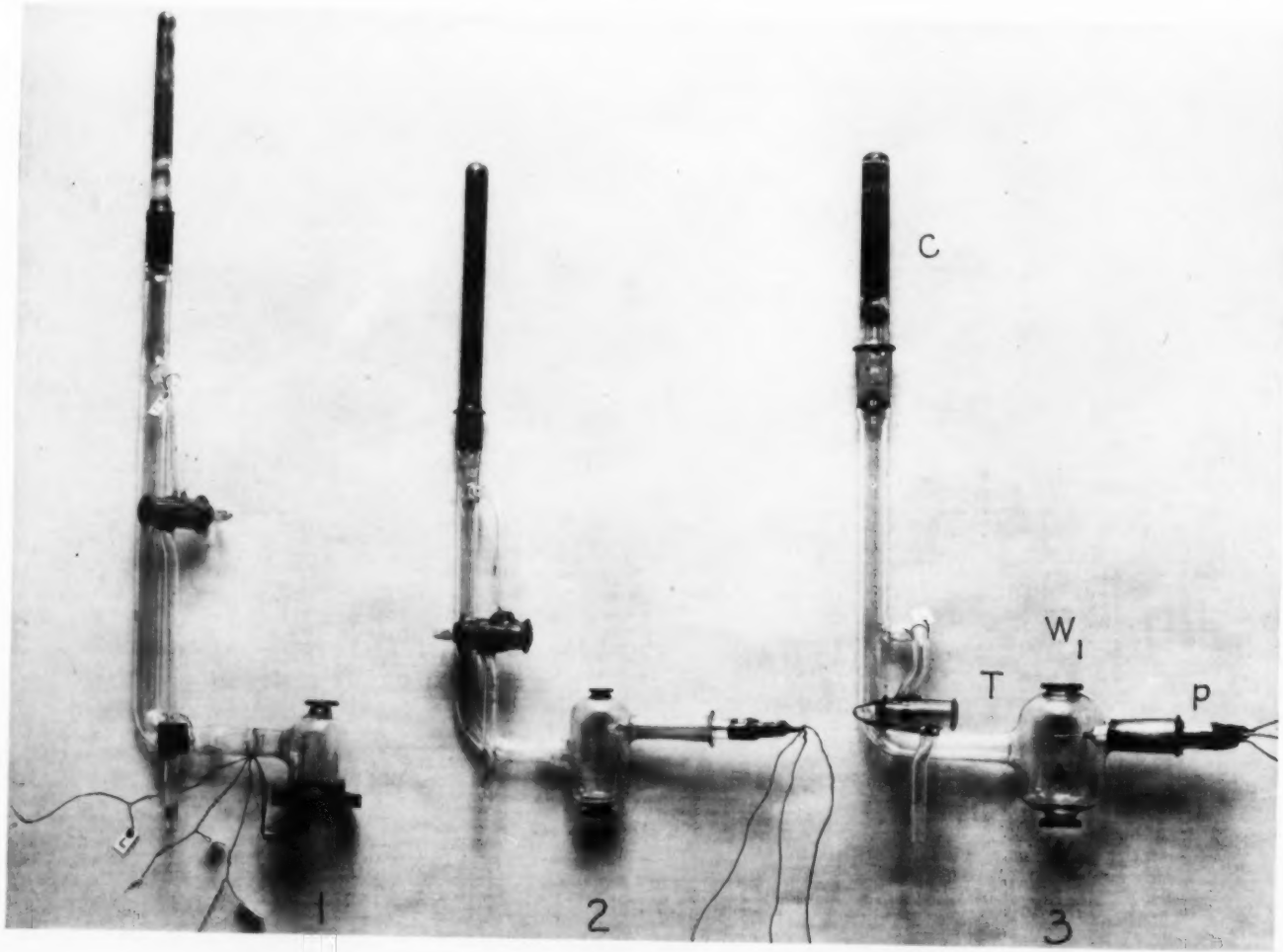

TYPES OF THERMOCOUPLE CELLS

(1) high electrical conductivity; (2) high thermoelectric power; (3) low heat conductivity; (4) low coefficient of brittleness; (5) approximately equal melting points; (6) low specific heat.

Of these six conditions (1) and (3) and also (2) and (4) are obviously antagonistic in nature. Generally the relative specific coefficients of thermal and electrical conductivity are nearly equal, and high thermoelectric power is associated with a crystalline structure making for great brittleness. There is a considerable range in the constants for some of the metals, especially those of more crystalline structure. This is due principally to two causes: differing conductivity and thermoelectric power in axial and equatorial directions, and impurities in the metal. Taking bismuth as an example, the thermoelectric power axially is $65\times10^{-6}V$/deg. C., and equatorially $45\times10^{-6}V$/deg. C. An impurity of $\frac{1}{3}$ of 1 per cent of tin will reduce the thermoelectric power to 0 relative to lead. The thermoelectric properties of alloys have been investigated by Mattheissen, Tait, Becquerel, Hutchins, and others, and it is found that most of the metals investigated are very sensitive to changes in the relative proportions of the alloy.

The current produced by the junction of a couple will depend on the thermoelectric power, p, the resistance, R, and the difference in temperature ΔT between the hot and the cold junction. The latter in turn depends on the specific heat of the junction, S; the mass, M; the quantity of heat, C, conducted away along the strips; the quantity C_1 conducted through the air; the quantity C_2 convected away; the quantity radiated, r; and the quantity incident on the junction, Q.

Then

$$I=\frac{kp}{SMR}[Q-(C_1+C_2+C+r)] \qquad (1)$$

where I is the current and k is a constant depending on the units employed.

Obviously C_1, C_2 may be eliminated by placing the couple in a vacuum. Then r will depend only on the absolute temperature and C should be made as small as possible. In only a few cases, however, will this be of any advantage, since C and R are physically connected, and a decrease in C will correspondingly increase R.

The values of C and $1/R$ are both directly proportional to M, so that after a certain limit is reached, the only advantage in reducing M lies in the quickness of action of the couple in responding to changes in Q. Some advantage is gained, however, by placing at the junction of the two metals a thin plate of a third metal, functioning only as a receiver of the radiation and chosen so that the specific heat will be low. If the plate is very thin and M is small, then its conductivity is unimportant.

The thermoelectric power, p, is itself dependent on the absolute temperature at which the thermocouple is working. Generally this is high for low temperatures and decreases for the higher temperatures, passing through zero and reversing sign at the "temperature of inversion." Considerable advantage would be gained in operating the couple at the temperature, let us say, of liquid air, but the difficulties attending this modification of the apparatus have thus far prevented its successful application.

We have employed chiefly the following metals: Bi, 95Bi+5Sn, Pb, Sn, Pt, Au, Cu, 806Sb+696Cd, Ag, 97Bi+3Sb, Te. When the metals are easily fusible, the simplest method of producing fine flat strips suitable for thermocouples is that first proposed by Pfund. About 10 gm of the metals to be fused and alloyed are placed in a Rose's crucible and heated in a current of hydrogen, which prevents oxidation from destroying the ratios of the metals introduced. The molten metal is then dashed with all possible force perpendicularly on a large plate of window glass. The spattered metal is thus transformed into a spray of fine radiating wires. An abundant supply of strips 0.005 mm or more thick and 0.05 mm or more wide is thus obtained.

The operation of forming the junctions is carried out on a large sheet of plate glass. As one must everywhere avoid adhesion when working with such small masses, the glass is kept warm by laying it on the planed surface of a large iron casting which has previously been heated. A sheet of white paper lies between the glass and the casting.

Because of its low specific heat and melting point, tin or ordinary tinner's solder is chosen for the receivers. Shavings of the metal are rolled out into thin sheets; these are cut into narrow strips,

which are cut into small pieces by means of a scalpel. The latter are fused with a bit of rosin by touching them with a loop of nichrome wire heated by a current of electricity. This immediately produces a minute sphere of the metal, which when pressed flat by a plate of glass produces a thin disk suitable for the receivers. By trial it is found that a sphere 0.15 mm in diameter can be pressed into a receiver 0.5 mm in diameter, which is almost as thin as can be handled. It is easy to find the length of strip necessary for these spheres, which can then be produced in quantity. After several dozens of them have been fused with a bit of rosin, the latter is dissolved away with amyl alcohol and the disks made as needed.

The operation of forming the couples, such as are shown in Figure 1, is carried out about as follows: The strips to be employed

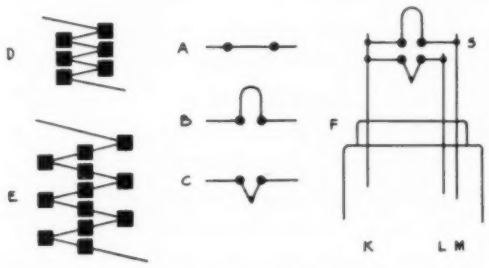

FIG. 1.—Types of thermopiles and thermocouples

are removed from the glass plates carrying the spattered metals by means of a razor blade attached to a convenient handle. These strips are first examined under a microscope to detect any defects which might weaken them, and then laid so that the ends overlap. One of the prepared receivers is then laid over the junction without rosin or other soldering flux. A strip of mica 12×30×.02 mm, bent in the middle so as to keep the center raised 1 or 2 mm above the glass is then laid over the junction and held down with the finger and two 10-gm weights laid close on either side of the couple to keep the mica in contact with it. The welding together of the junction and receiver is accomplished by touching the mica directly above the receiver with the electrically heated loop of nichrome wire. The loop must be heated just below redness and only the briefest

possible contact made with the mica. Only one junction at a time is welded, otherwise one may adhere to the glass and the other to the mica, in which case it is impossible to remove the mica without destroying the couple.

The receivers are painted with a mixture of lampblack, two parts; platinum black, one part; turpentine, five parts; and alcohol, twenty parts. This paint, put on with a fine camel's hair brush, forms a black mat surface which will dry quickly.

In Figure 1 are shown five forms of thermocouple; *A*, *B*, and *C* are compensated junctions adapted to stellar observations, *D* and *E* are piles adapted to spectroscopic work, and *F* shows the method of mounting the couples on the platinum wires *K*, *L*, *M*. Forms *B* and *C* have been adopted for stellar observations, since the deflections may be doubled by shifting the junctions alternately on the star image as first applied by Pfund. In *B* the middle strip is folded into a U form in order to bring the junctions close together and leave a space between them, but for some of the more brittle metals which cannot be folded without breaking them, type *C* is used, where two short strips are welded together in V form. Type *D* is a pile which we have used on the registering microphotometer, and *E* is another type of pile first employed by Rubens[1] in 1898 for spectroscopic work at atmospheric pressure, and used more recently by Coblentz[2] in a vacuum.

The platinum wires *K*, *L*, *M* (Fig. 1, *F*) are flattened out on the free ends and solder is run over them on one side. After being washed in alcohol, the thermocouples are laid in place and small disks of solder, *S*, formed in the same manner as above described for the receivers, except that they are flattened out without first removing the rosin, are laid upon the ends of the couples where they cross the platinum wires at *S*. The solder on the platinum wires is then melted by touching it with the nichrome loop.

The masses of the couples so constructed are exceedingly small. The mass of the entire couple *A*, *B*, or *C* is approximately $\frac{1}{30}$ to $\frac{1}{40}$ mg, while the mass of the portion heated by the incident stellar radiation is only 0.012 mg. The metal strips forming the couple are

[1] *Zeitschrift für Instrumentenkunde*, **18**, 65, 1898.

[2] *Scientific Papers, Bureau of Standards*, **17**, 188, 1921.

each approximately 3 mm long and 0.008 × 0.10 mm in cross-section, and the receivers are $\frac{1}{2}$ mm in diameter by 0.009 mm thick. The resistance of course depends on the metals employed, but generally is 8 to 20 ohms.

VACUUM EFFECTS

Lebedew[1] determined the law of sensitivity change with change in pressure for a constantan-platinum couple, and found that for the blackened couple the increase was 7.4 times and for the unblackened couple 34 times, for the highest vacuum attained, estimated less than 0.0001 mm. Pfund[2] found an increase of "six times," and Coblentz[3] a "four and one-half fold" increase. In the present investigation we have found increases of two to eleven fold for the vacuum effect.

The effect of the vacuum on the sensitivity does not appear to be the same for all thermocouples, even of the same construction and materials, though the effect of differing materials seems to be the most pronounced. Graphs of the galvanometer deflection against the pressure for three thermocouples are given in Figure 2. It will be seen that the vacuum has little effect upon the sensitivity until the region of 1 mm mercury pressure is reached. Then for the Ag-Te couple the entire increase takes place between 1 mm and 0.01 mm, while the Bi-Bi Sn couple shows an increase of 20 per cent between 0.01 mm and 0.0001 mm. From this it appears that the vacuum which must be maintained in order to keep the sensitivity constant depends on the metals employed in the thermocouple. Thus for Ag-Te couples a vacuum of 0.01 mm is sufficient; but for Bi-Bi Sn this vacuum would occur on a steep part of the curve and in order to insure constant sensitivity a vacuum of 0.0001 mm should be maintained.

A general explanation of the character of the curve is easily given. It is known that the thermal conductivity of a gas is independent of the pressure until the region of 1 mm is reached, when it begins to drop rapidly to zero as the mean free path of the molecules becomes comparable to the dimensions of the container.

[1] *Annalen der Physik*, **9**, 209, 1902.

[2] *Physikalische Zeitschrift*, **13**, 870, 1912.

[3] *Bulletin of the Bureau of Standards*, **11**, 636, 1915.

The thermal conductivity also depends on the nature of the gas; for hydrogen it is much greater than for any other. This should make a thermocouple less sensitive in this gas than in air, say. Figure 2 shows how this effect appears in the sensitivity curves when this gas is employed.

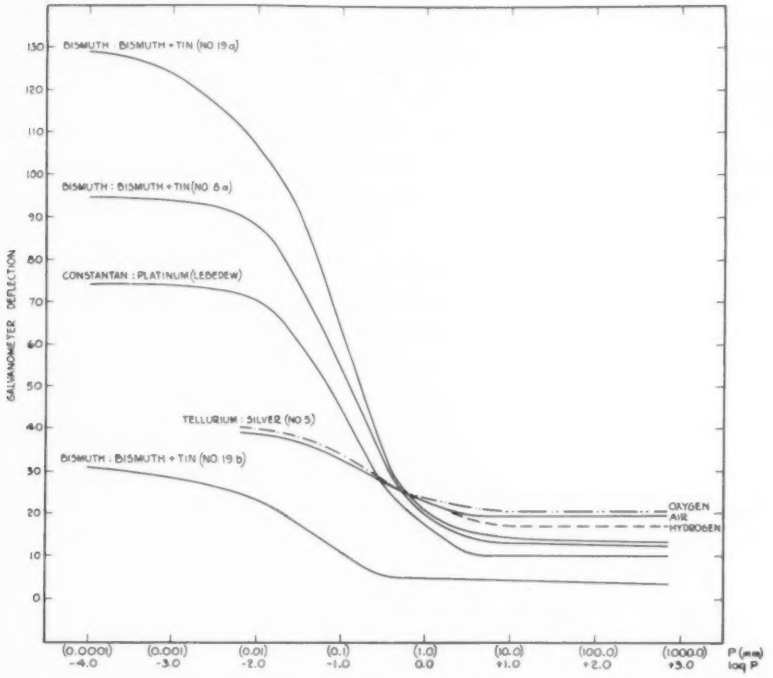

FIG. 2.—Variation of thermocouple sensitivity with pressure

The use of metallic calcium to maintain the vacuum has been studied by both Soddy[1] and Coblentz.[2] The calcium is heated while the pump is in operation to remove the hydrocarbon vapors. We have found it necessary to pump a considerable time to remove these gases completely. After the vacuum has been raised by the pump to a desired limit, it may thereafter be brought back to this point by merely heating the calcium tube to a low red heat with a small electric heater or lamp. After the lamp is removed the

[1] *Proceedings of the Royal Society*, A, **78**, 429, 1907. [2] *Op. cit.*, **11**, 625, 1915.

absorption of the gases continues for about twenty minutes until the tube has cooled considerably.

Coblentz uses a discharge between two platinum terminals inserted in that part of the tube connecting the calcium tube to the thermocouple cell, to test the degree of evacuation obtained while heating the calcium. Since our cells are made of Pyrex glass, it was not feasible to use sealed-in electrodes for this purpose; outside electrodes were therefore substituted. It was found, however, that after the discharge passed, the sensitivity decreased to about 30 per cent to 50 per cent and remained at this level for some hours. On opening the stop-cock to the pump which was maintained at about 0.001 mm pressure, the sensitivity immediately rose to normal again, and this could be repeated at will. Apparently the discharge did not produce a change in pressure, for none was detectable on opening the stop-cock to the gauge. On this account, the discharge test was discarded and tests of the sensitivity by use of a standard lamp were substituted. This is more satisfactory in another way, for it gives a quantitative test of the sensitivity which the discharge test does not give, and all that is necessary is to heat the calcium tube till the sensitivity rises to normal.

SOME PROPERTIES OF VACUUM THERMOCOUPLES

In thermocouples of these small dimensions some interesting properties were observed. Generally in a compensated couple, such as Figure 1 (*A*, *B*, *C*), the two junctions do not give the same deflections, i.e., the compensation is not exact. One case was observed in a couple of Bi-Bi Sn where the deflections for the two junctions were 125 mm and 25 mm and both in the same direction, the current flowing normally across the first junction and in reverse across the second. How this could occur we are unable to explain. As a rule, however, the compensation is so complete that, while observing star deflections, we can turn on all the lights in the dome, without disturbing the galvanometer. With this couple the Peltier effect was quite pronounced. When a deflection was observed with the first junction, the galvanometer mirror swung rapidly at first, then suddenly slowed down and crept up to maximum over 8 or 10 mm, but when a deflection was observed with

the second junction the galvanometer mirror over-ran its maximum 2 or 3 mm and returned to normal deflection after one or two seconds.

The absorbing power of the black paint of course depends on the wave-lengths of the incident radiation, being somewhat greater for the shorter waves. Coblentz has found that the reflecting power of this paint is only about 2 per cent. Tests were made with both blackened and unblackened sides of the receivers turned to the window admitting the radiation. The ratio of deflections for the unblackened side to the blackened side was $\frac{1}{3}$ to $\frac{1}{4}$. It was thought that the sensitiveness of the couple might be increased by blackening, on both sides, the entire couple and strips except the receiver, but the effect was very slight. Several couples were repainted after testing, but this seemed to have little effect on the sensitivity.

The efficiency of a thermocouple is exceedingly low. An approximate value of this quantity may be obtained from data relating to the sensitivity tests of No. 19, for example. This efficiency is the ratio between the electrical energy produced and the quantity of the incident radiation, expressed in the same units. If W is the wattage of the lamp, D its distance from the couple, r the radius of the receiver of the thermocouple, R its resistance, i the galvanometer sensitivity in amperes, S the observed deflection, then the efficiency is

$$E=\frac{4R(DSi)^2}{Wr^2}. \qquad (2)$$

Now for No. 19, $W=90$, $r=\frac{1}{4}$ mm, $R=20$ ohms, $D=3000$ mm, $S=125$ mm, $i=4.75\times10^{-10}$ amp./mm. Hence, $E=4.5\times10^{-7}$, i.e., only about half a millionth of the incident radiation actually produces deflection in the galvanometer. Of course we are assuming a uniform distribution of radiation about the lamp, and neglecting the heat convected away from it, as well as the absorption of the air through which the beam must pass. For a value of E so small, however, these quantities could hardly affect the order of the result.

We may approach the problem in another way. The receiver of the thermocouple will continue to increase in temperature until

the heat lost and converted into electrical energy equals the amount being absorbed from the incident ray. The ratio of the heat converted into electrical energy to the total heat received is the desired value of E. As was seen in equation (1), since the thermocouple is in a vacuum, the only sources of lost heat are the quantity C, conducted away by the strips, and the quantity radiated, r.

In order to determine these values, let us assume the temperature at which the couple is working to be 20° C., and that a difference of 1° C. between the two junctions is produced by the incident radiation. Let us take couple No. 19 already cited. Since the area of the receiver is about $\frac{1}{5}\times 10^{-2}$ sq. cm, and since, as already seen, it radiates about $\frac{1}{3}$ as much from the unblackened as from the blackened side, then Stefan's law becomes

$$r=\tfrac{1}{3}\times\tfrac{1}{5}\times 10^{-2}\times 1.28\times 10^{-12}(T_1^4-T^4)\text{ cal./sec.}=$$
$$3.4\times 10^{-15}(T_1^4-T^4)\text{ cal./sec.} \quad (3)$$

and since $T_1=293$ and $T=292$, then

$$r=3.4\times 10^{-7}\text{ cal./sec.}$$

The amount conducted away varies directly as the cross-section of the metal strips A, and inversely with their length L, the constant of proportionality K being the amount conducted through one centimeter cube in one second per degree centigrade. This constant for bismuth is 0.02 cal./sec. Since there are two strips 3 mm long at each junction, one of which contains only 5 per cent tin, we may compute the heat conducted through one strip and call the total amount just double this. Hence the amount of heat conducted away is

$$C=\frac{2KA}{L}\text{ cal./sec.}=2\times 0.02\times 0.000008\times 3\text{ cal./sec.}$$
$$=9.6\times 10^{-7}\text{ cal./sec.} \quad (4)$$

Now the amount of heat, I, converted into electricity, expressed in cal./sec., varies directly with the square of the thermoelectric power p, the square of the difference in temperature ΔT, and the reciprocal of the resistance R, the constant of proportionality being

the Joule equivalent, 0.24. Since $\Delta T = 1°$ C., p = about 50×10^{-6} volts, and $R = 20$ ohms, we have

$$I = \frac{0.24(p\Delta T)^2}{R} \text{ cal./sec.} = \frac{0.24 \times (50 \times 10^{-6})^2}{20} \text{ cal./sec.} = 3 \times 10^{-11} \text{ cal./sec.}$$

The efficiency then is

$$E = \frac{I}{r + C + I} = \frac{3 \times 10^{-11} \text{ cal./sec.}}{3.4 \times 10^{-7} + 9.6 \times 10^{-7} + 3 \times 10^{-11} \text{ cal./sec.}} \qquad (5)$$

or

$$E = 2.3 \times 10^{-5}.$$

These low values of the efficiency computed here are in part due to the small range in temperature over which the thermocouple works. From the principle of Carnot's Cycle it is known that the efficiency of the theoretically perfect heat engine is

$$E = \frac{T_1 - T}{T_1}. \qquad (6)$$

The efficiency of the thermocouple, then, considered as a converter of available heat, may be obtained by multiplying the values of E found in equations (2) and (5) by the reciprocal of equation (6). For equation (2) the value of T_1 is the room temperature at which the thermocouple was tested, which was 293° C. absolute. The difference in temperature $(T_1 - T)$ between the hot and cold junction for this thermocouple will be shown in equation (7) to be 16×10^{-5} deg. C. per mm deflection. Since in equation (2) the deflection was 125 mm, then $(T_1 - T) = 2 \times 10^{-2}$. The value then of $T_1/(T_1 - T)$ is 1.5×10^4. Multiplying the value of E obtained in equation (2) by this coefficient, we obtain for the relative efficiency $E = 6.7 \times 10^{-3}$. For the value of E in equation (5) $T_1 = 293$, $T = 292$, which gives for the coefficient 2.93×10^2. Multiplying the value of E in equation (5) by this quantity we obtain for the relative efficiency $E = 6.7 \times 10^{-3}$. It is, then, theoretically possible to construct a thermocouple over one hundred times as sensitive as No. 19 considered here.

Ganot states that Clamond's thermoelectric battery of Fe-Sb Zn heated directly with coal gas under favorable conditions has an efficiency of $E = 5 \times 10^{-3}$.

Some attempts to prevent the losses by radiation have been made by placing the couple at the center of curvature of a hemispherical mirror, the radiation being admitted through a hole in its center. We have not found it possible to apply this principle with the present apparatus since a slight displacement of the junction would render the mirror inactive. Again this would be effective on only one junction. The effect of a hemispherical mirror would be to reduce the losses by radiation to that emitted by the unblackened surface of the receiver, which is approximately one-fourth of the whole amount. Reducing the value of r in equation (5) to one-fourth of its value, we obtain a value for E which is just five-fourths its original value. Hence we may say that the effect of a hemispherical mirror is to increase the sensitivity one-fourth, assuming the mirror to reflect perfectly and the central hole to be of negligible area. In the case of the stellar thermocouples, Figure 1, *B* and *C*, the increase would be only one-eighth when the method of double deflections is used.

It is of interest to know the temperature sensitivity of the thermocouple. This may be determined from the current relations in the circuit.

Let us determine what change in temperature of the receiver will be required to give a deflection of 1 mm on the scale. If we let

P = the potential produced in the circuit expressed in volts
p = the thermoelectric power of the junction in volts
i = the sensitivity of the galvanometer in amperes/mm
R = the total resistance of the circuit
Δt = the required change of temperature in deg. C.
T = temperature of cold junction

then all the constants are known for any particular couple. Let us take No. 19 cited above. Here p normally should be about 150×10^{-6} *V*, but on account of the impurity of the bismuth, probably it is not greater than about 60×10^{-6} *V*. $i=4.75\times10^{-10}$ amp., $R=20$ ohms. Then

$$\Delta t=\frac{P}{p}=\frac{iR}{p}=\frac{4.75\times10^{-10}\times20}{60\times10^{-6}}=16\times10^{-5}\text{ deg. C.} \qquad (7)$$

and with a more sensitive galvanometer this figure could easily be pushed to one-millionth of a degree.

Since deflections of about 150 mm are employed ordinarily on recording apparatus, the difference in junction temperature must be approximately 2.4×10^{-2} deg. C. at maximum working deflection for the galvanometer employed. We may now form an estimate of the speed of action of the couple.

We may state the speed of action in terms of the time required for the heat to travel from the blackened face of the receiver to the junction on the rear side and reach a state of steady flow. The increase $\Delta t_2 = 2.4\times10^{-2}$ deg. C. is that reached by the rear side of the receiver after the steady state is established. To determine the time required, it will be necessary to know the increase in temperature of the front (blackened) face also. This is given by

$$W = \frac{k(\Delta t_1 - \Delta t_2)}{u} \text{ or } (\Delta t_1 - \Delta t_2) = \frac{Wu}{k} \tag{8}$$

where W is the rate at which heat flows through unit cross-section, k is the conductivity, $\Delta t_1 - \Delta t_2$ is the difference of temperature between the two faces and u is the thickness of the receiver in cm. Now $W = (C_1 + R_1)/A$, where C_1 = heat conducted away along the two strips, R_1 = heat radiated from the rear face, and A is the area of the receiver in square centimeters.

Now taking couple No. 19 again as an example,

$$\begin{aligned} C_1 &= \Delta t_2 C \text{ [where } C \text{ is the value in eq. (4)]} \\ &= 2.4\times10^{-2}\times9.6\times10^{-7} \text{ cal./sec.} = 2.3\times10^{-8} \text{ cal./sec.} \end{aligned} \tag{9}$$

The amount radiated from the rear face is given by

$$R_1 = \tfrac{1}{3}\times\tfrac{1}{5}\times10^{-2}\times1.28\times10^{-12}[(T+\Delta t_2)^4 - T^4]. \tag{10}$$

Let $T = 293°$ C. then

$$R_1 = \frac{1.28\times10^{-14}}{15}\times2.4\times10^{6} = 2.0\times10^{-9} \text{ cal./sec.},$$

hence the total loss is 2.5×10^{-8} cal./sec. and the value of W is

$$W = 2.5\times10^{-8}\times5\times10^{2} \text{ cal./sec.} = 1.25\times10^{-5} \text{ cal./sec.} \tag{11}$$

and from equation (8)

$$\Delta t_1 - \Delta t_2 = \frac{1.25 \times 10^{-5} \times 10^{-3}}{16 \times 10^{-2}} = 7.8 \times 10^{-8} \text{ deg. C.} \qquad (12)$$

This is the stable condition and is reached only after an indefinite period of time. Since $\Delta t_1 - \Delta t_2$ is insignificant compared to the value of $\Delta t_2 = 2.4 \times 10^{-2}$ deg. C., we may neglect it in the following computation. Let us inquire what time will be required for the rear face to reach a temperature 99 per cent of the steady state, i.e., the time required for the thermoelectric current to reach 99 per cent of its value under the influence of the incident radiation. We have Fourier's equation for the flow of heat

$$\frac{\Delta t_2}{\Delta t_1} = 99 \times 10^{-2} = \frac{2}{\sqrt{\pi}} \int_{\frac{u}{2h\sqrt{t}}}^{\infty} e^{-\beta^2} d\beta \qquad (13)$$

Since $u = 10^{-3}$ cm, $h^2 = 0.4$, this gives us

$$t = 6.2 \times 10^{-3} \text{ sec.}$$

It follows then that the lag of the thermocouple is negligible when applied to recording apparatus. If we multiply the equation (10) by the factor 4, we obtain the total radiation from both faces of the receiver. This gives us 8×10^{-9} cal./sec. as the loss by radiation. This is only one-third the loss by conduction along the strips, which is 23×10^{-9} cal./sec. Hence the desirability of using substances of low heat conductivity for the strips.

APPLICATIONS TO THE ASTROPHYSICAL PROBLEMS

1. *Stellar radiation problems.*—To observe the total radiation from stars, the thermocouple is mounted on a plate provided with a low-power eyepiece and water cell which can be moved in front of the thermocouple or moved away by means of a lever on the face of the plate. The apparatus is adapted to the Newtonian double-slide plate holder of the 100-inch telescope. A four-wire cable 135 feet long connects the thermocouple with the galvanometer room in the basement of the dome. Two of these wires are used for the thermo-

couple circuit, and the other two connect the observer at the telescope with the observer at the galvanometer by telephone. The deflections are obtained by orienting the thermocouple so that the line connecting the two receivers is parallel to one of the guiding screws, and by shifting the receivers alternately upon the star image with a half-turn of this screw.

In order to test the fundamental sensitivity of the thermocouple during the observations, an electric lamp (100-watt "Peerless" mazda) is placed on a bracket in the Cassegrain plate holder. The light from this lamp is reflected from the Cassegrain flat to the Newtonian flat and is received by a small lens at the Newtonian plate holder and projected on the thermocouple. When not in use, the lens may be swung aside and the lamp turned off.

Two types of galvanometer have been employed, viz., Leeds and Northrup high sensitivity D'Arsonval No. 2285, and more recently the Coblentz-Thompson galvanometer of the same make. Of the D'Arsonval galvanometers, two of different electrical properties have been used. No. (1) has a period of 4.44 seconds, resistance of 9.1 ohms, and mirror sufficiently flat to use a scale at 8 m, which gives a sensitivity of 4.75×10^{-10} amp./mm. No. (2) has a period of 6.5 sec., resistance of 17.4 ohms, and sensitivity of 3.1×10^{-10} amp./mm with scale at 8 m.

This latter galvanometer had a mirror $\frac{5}{16}$ inch in diameter with very good figure when tested in the Pasadena laboratory, so good in fact that a scale could be read at 11 m. When the galvanometer was taken to Mount Wilson and set up in the 100-inch dome at a temperature of 34° F., the figure became so bad that a scale could scarcely be read at 1 m, and the projected image of a lamp filament at a distance of 4 m was a band 7 mm broad with sharp edges and dark center. On removing the galvanometer to Pasadena the figure was restored. The mirror was then detached and the beeswax which covered the entire back and was used as a cement to attach it to the moving coil was removed, and the mirror attached to the coil again by a bit of universal wax placed in the center of the back. This procedure effectually removed the annoying change in figure of the mirror, which has since performed admirably, although subjected to temperatures below freezing.

No. (1) was placed under a bell jar and subjected to variations in pressure. No change in sensitivity was observed, even when the pressure was reduced to 10^{-3} mm. At this pressure the period was reduced 4 per cent, while an enormous drift was introduced which could not be removed even by grounding various parts of the galvanometer.

Both visual and photographic methods have been employed to observe the galvanometer deflections. Visually two methods have been used. When the scale was at 8 m the highest power telescope it was found feasible to employ was approximately 45. But by placing a spectacle lens of 6 m focus directly in front of the galvanometer mirror and observing the image with an eyepiece with cross-hair in the field, a power of 350 could be employed advantageously, and the scale read with accuracy to tenths of a millimeter.

When visual observations are made, the drift of the galvanometer is difficult to allow for. This drift can be reduced to a minimum by inclosing the thermocouple cell in a wad of cotton wool, and surrounding the galvanometer by a double wall box, the space also being filled with cotton. With this arrangement the observed drift of the D'Arsonval galvanometer is at most only 1 or 2 mm per minute, and is often absent. By taking the observations at regular intervals, keeping the star on the receiver in the meantime, an approximate value of the drift may be obtained.

The method which we have adopted at Mount Wilson consists in recording photographically the deflections and drift. The photographic plate 7×17 inches, or 8×10 inches, is carried by a slide moving in cast-iron ways, which is driven by a screw so that the film is always in the focal plane of a cylindrical lens of semicircular cross-section, $\frac{1}{2}$-inch aperture and 8 inches long, set with its axis at right angles to the motion of the plate. The image of a straight filament lamp, formed by the spectacle lens before the galvanometer mirror, is at right angles to the axis of the cylindrical lens. That portion, then, which the lens intercepts, will form a point image on the plate, which in turn registers the motion of the galvanometer. The plate is driven 2 cm a minute by a motor-driven gear from which a large range of speeds can be had.

Plate VII is a reproduction of photographic records of Vega (mag. 0.1), Arcturus (mag. 0.2), α Herculis (mag. 3.0), and R Hydrae (mag. 8.0), respectively, made with this apparatus on the same night and reduced to one half the original scale. The larger deflections, on the left, for each star were taken without a water cell, those on the right with a water cell 1 cm thick interposed in the beam. The increasing absorption of the water cell with the advance in spectral type is well shown, as is also the increase in total radiation for a given magnitude. The effects of poor seeing are well shown in the deflections for α Herculis without the water cell.

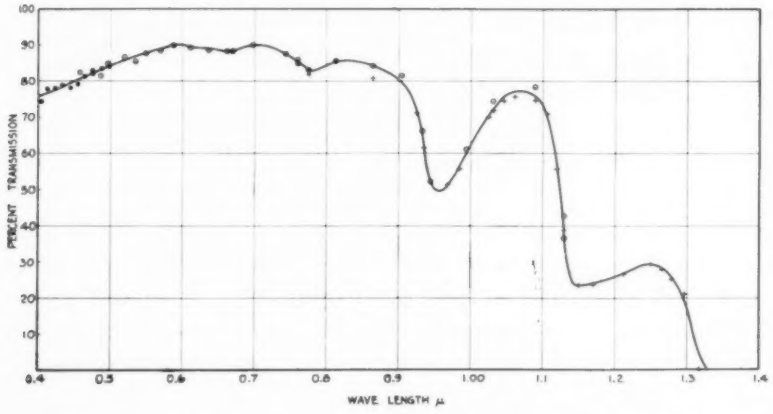

FIG. 3.—Transmission of a water cell 1 cm thick, having windows of microscope cover-glass 0.12 mm thick.

The water cell employed in these observations consists of a brass cylinder 1 cm long with microscope cover-glasses 0.12 mm thick cemented to the two ends. The transmission curve of this cell, filled with distilled water, as observed with the thermocouple in the Pasadena laboratory, is shown in Figure 3. From the curve it will be seen that very little energy is transmitted beyond 1.1 μ and none at all beyond 1.4 μ. It will also be noted that star deflections observed through the water cell cannot exceed 90 per cent of the deflections observed without it.

2. *Solar applications.*—The problems to which we have thus far applied the thermocouple may be listed as follows: (1) registration of the spectral energy curve of the sun; (2) registration of drift

PLATE VII

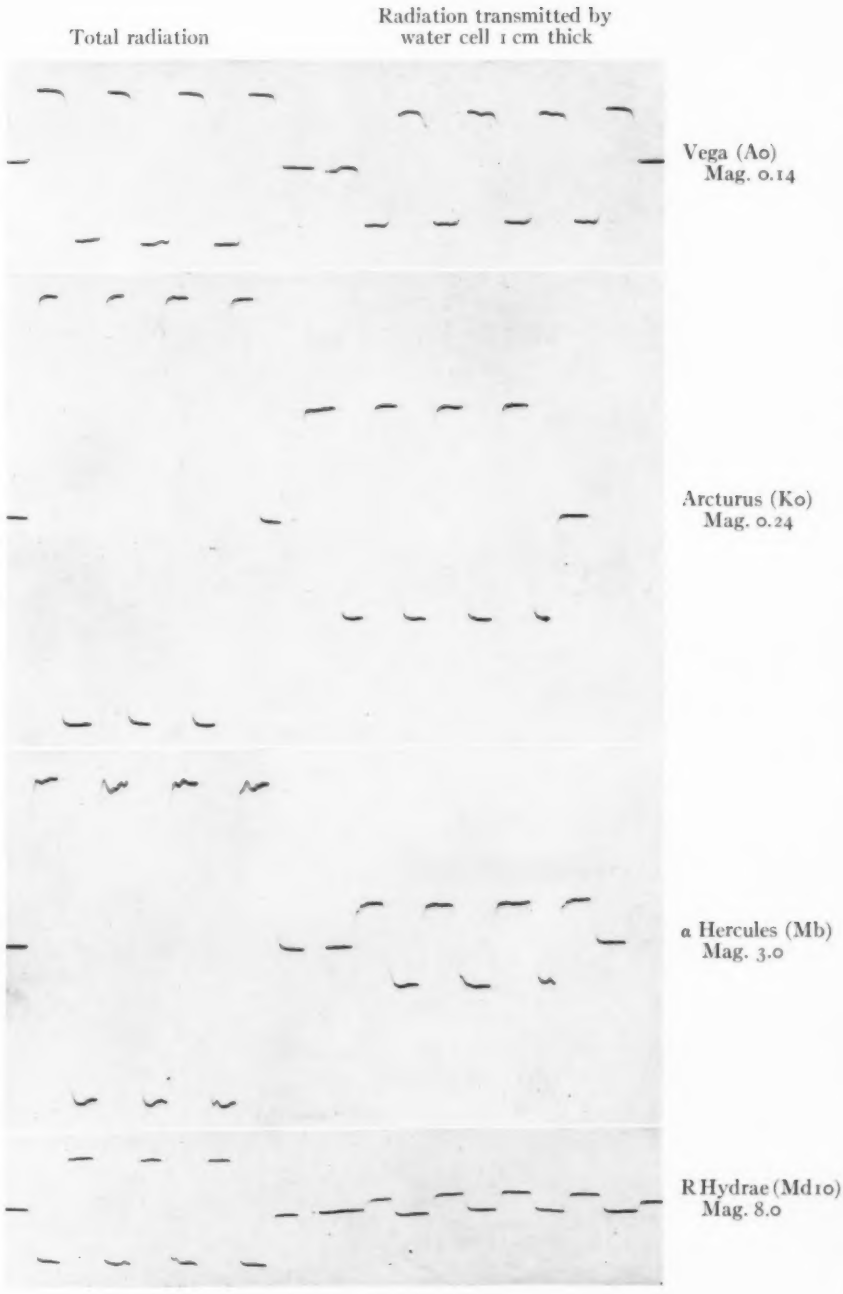
Total radiation
Radiation transmitted by water cell 1 cm thick
Vega (Ao) Mag. 0.14
Arcturus (Ko) Mag. 0.24
α Hercules (Mb) Mag. 3.0
R Hydrae (Md10) Mag. 8.0

PHOTOGRAPHIC RECORDS OF GALVANOMETER DEFLECTIONS MADE BY STARS OF VARIOUS SPECTRAL TYPES

curves across the disk in various wave-lengths; (3) energy relations across sun-spots and faculae.

The apparatus employed in these investigations consists of the photographic registering apparatus already described. For studying the energy relations across spots and faculae the apparatus is mounted on the head of the spectrograph of the 150-foot tower telescope. The thermocouple is contained in a wooden case carried horizontally by a screw-driven plate, which is connected by a back gear to the driving shaft of the photographic registering apparatus. A paper-covered metal shield, perforated with a needle point, is attached to the thermocouple case directly above one of the receivers in such a way that the needle hole can be adjusted by means of a screw so that the light from the solar image passing through it will fall on the receiver. An aperture in the side of the case, closed by a cork, enables the observer to effect this adjustment.

The spot is now brought by the slow motions of the coelostat in line with the pin hole, and the photographic registering apparatus set in motion. By means of the back gear, the ratio is so adjusted that the thermocouple is driven about 1 cm while the photographic plate travels 20 cm. The galvanometer, which is set on an arm of the spectrograph head, is connected to the photographic registering apparatus by means of an aluminum box 1 m long, which shuts out the light of the room from the cylindrical lens. By this apparatus the total radiation curve across the spot is obtained. By rotating the spectrograph head, curves may be obtained across the spot in any direction.

THE REGISTERING MICROPHOTOMETER

In 1912 Koch first introduced the principle of the registering microphotometer, using a photo-electric cell and string electrometer as the registering device. The curves were photographically registered on a falling plate controlled by clock work. In 1915 Stetson[1] modified the apparatus by substituting a thermopile and galvanometer for the photo-electric cell and electrometer, thus making the apparatus simpler and freer from the annoyances to which the photo-electric cell is subject. Stetson's apparatus

[1] *Astrophysical Journal*, **43**, 253, 1916.

was read visually and was not a self-recording apparatus. In 1921 Moll[1] applied the self-registering principle to the thermocouple, the negative and plate being driven by hand. In both Stetson's and Moll's apparatus the thermocouple operated at atmospheric pressure.

The new registering microphotometer now in use at Mount Wilson was built in the Pasadena shop after designs by Mr. Babcock and set in operation in 1914. The photo-electric cell and string electrometer were employed by him as in Koch's apparatus. The modifications introduced by Babcock consisted in (1) moving the plate by a motor-driven screw, (2) providing for plates 15 cm × 100 cm, (3) introducing a gear shift between the moving microscope stage and plate screw so that a number of magnifications of motion between the negative and moving plate could be used, (4) use of a cylindrical lens in place of a slit before the moving plate, and (5) taking all light used in the apparatus from one Nernst filament. The modifications introduced by us consist in (1) replacing the photo-electric cell and electrometer by a vacuum thermopile and D'Arsonval galvanometer, (2) the use of both sunlight and a nitrogen-filled straight-filament lamp as sources of illumination, (3) adding a second microscope for setting purposes, (4) introducing an adjustable second slit before the thermopile, (5) projecting an illuminated slit upon the photographic film as in Moll's apparatus instead of limiting a large beam by means of a slit directly above the film as in Koch's machine, and (6) the introduction of parallel silvered plates into the barrel of the microscope to increase the field of the objective and the deflections of the galvanometer.

Plate VIII shows the machine as it is now used, arranged for solar illumination. The whole instrument rests on a cast-iron bed-plate *AB*, 12 ft. long and 28 in. wide, which stands on a cement pier. The photographic registering device *C* and the traveling microscope stage *D* are connected by the shift-gear box *G* and driven by the motor *M*. The plate carrier *K* carries the plate *P* horizontally past the cylindrical lens *L*, and is moved by the long screw *Sc* of 2 mm pitch in the casting below. By means of two mirrors the

[1] *Proceedings of the Physical Society of London*, **33**, 207, 1921.

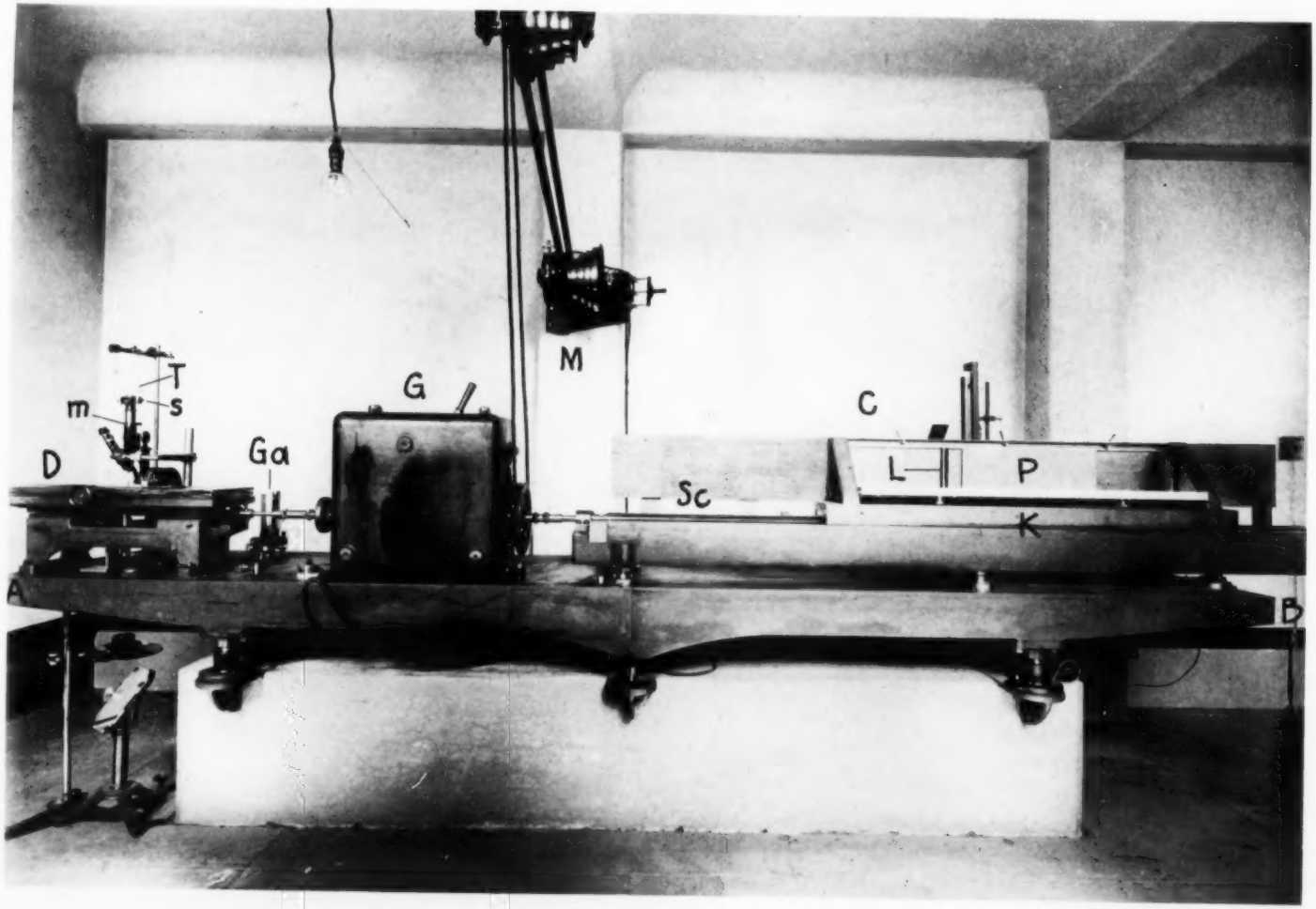

THE REGISTERING MICROPHOTOMETER

image formed by the galvanometer mirror is made to play up and down along the cylindrical lens, and thus the curves are produced. The microscope stage *D* rests on four steel balls and is driven by a screw of 1 mm pitch connected to the gear box *G*, in the same direction as the photographic plate *P*. By means of the gear box *G* the ratio of speeds between *C* and *D* may be varied from two to fifty fold. The microscope *m* contains at its upper end an adjustable slit *S* above which the thermopile *T* is placed. Lead-wires from the thermopile are connected with the registering galvanometer *Ga* on the bed plate of the instrument. A motor is also provided to drive the machine at high speed so that the plate may be returned to starting position when several curves are being compared. In this way all the runs may be made in the same direction, thus eliminating the lag of the galvanometer, due to its period.

In securing a curve representing the energy relations across a spectral line in a photograph, it is obvious that in order to avoid distortions of the curve it will be necessary to employ as narrow an element of the line as possible. This means, in effect, that the magnification of the microscope *m* should be large and that the second slit *S*, which limits the beam reaching the thermopile, should be narrow. There is, however, a limit to the width of the slit *S*, since too narrow a slit will introduce irregularities due to the clustering of silver grains in the film, or dust and defects in the film. With the present apparatus these irregularities begin to appear when the slit width is reduced to about 0.1 mm for the negatives employed. For very fine-grained plates this limit can of course be further reduced.

In order to remedy this defect it will be necessary to integrate over a greater length of line than is available with Koch's arrangement. The device adopted to facilitate this is shown in the diagram of the optical system now employed (Fig. 4). Artificial light or sunlight passes through a condenser and falls on a slit S_1, an image of which, formed by the objective O_1, is projected on the spectral line *L* of the negative on the moving microscope stage. An image of this illuminated portion of the spectral line *L* is pro-

jected by the microscope objective O_2 on to the second slit S placed just in front of the thermopile T. By means of the two parallel mirrors M_1, M_2 the portions of the beam which would otherwise fall outside of the field are thrown back upon the thermopile and become effective. From tests it was found that the 40 mm objective employed had fair field over 10°, so that a spectral line 9 mm long could be employed. By adjusting the length of the slit S_1, or the distance from the mirrors M_1, M_2 to the objective O_2, the field may be limited to this value. The full lines indicate the path of the rays in the present arrangement, and the dotted lines the same for the arrangements of Koch and Moll.

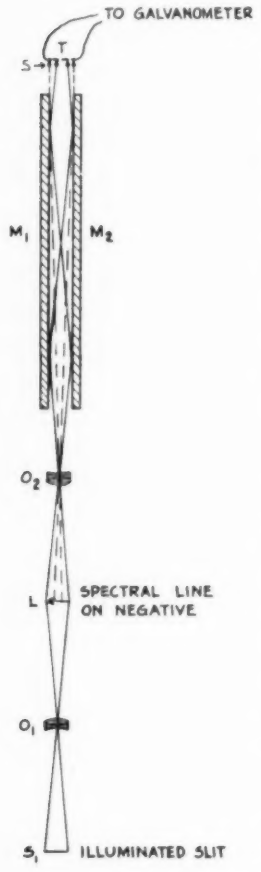

FIG. 4—Optical system of the registering microphotometer.

By adjusting the width of the first slit S_1, only that portion of the spectral line L is illuminated which is included in the image which passes through the second slit at S. This device employed by Moll reduces the scattering of the light in the film, but probably its greatest advantage is in eliminating the use of the first slit just above the moving plate at L, thus facilitating the adjustment of the negative.

When the thermocouple is employed to replace the photo-electric cell on the registering microphotometer, no means is available for compensating the apparatus against changes in the intensity of the illumination used. No mention of this is made in the descriptions of the apparatus employed by Stetson and Moll, who used storage batteries as a source of current for the illumination. While we cannot compensate the thermopile, we may, at the same time, however, register the variations in the illumination by

projecting a portion of the beam incident on the first slit S_1, on a second thermopile and registering the fluctuations in intensity on the photographic plate by means of a second galvanometer of the same period as the one employed with the first thermopile T. The results of investigations with the apparatus and methods here described will appear in a future paper.

MOUNT WILSON OBSERVATORY
July 1922

THE ELECTRIC FURNACE SPECTRUM OF IRON IN THE ULTRA-VIOLET, WITH SUPPLEMENTARY DATA FOR THE BLUE AND VIOLET[1]

By ARTHUR S. KING

ABSTRACT

Electric furnace emission and absorption spectra of iron in the ultra-violet, for various temperatures from 1400° to 2600° C.—This paper supplements one published in 1913 on the iron furnace spectrum from λ 3884 to λ 7208. Furnace emission spectra extend into the ultra-violet only as far as the continuous spectrum of a black body at the same temperature. It has now been found, however, that by using a very hot source, such as a gas-filled tungsten lamp or a series of fine wires exploded by Anderson's method, absorption spectra corresponding to either low or high temperatures of the vapor may be obtained extending to λ 2298 or beyond. The relative intensities in absorption spectra are the same as in emission spectra of the same temperature. A large number of spectrograms have been made in the first and second orders of a 15-foot concave grating. Tables I–III contain the *temperature classification of 904 lines, λ 2298 to λ 3878*, and the relative intensities in the arc and in high, medium, and low temperature furnace spectra, either emission or absorption, upon which the classification is based. For iron, the low-temperature lines, classes I and II, are well developed at 1600°, the medium, class III, at 2000°, and the high-temperature lines, class IV, at 2300°. About sixty lines, of various classes, are relatively very weak in the arc; they are denoted by I A, II A, etc. A *revised classification of 262 lines, λ 3884 to λ 4531*, based on later spectrograms, is given in Table IV; and Table V contains a list of the most persistent low-temperature lines, the twenty-one from λ 3745 to λ 4482 emitted by the vapor at 1400°, as photographed by long exposure with a 1-meter concave grating. On Plate XI a high-temperature absorption spectrum is shown between two arc spectra.

Discussion of the significance of the temperature classification of spectral lines.—Work with various metals indicates a parallelism between the successive temperature excitation stages and the radiation stages as the potential is increased in low-voltage vacuum arcs. For high boiling-point metals, the classification can perhaps be more readily made by the furnace method. To assist in the correlation of the two types of classification, elements which may have their spectra excited in either way should be carefully studied in both ways.

A paper on the electric furnace spectrum of iron from λ 3884 to λ 7208 was published by the writer[2] in 1913. The present paper begins at the violet limit of the former investigation and extends the study to λ 2298, which is as far as it has been possible to obtain lines by means of the furnace. Within this range, the lines given in tables of arc wave-lengths are covered with reasonable completeness, the missing lines generally being very faint in the arc or of the enhanced-line type, both of these classes requiring, as a rule, the stronger excitation of the electric discharge. As in other studies of

[1] *Contributions from the Mount Wilson Observatory*, No. 247.

[2] *Ibid.*, No. 66; *Astrophysical Journal*, **37**, 239, 1913.

furnace spectra, the purpose has been to show the changes in relative line intensity through various furnace temperatures and into the conditions of the arc, and from these data to classify the lines according to the temperatures at which they first appear and their rates of growth as the temperature rises.

The temperature stages for this purpose must be selected for each element according to the observed changes in its spectrum, and it is desirable that at each stage there be a marked change from the spectrum at the stage below. For iron, the low-temperature spectrum was found to be well developed at 1600° C. and the plates for this group of lines were taken from 1600° to 1700°. For the medium temperature, at which another set of lines appears, about 2000° was used. The high-temperature spectrum develops at about 2300° and still higher temperature has little effect beyond increasing the reversals and giving general intensification. Nevertheless, temperatures of 2500° to 2600° were used for most of the high-temperature spectra, in order to obtain the full effect of the conditions corresponding to this stage.

The same methods of classification have been used as in previous studies, but an important new feature is the use which has been made of absorption spectra, obtained by methods described in recent papers,[1] and by others still more recently developed.

It was noted in the first paper on the iron spectrum, and has been many times confirmed for this and other spectra, that at a given temperature of the furnace the emission spectrum stops at a point in the ultra-violet somewhat short of the limit of the continuous spectrum given by a black body at the same temperature. A close approach to such a black body is easily obtained by placing a graphite plug in the central part of the tube and heating the furnace to the temperature previously used for the emission spectrum.

A limit is thus set to the wave-length range within which the furnace at a certain temperature can give emission lines, and if appearance at this temperature is the criterion indicating that lines belong to a certain class, all lines of shorter wave-length automatically go into a higher class. It is often the case, however,

[1] *Mt. Wilson Contr.*, Nos. 174, 233; *Astrophysical Journal*, **51**, 13, 1920; **55**, 380, 1922.

that the lines of shorter wave-length, when produced by the furnace at a higher temperature or in the arc, show no features that would distinguish them from those in the region given by the low-temperature furnace. This forced distinction, due to the fact that the furnace cannot emit beyond a certain point, was noted in the study of the spectrum of calcium, strontium, barium, and magnesium.[1]

In the present investigation, trials were made to see if iron vapor at low temperature would absorb radiation of shorter wave-length than it was able to emit. This proved to be the case. When a beam of white light from a very hot source was passed through the moderately heated furnace, iron absorption lines appeared as far in the ultra-violet as the solid body was able to build up a continuous spectrum; and by using successively hotter sources behind it, the furnace at 1600° C. gave absorption lines as far as λ 2298. The emission spectrum at this temperature ends at λ 3440, though this is due partly to the fact that for a considerable range below this, no low-temperature lines occur.

There seems to be no reason why ultra-violet absorption lines obtained in this way should not be classed as low-temperature lines. A stellar spectrum produced by sufficient difference of temperature between the body of the star and cool iron vapor surrounding it should show no difference (disregarding atmospheric absorption) between these lines and the low-temperature lines of the visible spectrum.

It has therefore been considered legitimate to use the absorption spectrum for a certain temperature stage as a means of extending the data beyond the point where the emission lines die out. This has resulted in a division of the tabulated lines into three sections. In Table I, from λ 2298 to λ 2808, the comparison is between the absorption spectra at high and low temperatures. Both of these extend to shorter wave-lengths than the corresponding emission spectra. At high temperature, however, it has been possible to force the emission spectrum to λ 2462. The relative intensities of emission and absorption lines with the furnace at high and low

[1] *Mt. Wilson Contr.*, No. 150; *Astrophysical Journal*, **48**, 13, 1918.

PLATE IX

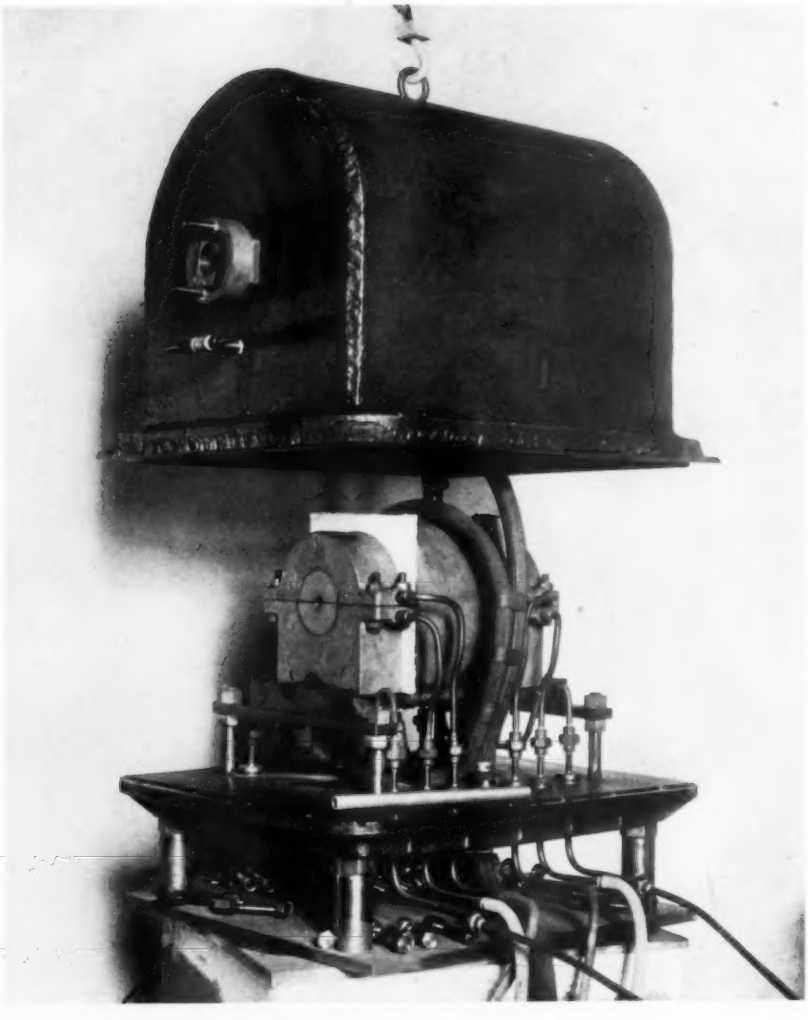

Vacuum Electric Furnace

temperatures were so nearly the same as to justify printing only a single list. Table II includes data from λ 2813 to λ 3437. The high- and medium-temperature columns are for emission lines, but intensities of the low-temperature lines are to be obtained only from the absorption spectrum. Table III, for the range λ 3440 to λ 3788, makes use of emission spectra at the three temperature stages, though in compiling it constant reference was made to the reversibility of lines as shown by their strength in absorption spectra.

EXPERIMENTAL METHOD

a) *Furnaces.*—Two electric furnaces have been employed. The first, in which the tube with its supports is inclosed in a strong cylindrical chamber, adapted for high pressure as well as vacuum, was used throughout the previous investigations. The other is for pressures not above the atmospheric limit, and consists of a heavy sheet-iron hood which is lowered upon a base-plate through which the connections for electric current and water pass to the supports of the furnace tube. These supports are hollow bronze blocks, water-cooled, and bored to hold cylindrical graphite bushings which make direct contact with the tube. The latter is of Acheson graphite, and various forms have been used in special experiments, but the size regularly employed has been of 13-mm bore, 19-mm outside diameter, and 30-cm length. The heated portion of the tube between the contact blocks is about 20 cm long. A tubular water jacket of cast iron, of 17.5 cm internal diameter, surrounds the furnace tube, so that no cooling of the outer inclosure is required. This furnace, and also the older one, were usually pumped out to a pressure of less than 1 cm of mercury, but numerous experiments were made at atmospheric pressure. An illustration of this furnace with the hood raised is shown in Plate IX.

Iron in powdered form was placed in the heated portion of the tube. A preliminary heat was given at a temperature sufficient to melt the iron, which then stuck to the wall of the tube, probably forming a carbide. A supply of iron thus remained in place during the life of the tube, and no fresh charging was needed. The presence of air appeared to cause a more vigorous combination of the metal with the material of the tube.

Alternating current of from 10 to 30 volts was usually employed on the furnace tube; but in the later work, direct current from a 500-kw generator was often used. This was especially useful in experiments with the furnace at atmospheric pressure, as the temperature changes caused by the thinning tube could be compensated by a close control of the voltage.

b) *Production of absorption spectra.*—Three methods of obtaining absorption spectra were used during the investigation. A very useful method was to place a cylindrical plug of graphite near the center of the tube and observe the absorption produced by iron vapor in front of this plug. Very high black-body temperatures are obtainable in this way, the plug frequently being heated above 3200° C., the highest temperature readable on the pyrometer. With this arrangement, however, it is a question as to the temperature of the vapor which absorbs. As in previous work with this method, the spectrum indicated a difference of about 400° between the plug and the absorbing layer, which would mean that the relatively cool vapor near the end of the tube is effective, while the main mass of vapor in the tube is too hot to give the required gradient. This method, especially when the tube was made thinner near the middle, so that the plug was much hotter than the main length of the tube, gave good results for the high-temperature absorption spectrum. An absorption spectrogram for which the plug was held at a temperature of 3000° gave lines as far as λ 2447, the relative intensities showing no important difference from an emission spectrum at 2600°. In another test, the emission spectrum at 2400° was compared with absorption spectra for which the plug was held closely at 2400°, 2600°, and 2800°, respectively. The 2800° spectrum was identical in all essential features with the emission spectrum at 2400°. At low temperatures, however, it is desirable to know as accurately as possible the temperature of the absorbing vapor. For this purpose it is best to use an open tube, the temperature of whose wall can be closely measured, and pass through the tube a beam of light from a source so much hotter that the vapor in the main section of the tube can be safely assumed to be in a condition to absorb. This was arranged by placing a 900-watt gas-filled lamp, operating at 30 amperes, behind the furnace, and directing its beam through

the tube. The rated temperature of the tungsten spiral in this lamp is 2900° C. To get the full benefit of the lamp in the ultra-violet region, a side tube closed by a quartz window was set in the bulb, which was then refilled with pure nitrogen.

A third method was to use as a source of continuous spectrum the light from exploding wires inclosed in a block of wood. This has been shown by Anderson[1] to give excellent absorption spectra of the material of the wire, extending far into the ultra-violet. Dr. Anderson kindly operated the explosion apparatus and the light was passed through the furnace heated at various temperatures. As it is necessary to use metals giving as few lines as possible in the region to be studied, wires of aluminium and of lead were tried. The latter was most nearly free from disturbing lines, both of the metal itself and of iron impurities, and a number of furnace absorption lines were added to the list obtainable by the other methods. The explosion method promises to be generally useful, the chief drawback, aside from the disturbing lines in the source, being the very large number of explosions required (on account of their almost infinitesimal duration) to build up a continuous spectrum with a high-dispersion spectrograph.

c) *Photography of the spectrum.*—The spectrograms for the various furnace temperatures were made as far as possible with the vertical concave-grating spectrograph of 15-foot radius. All of the photographs used for the final intensity estimates were made in this way, except when wire explosions were used as an absorption source, a 1-meter concave grating giving high intensity beyond λ 3000 then being employed. The second order of the 15-foot instrument, giving a scale of 1.86 A per millimeter, was used as far as λ 2800, while the first order was used for the shorter wave-lengths. Many spectrograms, especially for low-temperature spectra, were made with the 1-meter spectrograph and used for checking those of the higher dispersion. These were particularly useful in deciding whether certain lines can be brought out at a given temperature, since a long exposure with this instrument may be depended on to show lines which with higher dispersion are under-exposed.

[1] *Mt. Wilson Contr.*, No. 178; *Astrophysical Journal*, **51**, 37, 1920.

EXPLANATION OF THE TABLES

Tables I, II, and III contain in the first column the wave-lengths of iron lines on the international system. These are for the most part according to the measurements of Burns,[1] rounded off to two decimal places, though in some cases values from the table of iron lines given by Kayser[2] have been used. Lines in the arc tables which are not given by the furnace even at high temperature are entered only when they offer a striking contrast with neighboring lines which in the arc are of equal intensity or even weaker, but which appear distinctly in the furnace. This rule is not followed closely in the region of wave-lengths shorter than λ 2500, where a large proportion of the strong arc lines are of polar type and are usually absent from the furnace spectrum.

The arc intensities in the tables are graded so that a large proportion of the lines are given values comparable with those for the high-temperature furnace. In the ultra-violet, the arc spectrum taken close to the poles is very different from that emitted by the central region, and it is the lines of the latter which in the main make up the furnace spectrum. The photographs for estimation of arc intensities were therefore made with the slit across the image of the arc and about midway between the poles. For the arc, as for the emission furnace, "r" and "R" refer to degrees of reversal, while a line of nebulous structure is denoted by "n."

In the gradation of furnace intensities, "tr" indicates that a trace is visible on a strongly exposed spectrogram, while a line distinctly outlined is given intensity "1." Lines of strength above 20 are likely to show some degree of reversal, and before this intensity is reached, the line has a softened appearance which may be mistaken for faintness. Some plates out of the large collection for each temperature stage usually showed the true condition of the line. The scale for absorption lines was made as closely comparable as possible with that for emission lines.

The "arc type," in the fifth column of Table I, refers to the relative strength of a line at the center and near the poles of the arc. Type "C" is strong in the center of the arc, while type "C–P"

[1] *Lick Observatory Bulletin*, **8**, 27 (No. 247), 1913.

[2] *Handbuch der Spektroscopie*, **6**, 896.

TABLE I

TEMPERATURE CLASSIFICATION OF IRON LINES, λ 2298–λ 2808

λ (I.A.)	Arc Intensity	Furnace Intensities		Arc Type	Class
		High-Temp. Absorption	Low-Temp. Absorption		
2298.18	10r	4	2	C	II
2299.25	2	1	.....	C	III
2303.57	3	2	1	C	II
2309.00	2	1	.....	C	III
2313.12	2	1	.....	C	III
2320.37	2	1	.....	C–P	III
2354.88	3	2	1	C–P	II
2368.60	10	1	.....	C–P	III
2373.74	15	2	1	C–P	II
2382.04	20	2	1	C–P	II
2438.19	2	1	.....	C	III
2447.72*	4	4	?	C	II ?
2453.48	5	1	.....	C	III
2457.60	6	3	1	C–P	II
2462.19	4	4	.....	C	III
2462.65	10r	12	3	C	II
2465.16*	6	3	.....	C–P	III
2468.89	4	2	.....	C–P	III
2472.37	5	2	.....	C–P	III
2472.90	12R	20	4	C	II
2473.07	?			C	II
2476.67	3	2	.....	C	III
2479.48	6	10	2	C	III
2479.78	20R			C	II
2483.28	60R	40	10	C	II
2483.54	10			C	II ?
2484.19*	15R	8	2	C	II
2488.15	40R	30	8	C	II
2489.76*	15r	8	2	C	II
2490.66	30R	20	4	C	II
2491.16	20R	15	4	C	II
2496.54	6	1	.....	C–P	III
2498.90	10	tr	.....	P	IV
2501.14	20R	15	3	C	II
2507.90	6	2	.....	C–P	III
2510.84	15R	12	2	C	II
2512.37	5r	3	tr	C	III
2518.11	12r	10	2	C	II
2522.86	40R	30	5	C	II
2524.29	8r	5	2	C	II
2527.44	15r	12	3	C	II
2529.27	10r	8	tr	C	III
2529.83	3	2	.....	C	III
2530.70	3	2	.....	C	III
2533.80	4	tr	.....	C	IV
2535.61	8r	6	.....	C	III
2540.98	10R	10	1	C	III
2542.11	6	tr	.....	C–P	IV
2543.93	6	tr	.....	C–P	IV
2544.72	6	tr	.....	C	IV
2545.98	10r	10	1	C	III
2549.62	10r	10	1	C	III
2552.03	2	2	.....	C	III
2556.87	1	1	.....	C	III
2576.70	4	2	.....	C–P	III
2582.31	6	1	.....	C	III
2584.54	8	3	.....	C–P	III
2585.89*	20	1	.....	P	IV
2588.01*	8	1	.....	C	III
2594.05	1	1	.....	C	III
2594.16	1			C	III
2599.58	6	3	.....	C–P	III
2605.69	6	1	.....	C–P	III
2606.84	6	3	.....	C–P	III
2610.76	1	1	.....	C	III
2612.79	2	2	.....	C	III
2614.51	1	1	.....	C	III
2618.03	5	2	.....	C–P	III
2618.72	2	2	.....	C	III
2623.38	2	2	.....	C	III
2623.54	5	2	.....	C–P	III
2629.60*	2	2	.....	C	III
2632.25	4	2	.....	C–P	III
2632.60	2	4	.....	C	III A
2635.82	8	4	.....	C–P	III
2636.49	1	1	.....	C	III
2641.65	4	2	.....	C	III
2644.01	8	3	.....	C–P	III
2645.43	1	2	.....	C	III A
2647.57	3	4	.....	C	III
2651.72	2	1	.....	C	III
2656.15	3	tr	.....	C	III
2660.41	1	1	.....	C	III
2662.07	3	2	.....	C	III
2666.41	2	1	.....	C	III
2666.82	8	4	.....	C–P	III
2666.97	3			C	III
2667.92	1	2	.....	C	III A
2669.50*	2	.....	.....	C	IV
2673.22	1	tr	.....	C	III
2679.07	10	3	.....	C–P	III
2680.46	2	1	.....	C	III
2689.22	8	3	.....	C–P	III
2689.84	2	tr	.....	C	III
2690.07	2	2	.....	C	III
2695.04	1	tr	.....	C	III
2697.03	2	tr	.....	C	III
2699.11	6	2	.....	C–P	III
2706.02	4	tr	.....	C	IV
2706.59	8	3	.....	C–P	III
2708.58*	4	.....	.....	C	IV
2710.55	2	tr	.....	C	III
2711.66	4	2	.....	C–P	III
2714.88	1	tr	.....	C	III
2715.33	1	tr	.....	C	III
2717.79	2	1	.....	C	III
2718.45*	6	?	.....	C–P	III ?
2719.04	60R	60	10	C	II
2719.43*	3	?	.....	C	III ?
2720.91	40r	40	6	C	II
2723.58	15	15	3	C	II
2724.96*	10	3	.....	C–P	III
2726.06	6	2	.....	C–P	III
2728.03	3	2	.....	C	III
2728.83	2	2	.....	C	III
2730.98	2	2	.....	C	III
2733.58	15	5	1	C	II
2734.01	2	tr	.....	C	III
2734.27	2	tr	.....	C	III
2735.48*	8	5	.....	C–P	III
2735.61*	8			C	III
2737.31	20r	20	2	C	II

TABLE I—*Continued*

λ (I.A.)	Arc Intensity	Furnace Intensities: High-Temp. Absorption	Furnace Intensities: Low-Temp. Absorption	Arc Type	Class	λ (I.A.)	Arc Intensity	Furnace Intensities: High-Temp. Absorption	Furnace Intensities: Low-Temp. Absorption	Arc Type	Class
2742.02	2	1	.....	C	III	2769.67	1	1	.....	C	III
2742.26	20	30	5	C–P	III	2772.08	20	6	2	C–P	II
2742.41	30r			C	II	2772.11	1	.....	.....	C	III
2743.57	3	1	.....	C–P	III	2773.23	2	tr	.....	C	III
2744.07	10	8	2	C	II	2774.73*	3	2	.....	C	III
2744.53	8	2	.....	C–P	III	2778.08	3	5	.....	C	III
2746.99*	20	2	.....	P	III	2778.23	20			C–P	III
2750.15	25r	20	4	C	II	2778.85	3	3	.....	C	III
2753.69	3	2	.....	C	III	2780.70	1	tr	.....	C	III
2754.03	3	2	.....	C	III	2781.84	4	2	.....	C	III
2754.43	2	1	.....	C	III	2787.94	5	8	.....	C–P	II
2756.33	20	10	6	C	I	2788.11	30		2	C	II
2757.32	10	3	.....	C–P	III	2792.40	1	1	.....	C	III
2759.82	4	2	.....	C	III	2795.01	3	2	.....	C	III
2761.79*	18	3	.....	C–P	III	2797.78	15	3	.....	C–P	III
2762.03	15	3	.....	C–P	III	2799.15	1	tr	.....	C	III
2763.11	4	2	.....	C	III	2804.52	20	3	1	C–P	II
2764.33	3	1	.....	C	III	2806.99	20	3	1	C–P	II
2766.91	2	2	.....	C	III	2807.24	2	1	.....	C	III
2767.52*	20	3	.....	P	III	2808.33	2	1	.....	C	III

2447.72 Probably present at low temperature close to Pb absorption line. Blends in arc with close polar line to red.
2465.16 Some strengthening at pole in arc. Possibly blend with polar line.
2484.19 Blend in arc with polar line to red.
2489.76 Blend in arc with polar line to red.
2585.89 Strong throughout arc, enhanced at poles.
2588.01 Blend in arc with polar line to red.
2629.60 Close blend in arc with polar line.
2669.50 Appears faintly in high-temperature emission spectrum.
2708.58 Appears faintly in high-temperature emission spectrum.
2718.45, 2719.43 Blend in furnace with λ 2719.04.
2724.96 Blends in arc with polar line λ 2724.89.
2735.48–.61 Furnace line is chiefly λ 2735.61.
2746.99 Strong throughout arc, enhanced at poles.
2761.79 Slightly strengthened at poles.
2767.52 Much enhanced at pole.
2774.73 Blend in arc with polar line to violet.

indicates that the line is emitted with little change of intensity from center to pole. Polar lines, denoted by "P," are rarely visible in the furnace spectrum.

The classification of lines given in the last column of each table has been carried out in the same manner as in previous papers, except that class I B of the former paper on the iron spectrum is here replaced, as has been the case for the other metals studied, by class I.

Classes I and II are low-temperature lines, but those of class I maintain their strength at low temperature longer than do the lines of class II. These classes include practically all of the lines which

TABLE II

TEMPERATURE CLASSIFICATION OF IRON LINES, λ 2813–λ 3437

λ (I.A.)	Arc Intensity	Furnace Intensities			Class	λ (I.A.)	Arc Intensity	Furnace Intensities			Class
		High-Temp. Emission	Med.-Temp. Emission	Low-Temp. Absorption				High-Temp. Emission	Med.-Temp. Emission	Low-Temp. Absorption	
2813.29	30R	8	5	3	II	2945.07	3	1	.....	.....	IV
2815.51	3	2	.....	.....	IV	2947.66*	6	.....	.....	.....	V
2817.51	6	5	2	.....	III	2947.88	60R	50R	20r	15	I
2820.81	2	2	.....	.....	IV	2948.44	4	1	.....	.....	IV
2823.28	20	4	3	1	II	2949.21*	8	.....	.....	.....	V
2825.56	20	6	3	2	II	2950.25	20n	3	.....	.....	IV
2825.69	6	2	1	1	II	2953.49	5	1	.....	.....	IV
2827.89	5	3	2	.....	III	2953.78*	5	.....	.....	.....	V
2828.81	7	3	2	.....	III	2953.94	50R	35R	15r	10	II
2832.43	25r	4	3	1	II	2954.66	5	2	.....	.....	IV
2835.46	6	4	4	4	I	2957.37	30R	25R	12r	8	II
2838.12	10	5	3	.....	III	2960.00	10	3	.....	.....	IV
2840.42	6	4	2	2	II	2960.30	1	1	.....	.....	IV
2843.63	10	3	2	.....	III	2965.26	20	15r	10	6	II
2843.97	20r	6	5	2	II	2965.82	2	1	.....	.....	IV
2845.60	8	6	3	.....	III	2966.90	125R	100R	40R	20	II
2846.83	3	1	.....	.....	IV	2969.36	5	3	2	1	II
2848.71	5	3	1	.....	III	2969.48	10	6	4	4	I
2851.80	15r	5	3	1	II	2970.11	40R	30R	10r	10	I
2858.90	5	3	2	1	II	2970.52*	4	.....	.....	.....	V
2862.50	4	2	.....	.....	IV	2972.28	3	1	.....	.....	IV
2863.43	8	3	1	.....	III	2973.14	60R	50R	20r	15	I
2863.87	8	6	3	3	I	2973.24	60R	50R	20r	15	I
2866.63	7	3	2	.....	II	2976.13	5	2	.....	.....	IV
2867.31	3	1	.....	.....	IV	2980.54	5	1	.....	.....	IV
2867.57	3	1	.....	.....	IV	2981.45	20r	15r	12	8	I
2868.44	3	1	.....	.....	IV	2981.86	6	4	.....	.....	IV
2869.31	10	6	6	6	I	2983.57	125R	100R	30r	25	I
2872.34	7	4	4	.....	III	2984.83*	10	6	1	.....	IV
2874.18	10	8	6	6	I	2985.55	4	.....	.....	.....	V
2875.31*	5	3	.....	.....	IV	2986.40	3	5	5	1	III
2877.30	8	4	2	.....	III	2987.29	10	8	6	1	III
2880.58	2	1	.....	.....	IV	2988.47	2	3	.....	.....	IV
2880.76*	5	.....	.....	.....	V	2990.39	6	4	.....	.....	IV
2883.73*	4	.....	.....	.....	V	2991.65	5n	3	.....	.....	IV
2886.32	3	1	.....	.....	IV	2994.43*	100R	80R	40R	35	I
2887.81*	5	.....	.....	.....	V	2994.50*					
2893.76	1	2	.....	.....	IV A	2996.39	5	2	.....	.....	IV
2893.88	2	1	.....	.....	IV	2999.52	30R	30R	12	5	II
2894.51	10	3	1	.....	III	3000.45	8	8	3	.....	III
2895.04	8	3	1	.....	III	3000.95	100R	80R	30r	25	I
2899.42	8	3	.....	.....	IV	3002.05*	5	.....	.....	.....	V
2901.38	5	4	.....	.....	IV	3003.03	10	10	6	tr	III
2901.92	5	2	.....	.....	IV	3005.31	3	1	.....	.....	IV
2907.52	5	.....	.....	.....	V	3007.15	8	8	3	.....	III
2912.16	20r	12	10	8	I	3007.28	12r	10r	7	5	I
2912.26	3	3	.....	.....	IV	3008.14	60R	50R	20r	12	I
2914.31	3	1	.....	.....	IV	3009.10	5	3	.....	.....	IV
2918.03	10	1	.....	.....	IV	3009.58	25r	20r	10	3	II
2918.35	3	1	.....	.....	IV	3011.48	7	3	.....	.....	IV
2920.69	5	4	.....	.....	IV	3014.18	3	5	.....	.....	IV
2923.29	7	1	.....	.....	IV	3014.92	1	2	.....	.....	IV A
2923.85	7	1	.....	.....	IV	3015.93	4	1	.....	.....	IV
2925.30	4	.....	.....	.....	V	3016.18	12	8	8	tr	III
2925.90	4	3	.....	.....	IV	3017.63	15r	30R	15r	10	I A
2926.58*	10	tr	.....	.....	V	3018.99	15r	12r	10	1	III
2929.01	25r	15r	10	8	I	3020.50	100R	75R	30R	10	II
2929.12	6	4	.....	.....	IV	3020.64	200R	150R	80R	50	I
2929.62	2	1	.....	.....	IV	3021.08	150R	100R	40R	30	I
2936.90	60R	50r	20r	15	I	3024.04	15r	30R	15r	10	I A
2937.81	10n	1	.....	.....	IV	3025.28	3	5	2	.....	III
2941.34	15r	15r	10	8	I	3025.64	15	8	1	.....	IV
2944.40*	6	.....	.....	.....	V	3025.85	50R	50R	25r	20	I

TABLE II—*Continued*

λ (I.A.)	Arc Intensity	Furnace Intensities			Class	λ (I.A.)	Arc Intensity	Furnace Intensities			Class
		High-Temp. Emission	Med.-Temp. Emission	Low-Temp. Absorption				High-Temp. Emission	Med.-Temp Emission	Low-Temp. Absorption	
3026.47	15	10	8	1	III	3165.86	4	2	.....	.....	IV
3029.24	3	3	.....	.....	IV	3166.44	6	3	.....	.....	IV
3030.15	15	8	1	.....	IV	3168.86	2	1	.....	.....	IV
3031.22	12	6	.....	.....	IV	3171.35	5	1	.....	.....	IV
3031.64	15	10r	10	tr	III	3171.66	2	1	.....	.....	IV
3037.39	80R	60R	30r	20	I	3172.07	2	1	.....	.....	IV
3037.78	2	5	tr	.....	IV A	3175.45	12	6	tr	.....	IV
3040.43	15	10	8	1	III	3176.37	2	1	.....	.....	IV
3041.04	10	6	1	.....	IV	3178.01	10	5	1	.....	IV
3041.75	15	10	8	.....	III	3178.55	2	1	.....	.....	IV
3042.03	15	8r	8	.....	III	3178.97	3	1	.....	.....	IV
3042.67	15	10r	8	.....	III	3179.54	3	1	.....	.....	IV
3045.08	5	4	3	.....	III	3180.22	20	7	1	.....	IV
3047.61	100R	80R	40r	25	I	3180.76	5	10	10	3	II A
3053.07	5	2	.....	.....	IV	3181.53	4	1	.....	.....	IV
3055.27	12	6	2	.....	III	3182.08	3	1	.....	.....	IV
3057.45	40R	20R	10r	5	II	3182.99	3	1	.....	.....	IV
3059.09	100R	80R	40r	25	I	3184.63	3	1	.....	.....	IV
3060.99	4	3	.....	.....	IV	3184.90	7	15r	8	7	I A
3066.49	3	3	.....	.....	IV	3186.75	3	.....	.....	.....	V
3067.12	8	6	tr	.....	IV	3188.59	4	2	.....	.....	IV
3067.25	30r	15r	8	4	II	3188.84	7	3	.....	.....	IV
3068.18	8	8	1	.....	IV	3191.67	7	15r	10	10	I A
3075.73	25r	15r	8	3	II	3192.81	8	5	tr	.....	IV
3078.02	4	8	1	.....	IV A	3193.21	10	25r	10	10	I A
3078.44	3	1	.....	.....	IV	3193.31	8	5	.....	.....	IV
3083.75	20	12	6	2	II	3194.42	3	1	.....	.....	IV
3091.58	20	12	6	2	II	3196.09	2	}	.....	.....	IV
3092.79*	2	2?	?	.....	III ?	3196.15	2	1	.....	.....	IV
3093.81	3	6	.....	.....	IV A	3196.94*	20	8	6	4	II
3098.19	6	2	.....	.....	IV	3199.53	15	8	6	3	II
3099.90	20	20	8	2	II	3200.48	15	5	tr	.....	IV
3099.97	15	}	8	2	II	3200.79	2	6	4	tr	III A
3100.31	20	12	8	2	II	3202.56	2	1	.....	.....	IV
3100.67	20	15	8	2	II	3205.40	15	5	tr	.....	IV
3112.08	3	1	.....	.....	IV	3207.09	2	1	.....	.....	IV
3116.63	12	8	6	.....	III	3208.48	4	1	.....	.....	IV
3117.63	1	3	1	.....	III A	3209.33	6	2	.....	.....	IV
3119.50	6	4	.....	.....	IV	3210.25	8	4	.....	.....	IV
3120.44	6	3	.....	.....	IV	3210.83	10	4	tr	.....	IV
3125.66	15	10	7	.....	III	3211.49	4	1	.....	.....	IV
3126.17	8n	1	.....	.....	IV	3211.69	8	1	.....	.....	IV
3128.88	1	1	.....	.....	IV	3211.87	4	1	.....	.....	IV
3129.33	5	5	tr	.....	IV	3212.00	10	5	1	.....	IV
3132.51	4n	.....	.....	.....	V	3214.04*	20	8	2	.....	III
3134.11*	10	8	5	.....	III	3214.30	8	15r	8	8	I A
3139.91	4n	.....	.....	.....	V	3215.94	12	5	1	.....	IV
3140.30	5n	.....	.....	.....	V	3217.30	10	5	tr	.....	IV
3142.45	6	2	.....	.....	IV	3219.58	12	5	1	.....	IV
3142.89	5	2	.....	.....	IV	3219.82	10	8	3	.....	III
3143.24	2	5	3	.....	III A	3221.94	2	1	.....	.....	IV
3143.98	8	1	.....	.....	IV	3222.07	20	6	4	.....	III
3144.49	6n	1	.....	.....	IV	3225.79	25	8	5	.....	III
3151.34	10	2	.....	.....	IV	3226.73	2	5	2	.....	III A
3153.21	5	3	.....	.....	IV	3227.07	3	1	.....	.....	IV
3154.51	2	1	.....	.....	IV	3227.76	15	6	1	.....	IV
3155.29	2	1	.....	.....	IV	3227.81	}				
3156.27	5n	1	.....	.....	IV	3228.26	5	3	.....	.....	IV
3157.04	8	5	.....	.....	IV	3228.92	3	1	.....	.....	IV
3157.88	6	3	.....	.....	IV	3229.13	4	8	8	3	II A
3160.65	10	5	.....	.....	IV	3230.21	6	3	tr	.....	IV
3161.37	4	4	tr	.....	IV	3230.98	10	5	tr	.....	IV
3161.95	8	4	tr	.....	IV	3233.06	8	1	.....	.....	IV
3162.34	2n	1	.....	.....	IV	3233.98	12	6	tr	.....	IV
3165.01	3	1	.....	.....	IV	3234.62	7	15r	8	8	I A

TABLE II—*Continued*

λ (I.A.)	Arc Intensity	Furnace Intensities: High-Temp. Emission	Furnace Intensities: Med.-Temp. Emission	Furnace Intensities: Low-Temp. Absorption	Class
3236.23	8	20r	10	10	I A
3239.45	15	8	1	.....	IV
3243.41	3	1	.....	.....	IV
3244.19	15	8	1	.....	IV
3246.02	8	12	10	8	I
3246.49	3	1	.....	.....	IV
3246.97	6	3	.....	.....	IV
3247.30	3	1	.....	.....	IV
3248.22	10	5	.....	.....	IV
3249.20	3	1	.....	.....	IV
3250.63	4	2	.....	.....	IV
3251.24	8	1	.....	.....	IV
3252.93	4	1	.....	.....	IV
3253.61	4	1	.....	.....	IV
3254.37	10	2	.....	.....	IV
3257.24	2	1	.....	.....	IV
3257.60	8	4	tr	.....	IV
3260.00	6	2	.....	.....	IV
3260.28	4	1	.....	.....	IV
3262.28	4	1	.....	.....	IV
3264.52	5	2	.....	.....	IV
3265.06	8	15r	10	8	I A
3265.63	15	6	2	.....	III
3268.25	5	2	.....	.....	IV
3271.01	15	6	2	.....	III
3276.48	4	2	.....	.....	IV
3278.74	4	1	.....	.....	IV
3280.27	8	2	.....	.....	IV
3284.60	5	3	.....	.....	IV
3286.03	2	1	.....	.....	IV
3286.76	20	8	4	.....	III
3288.97	2	1	.....	.....	IV
3291.00	5	3	.....	.....	IV
3292.03	8	2	.....	.....	IV
3292.60	8	5	1	.....	IV
3298.14	6	5	1	.....	IV
3305.98	20	8	4	.....	III
3306.36	20	8	4	.....	III
3307.24	5	1	.....	.....	IV
3310.35	4	1	.....	.....	IV
3314.75	7	2	.....	.....	IV
3317.13	3	2	.....	.....	IV
3319.26	2	1	.....	.....	IV
3322.50	5n	1	.....	.....	IV
3323.74	7	3	.....	.....	IV
3324.54	4	2	.....	.....	IV
3325.47	4	2	.....	.....	IV
3328.87	5	1	.....	.....	IV
3331.62	3	1	.....	.....	IV
3335.78	4	1	.....	.....	IV
3337.67	6	3	.....	.....	IV
3339.20	2	1	.....	.....	IV
3340.57	6	4	.....	.....	IV
3341.91	5	10	10	.....	III A
3342.23	5	2	.....	.....	IV
3342.30	4	.....	.....	.....	V
3346.94	1	1	.....	.....	IV
3347.93	6	4	.....	.....	IV
3351.53	2	1	.....	.....	IV
3351.75	3	1	.....	.....	IV
3354.07	3	1	.....	.....	IV
3355.24	6	1	.....	.....	IV
3356.33	1	2	.....	.....	IV A
3356.41	3	2	.....	.....	IV
3359.50	2	5	2	.....	III A
3366.79	5	1	.....	.....	IV
3366.87	5	2	.....	.....	IV
3369.57*	8	3?	2?	.....	III
3370.79	10	6	tr	.....	IV
3372.08	3	1	.....	.....	IV
3378.68	6	3	.....	.....	IV
3379.02	6	4	.....	.....	IV
3380.12	8	4	.....	.....	IV
3382.41	3	2	.....	.....	IV
3383.70	5	4	tr	.....	IV
3383.99	8	6	1	.....	IV
3387.41	2	1	.....	.....	IV
3389.75	2	1	.....	.....	IV
3392.02	2	tr	.....	.....	IV
3392.31	8	6	tr	.....	IV
3392.66	15	9	3	.....	III
3394.59	5	5	tr	.....	IV
3396.98	4	8	5	.....	III A
3397.64	2	4	1	.....	III A
3399.34	15	8	2	.....	III
3401.52	6	10	9	.....	III
3402.26	5	2	.....	.....	IV
3404.30	3	7	3	.....	III A
3404.36	6	5	1	.....	IV
3406.45	3	1	.....	.....	IV
3406.81	6	5	1	.....	IV
3407.47*	20	15	7	.....	III
3410.18	3	tr	.....	.....	IV
3411.36	3	2	.....	.....	IV
3413.14	15	10	4	.....	III
3415.54	4	4	.....	.....	IV
3417.85	12	7	2	.....	III
3418.51	10	6	2	.....	III
3422.50	3	1	.....	.....	IV
3422.67	7	5	1	.....	IV
3424.29	10	8	2	.....	III
3425.02	4	2	.....	.....	IV
3426.39*	5	10	6	.....	III A
3426.65	5	6	tr	.....	IV
3426.99	2	4	2	.....	III A
3427.13	20	8	6	.....	III
3428.20	8	6	2	.....	III
3431.83	3	1	.....	.....	IV
3437.05	3	1	.....	.....	IV

2875.31 Blend in arc with polar line.
2880.76, 2883.73 Strong polar lines.
2887.81 Not a polar line, though absent in furnace.
2926.58, 2944.40, 2947.66, 2949.21, 2953.78, 2970.52 Polar lines.
2984.83 Blend in arc with polar λ 2984.79.
2994.43–.50 λ 2994.43 is chief part of blend, which shows in furnace as a reversed line with violet side strongest.
3002.65 Polar line.
3092.79 Blend with strong Al line.
3134.11 Blend Ni. but arc and furnace lines chiefly Fe.
3196.94 Blend Ni on red side.
3214.04 Apparently a close double with components of equal strength.
3369.57 Blend Ni. Probable intensity of Ni line subtracted.
3407.47 Probably double.
3426.39 Double with faint violet component.

TABLE III

Temperature Classification of Iron Lines, λ 3441–λ 3878

λ (I.A.)	Arc Intensity	Furnace Intensities (Emission)			Class	λ (I.A.)	Arc Intensity	Furnace Intensities (Emission)			Class
		High Temp.	Med. Temp.	Low Temp.				High Temp.	Med. Temp.	Low Temp.	
3440.61	150R	125R	125R	125r	I	3552.84	3	2	.....	.....	IV
3440.99	75R	75R	75r	60	I	3553.74	6	2	.....	.....	IV
3442.36	5	4	tr	.....	IV	3554.12	4	12	10	1	III A
3442.68	3	8	5	.....	III A	3554.52	2	2	.....	.....	IV
3443.88	50r	50R	50r	50	I	3554.92	40	15	3	.....	III
3445.16	20	8	4	.....	III	3556.88	7	10	tr	.....	IV
3447.28	8	6	1	.....	IV	3558.52*	30	30R	20	10	II
3450.33	10	7	1	.....	IV	3559.51	2	1	.....	.....	IV
3451.62	2	1	.....	.....	IV	3560.71	5	1	.....	.....	IV
3451.92	10	7	1	.....	IV	3565.38	60r	60R	60r	50	II
3452.28	10	12	8	1	III	3565.58	3	2	.....	.....	IV
3458.31	4	2	.....	.....	IV	3567.05	2	1	.....	.....	IV
3459.92	4	1	.....	.....	IV	3568.98	4	2	.....	.....	IV
3462.35	2	1	.....	.....	IV	3570.10	100R	100R	100r	75	I
3463.31	2	2	.....	.....	IV	3570.24	20	10	4	.....	III
3465.86	60r	60R	60r	50	I	3571.23	2	4	.....	.....	IV A
3466.50	3	6	4	.....	III A	3572.00	6	5	.....	.....	IV
3468.85	4	2	.....	.....	IV	3573.40	2	tr	.....	.....	IV
3469.83	2	1	.....	.....	IV	3573.84*	3	4	.....	.....	IV
3471.27	5	3	.....	.....	IV	3573.89*	4				IV
3471.34	6	3	.....	.....	IV	3575.25	2	1	.....	.....	IV
3475.45	70r	75R	75r	60	I	3575.38	4	4	2	.....	III
3475.65	6	6	tr	.....	IV	3575.98	2	1	.....	.....	IV
3476.71	40	40R	40	40	I	3576.76	2	1	.....	.....	IV
3483.01	3	6	5	tr	III A	3581.20	250R	200R	150R	150r	I
3485.34	7	6	tr	.....	IV	3581.65	1	1	.....	.....	IV
3489.67	4	2	.....	.....	IV	3582.20	5	2	.....	.....	IV
3490.58	100r	100R	75r	75	I	3583.32	2	1	.....	.....	IV
3495.29	8	4	.....	.....	IV	3584.66	8	7	1	.....	IV
3497.11	10	10	2	.....	III	3584.79	1	1	.....	.....	IV
3497.84	40	40R	40r	40	I	3584.96	4	2	.....	.....	IV
3500.57	2	2	.....	.....	IV	3585.32*	30	30R	15	10	II
3504.87	2	2	.....	.....	IV	3585.71*	20	20R	15	8	II
3505.07	2	1	.....	.....	IV	3586.12	10	6	.....	.....	IV
3506.50	6	4	.....	.....	IV	3586.99*	30	25R	18	12	II
3508.49*	5	3	.....	.....	IV	3587.25	2	1	.....	.....	IV
3513.82	30	25R	20	10	II	3587.42	2	1	.....	.....	IV
3516.41	5	1	.....	.....	IV	3587.75	3	2	.....	.....	IV
3521.26*	25	20R	20	10	II	3588.62	3	3	.....	.....	IV
3521.84	2	4	.....	.....	IV A	3588.92	2	1	.....	.....	IV
3524.08	3	3	.....	.....	IV	3589.11	8	12r	12	2	III
3524.24	4	6	tr	.....	IV	3589.45	3	2	.....	.....	IV
3526.02	1	1	.....	.....	IV	3594.63	8	6	tr	.....	IV
3526.07	20	30R	30r	30	I	3595.29	2	1	.....	.....	IV
3526.17	15	15r	10	6	II	3596.20	1	1	.....	.....	IV
3526.38	4	3	.....	.....	IV	3597.05	3n	1	.....	.....	IV
3526.47	4	5	tr	.....	IV	3598.71	1	2	.....	.....	IV A
3526.67	5	4	.....	.....	IV	3599.63	3	tr	.....	.....	IV
3527.80	4	4	.....	.....	IV	3602.10	1	3	.....	.....	IV A
3529.82	6	8	3	.....	III	3602.46	2	1	.....	.....	IV
3530.38	2	2	.....	.....	IV	3602.54	3	2	.....	.....	IV
3533.00	5	4	.....	.....	IV	3603.20	10	7	1	.....	IV
3533.20	10	7	.....	.....	IV	3603.82	1	1	.....	.....	IV
3536.55	15	10	1	.....	IV	3605.45*	15	12	tr	.....	IV
3537.50	1	1	.....	.....	IV	3606.68	20	10	4	.....	III
3537.73	3	3	.....	.....	IV	3608.15	3	2	.....	.....	IV
3537.89	4	4	.....	.....	IV	3608.86	100r	80R	60r	60	I
3540.13	3	3	.....	.....	IV	3610.15	20	9	2	.....	III
3540.71	3	8	6	.....	III A	3610.71	2	1	.....	.....	IV
3541.09	15	10	1	.....	IV	3612.08	8	3	.....	.....	IV
3542.08	15	10	1	.....	IV	3612.94	1	4	.....	.....	IV A
3542.24	1	1	.....	.....	IV	3614.56	2n	tr	.....	.....	IV
3545.64	5	4	.....	.....	IV	3616.58	3n	tr	.....	.....	IV
3549.87	4	4	1	.....	III	3617.32	2	tr	.....	.....	IV
3552.11	4	1	.....	.....	IV	3617.79	12	6	tr	.....	IV

TABLE III—*Continued*

λ (I.A.)	Arc Intensity	Furnace Intensities (Emission)			Class
		High Temp.	Med. Temp.	Low Temp.	
3618.39	2	2	.....	.....	IV
3618.77	125R	100R	80r	80	I
3621.46	15	8	1	.....	IV
3622.01	12	7	1	.....	IV
3623.19	8	7	1	.....	IV
3623.45	1	1	.....	.....	IV
3623.78	2	1	.....	.....	IV
3625.15	6	3	.....	.....	IV
3628.09	1	1	.....	.....	IV
3630.35	4	2	.....	.....	IV
3631.09	7	4	tr	.....	IV
3631.46	125R	100R	75r	75	I
3632.04	10	5	.....	.....	IV
3632.55	3	1	.....	.....	IV
3632.98	3	2	.....	.....	IV
3633.84	1	tr	.....	.....	IV
3634.34	6n	1	.....	.....	IV
3634.68	4n	tr	.....	.....	IV
3635.19	2	6	1	.....	IV A
3636.19	2	3	.....	.....	IV
3636.65	1	tr	.....	.....	IV
3636.99	2	1	.....	.....	IV
3637.25	1	1	.....	.....	IV
3637.86	3n	tr	.....	.....	IV
3638.30	12	7	tr	.....	IV
3640.39	15	10	1	.....	IV
3643.62	2	1	.....	.....	IV
3643.72	1	1	.....	.....	IV
3645.09	2	1	.....	.....	IV
3645.49	1	1	.....	.....	IV
3645.83	6	2	.....	.....	IV
3647.43	3	1	.....	.....	IV
3647.85	100R	100R	75r	75	I
3649.31*	5	20r	25	20	I A
3649.51	12	10	1	.....	IV
3650.03	4	2	.....	.....	IV
3650.28	5	5	1	.....	IV
3651.47	20	12	2	.....	IV
3653.76	1	1	.....	.....	IV
3655.47	4	2	.....	.....	IV
3656.23	3n	tr	.....	.....	IV
3657.14	1	tr	.....	.....	IV
3657.89	1	1	.....	.....	IV
3659.52	8	6	1	.....	IV
3663.46	1	1	.....	.....	IV
3664.56	2	1	.....	.....	IV
3666.24	1	tr	.....	.....	IV
3667.28	3n	1	.....	.....	IV
3668.00	1	tr	.....	.....	IV
3669.16	3	tr	.....	.....	IV
3669.53	10	8	1	.....	IV
3670.04	3	2	.....	.....	IV
3670.09	3	2	.....	.....	IV
3670.81	1	1	.....	.....	IV
3672.69	1	1	.....	.....	IV
3674.77	2	1	.....	.....	IV
3676.31	6	6	tr	.....	IV
3677.31	2	tr	.....	.....	IV
3677.63	12	9	1	.....	IV
3678.86	3	3	.....	.....	IV
3679.92	40r	100R	80r	80	I A
3680.69	2n	tr	.....	.....	IV
3680.80	1	tr	.....	.....	IV
3681.77	1	tr	.....	.....	IV
3682.24	20	8	tr	.....	IV
3683.06*	10	20r	20	20	I A
3684.11	15	8	1	.....	IV
3686.00	15n	7	1	.....	IV
3686.26	2	2	.....	.....	IV
3687.10	2	3	.....	.....	IV
3687.46	40r	40R	40	30	I
3687.66	4	3	1	.....	III
3689.46	12	6	1	.....	IV
3690.73	4	1	.....	.....	IV
3693.02	1	tr	.....	.....	IV
3694.00	20	8	1	.....	IV
3695.05	8	4	.....	.....	IV
3697.44	6n	3	.....	.....	IV
3698.61	2	1	.....	.....	IV
3699.14	1	tr	.....	.....	IV
3701.08	20	9	1	.....	IV
3702.03	3	2	.....	.....	IV
3702.49	1	2	.....	.....	IV A
3703.56*	5	?	?	.....	IV ?
3703.70	3	1	.....	.....	IV
3703.82	3	1	.....	.....	IV
3704.46	10	4	tr	.....	IV
3705.57	100r	100R	80r	80	I
3707.05	8	3	.....	.....	IV
3707.83	20	20r	20	20	I
3707.92	8	10	5	.....	III
3709.25	75r	40R	30	15	II
3711.23	3	2	.....	.....	IV
3711.41	2	tr	.....	.....	IV
3715.92	4	4	tr	.....	IV
3716.45	12	6	tr	.....	IV
3718.41	3	2	.....	.....	IV
3719.94	250R	300R	300R	300r	I
3721.28	2	2	.....	.....	IV
3721.40	1	1	.....	.....	IV
3721.51	2	1	.....	.....	IV
3722.57	50r	100R	80r	80	I A
3724.38	8	8	2	.....	III
3726.92	6	4	tr	.....	IV
3727.10	4	2	tr	.....	IV
3727.62	50r	40R	30	20	II
3727.81	3	2	.....	.....	IV
3728.67	1	1	.....	.....	IV
3730.39	3	2	.....	.....	IV
3730.95	2	1	.....	.....	IV
3731.37	2	1	.....	.....	IV
3732.40	10	10	6	1	III
3733.32	40r	80R	60r	60	I A
3734.87	300r	150R	100R	100r	II
3735.33	6	4	.....	.....	IV
3737.14	150R	200R	200R	200r	I
3738.31	10	4	.....	.....	IV
3739.11	1	1	.....	.....	IV
3739.32	1	1	.....	.....	IV
3739.54	3	2	.....	.....	IV
3740.26	3	2	.....	.....	IV
3742.62	4	3	.....	.....	IV
3743.36	20	40R	25	20	II A
3743.47*	6	?	?	.....	IV ?
3744.10	4	3	.....	.....	IV
3745.56	100R	150R	150R	150r	I
3745.90	40r	80R	80r	75r	I A
3746.48	1	1	.....	.....	IV
3746.93	6	4	.....	.....	IV
3748.26	60R	125R	100r	100r	I A
3748.49*	7	?	?	.....	IV ?
3748.96	5	3	.....	.....	IV
3749.49	200R	125R	80r	50	II
3753.61*	8	5?	3?	.....	III

TABLE III—*Continued*

λ (I.A.)	Arc Intensity	Furnace Intensities (Emission)			Class	λ (I.A.)	Arc Intensity	Furnace Intensities (Emission)			Class
		High Temp.	Med. Temp.	Low Temp.				High Temp.	Med. Temp.	Low Temp.	
3754.50	1	1	.....	.....	IV	3813.06*	5?	?	.....	.....	IV
3756.07	1	2	.....	.....	IV A	3813.64	2	1	.....	.....	IV
3756.94	4	1	.....	.....	IV	3813.89	2	.....	.....	.....	V
3757.46	1	tr	.....	.....	IV	3814.53	5	10	8	2	III A
3758.23	150R	125R	75r	40	II	3815.84	100r	50R	30	20	II
3760.05	8	6	3	.....	III	3816.34	4	5	1	.....	IV
3760.53	6	5	2	.....	III	3817.64	3n	1	.....	.....	IV
3761.41	1	1	.....	.....	IV	3820.43	250R	200R	200R	60	II
3763.79	100r	80R	50	30	II	3821.18	10	4	tr	.....	IV
3765.54	20	6	1	.....	IV	3821.84	3	2	.....	.....	IV
3766.07	1	tr	.....	.....	IV	3824.08	1	1	.....	.....	IV
3767.19	80r	60R	40	25	II	3824.31*	2	?	.....	.....	IV ?
3768.03	3	3	tr	.....	IV	3824.44	50r	100R	100r	100r	I A
3770.00	4	1	.....	.....	IV	3825.89	200R	125R	80r	40	II
3770.31	3	1	.....	.....	IV	3826.84	1	1	.....	.....	IV
3770.41					IV	3827.57	1	1	.....	.....	IV
3773.09	1	tr	.....	.....	IV	3827.83	75r	50R	30	20	II
3774.83	5	4	tr	.....	IV	3829.46	1	1	.....	.....	IV
3776.46	6	5	tr	.....	IV	3830.76	1	1	.....	.....	IV
3777.45	2	1	.....	.....	IV	3830.87	1	1	.....	.....	IV
3778.52	4	tr	.....	.....	IV	3833.31	5	5	1	.....	IV
3779.42	3	1	.....	.....	IV	3834.23	100r	80R	60	30	II
3779.50	2	1	.....	.....	IV	3836.34	4	2	.....	.....	IV
3781.19	2	3	tr	.....	IV	3837.14	1	1	.....	.....	IV
3782.46	1	tr	.....	.....	IV	3839.26	7	3	.....	.....	IV
3785.95	6	4	tr	.....	IV	3840.44	80r	60R	40	25	II
3786.18*	4	1	.....	.....	IV	3841.05	80r	25r	25	15	II
3786.68	8	8	8	2	III	3843.26	8	4	tr	.....	IV
3787.88	50	30R	20	20	II	3846.41	2	tr	.....	.....	IV
3789.18	3	1	.....	.....	IV	3846.81	8	2	.....	.....	IV
3790.09	12	10	10	6	II	3849.97	40	40r	30	25	II
3790.76	1	2	tr	.....	IV A	3850.82	12	15r	20	10	II
3792.16	2	2	.....	.....	IV	3852.58	6	6	1	.....	IV
3792.83	1	1	.....	.....	IV	3856.37	50r	100R	100r	100	I A
3793.35	1	1	.....	.....	IV	3859.22	10	6	2	.....	III
3793.87	1	1	.....	.....	IV	3859.91	300R	250R	200R	200r	I
3794.34	8	4	1	.....	III	3861.34	2	1	.....	.....	IV
3795.00	60	40R	30	25	II	3863.75	2	1	.....	.....	IV
3797.52	12	4	1	.....	III	3865.53	30	40r	25	20	II
3798.51	40	30R	20	20	II	3867.22	7	4	.....	.....	IV
3799.55	50	40R	20	20	II	3867.93	1	tr	.....	.....	IV
3801.68	3	2	.....	.....	IV	3869.56	3	2	.....	.....	IV
3801.81	1	tr	.....	.....	IV	3869.59					IV
3805.35	12	5	tr	.....	IV	3871.75	4	3	.....	.....	IV
3806.22	2	tr	.....	.....	IV	3872.51	60	60R	35	20	II
3806.70	10	4	1	.....	III	3872.92	1	tr	.....	.....	IV
3807.54*	7	8?	3?	.....	III	3873.77	8	8	1	.....	IV
3808.73	4	3	.....	.....	IV	3876.04	4	15	12	1	III
3810.76	2	tr	.....	.....	IV	3878.02	60	60R	40	20	II
3811.89	2	tr	.....	.....	IV	3878.58	100r	100R	100r	75r	II
3812.97	40	25R	20	20	II						

3508.49 Probably double.
3573.84–.89 Blend in furnace. Violet component appears strongest.
3521.26, 3558.52, 3585.32–.71, 3586.99 Become very faint at 1600°.
3605.45 Blend Cr on violet side.
3649.31 Between Classes I and II. Weak at 1600°.
3583.06 Blend V on red side.
3703.56 Blend V.
3743.47 Blend with preceding line.
3748.49 Blend with preceding line.
3753.61 Blend V. Probable intensity of V line subtracted.
3786.18 Probably double.
3807.54 May be partly V.
3813.06 Blend with preceding line.
3824.31 Blend with following line.

reverse readily in the furnace or in the arc with moderate current. The distinction between the two classes will be considered further in the discussion. Lines of class III are absent or at least very faint at low temperature, and first appear distinctly at medium temperature. There is much variety among these lines, but a large proportion show a rapid increase in intensity through the high-temperature stage and under the conditions of the arc. Class IV lines require strong excitation and usually appear only at high temperature, though perhaps faintly at medium temperature. Most of the fainter arc lines belong in this class, but many lines of intensity 10 or higher in the arc require the high-temperature furnace for their appearance. Class V lines appear in the arc but are absent from the furnace. Lines of this character are listed in Tables I–III only when they show considerable strength in the arc. Their number is relatively few, since polar lines are seldom included, and, except for these, class V is made up chiefly of very faint arc lines.

"A" after the class number denotes that the line is relatively weak in the arc. The selection depends to some extent on the average intensity adopted for arc and furnace spectra. In the tables, a line whose arc intensity is not more than half of that for the high-temperature furnace is placed in this division.

An asterisk after the wave-length refers to a note at the end of the tables.

REVISED CLASSIFICATION OF BLUE AND VIOLET IRON LINES

Table IV contains 262 lines, from λ 3884 to λ 4531, which are within the range covered by the former paper. A revision of the classification seemed desirable to make this portion of the spectrum uniform with the ultra-violet region treated in the present paper. This is chiefly on account of the change in the temperature steps, 1600°–1700° now being used for the low temperature stage instead of 1800°–1900°. Twenty-six lines not in the former list are included in Table IV, and ninety lines have their classes changed. About half of the changes are from class V to class IV, due to improved high-temperature spectrograms, which show distinctly many faint lines not obtained before with the furnace. Of the remaining changes, a few are due to errors incident to the first attempt at a

TABLE IV

Classification of Iron Lines, λ 3884–λ 4531

λ	Class	λ	Class	λ	Class	λ	Class
3884.37	IV	3971.33	III	4143.42	III	4267.83	IV
3885.51	III	3973.66	V	4143.87	I	4268.75	IV
3886.29	I	3976.62	IV	4147.68	III	4271.17	III
3887.05	I	3977.75	III	4149.37	V	4271.76	II
3888.52	II	3981.78	III	4152.18	II A	4282.41	III
3888.83	IV	3983.96	III	4153.92	IV	4285.45	IV
3890.84	IV	3985.39	IV	4154.50	III	4291.47	I A
3891.93	V	3986.18	IV	4154.82	IV	4294.13	II
3893.40	IV	3989.86	V	4156.81	III	4298.04	IV
3893.92	IV	3990.38	V	4157.81	IV	4299.25	III
3894.01	III	3994.12	V	4158.81	V	4305.46	IV
3895.66	I	3995.99	IV	4170.91	IV	4307.91	II
3897.45	IV	3997.40	III	4172.13	IV	4309.38	IV
3897.89	IV	3998.06	III	4172.75	II A	4315.09	III
3898.01	II	4001.67	III	4173.32	IV	4325.77	II
3899.03	IV	4005.25	II	4173.93	II A	4337.05	II
3899.71	I	4006.31	IV	4174.92	II A	4351.55	IV
3900.52	V	4006.63	IV	4175.64	III	4352.74	III
3902.95	II	4007.27	IV	4176.57	IV	4358.51	IV
3903.90	IV	4009.72	III	4177.60	II A	4367.58	IV
3906.48	I	4014.54	III	4181.76	III	4367.91	III A
3907.47	III	4017.15	III	4182.39	IV	4369.78	III
3907.94	IV	4021.87	III	4184.89	III	4375.93	I
3909.67	V	4024.75	V	4187.05	III	4383.55	II
3909.83	III	4030.51	IV	4187.81	III	4387.90	IV
3910.85	IV	4032.64	III	4191.45	III	4388.42	IV
3913.64	III	4043.90	IV	4195.34	IV	4389.25	II A
3916.74	IV	4044.62	IV	4196.22	IV	4390.96	IV
3917.19	II	4045.82	II	4198.31	III	4404.75	II
3918.42	IV	4058.23	IV	4199.10	III	4415.13	II
3918.65	IV	4058.77	IV	4199.97	I A	4422.57	III
3920.26	I	4062.45	III	4202.03	I	4427.31	I
3922.92	I	4063.60	II	4203.99	III	4430.20	IV
3925.65	IV	4066.98	III	4206.70	I A	4430.62	III
3925.95	IV	4067.28	III	4207.13	IV	4433.22	IV
3927.93	I	4067.99	III	4208.61	V	4435.15	II A
3930.30	I	4070.78	III	4210.36	III	4439.89	IV
3932.64	IV	4071.75	II	4213.65	IV	4442.35	III
3933.61	IV	4074.79	IV	4215.42	IV	4442.84	IV
3935.82	III	4076.64	IV	4216.19	I	4443.20	III
3937.33	IV	4078.36	IV	4217.56	IV	4445.43	I A
3940.89	II	4079.25	IV	4219.36	IV	4447.14	IV
3942.45	IV	4079.85	IV	4220.34	IV	4447.73	III
3943.35	IV	4080.23	IV	4222.23	III	4454.39	III
3944.90	IV	4083.78	IV	4224.17	IV	4459.13	III
3945.12	IV	4084.51	IV	4224.51	IV	4461.66	I
3947.00	IV	4085.01	IV	4225.46	IV	4462.01	IV
3947.54	IV	4085.31	IV	4225.96	IV	4464.77	IV
3948.11	IV	4095.98	IV	4226.43	IV	4466.56	II
3948.78	IV	4098.19	IV	4227.45	III	4469.39	IV
3949.96	III	4100.75	II A	4229.75	III	4476.02	III
3951.17	IV	4104.14	V	4232.72	I A	4479.61	IV
3952.61	IV	4107.50	III	4233.61	III	4480.14	IV
3953.16	IV	4109.81	IV ?	4235.95	III	4482.18	I
3955.37	IV	4114.45	IV	4237.16	III A	4482.26	
3956.46	IV	4118.56	IV	4238.04	IV	4484.24	IV
3956.68	III	4120.21	IV	4238.83	IV	4485.67	IV
3957.04	IV	4121.81	IV	4239.85	III	4488.92	IV
3963.12	V	4122.52	IV	4245.26	III	4489.74	I A
3964.52	V	4126.19	IV	4247.44	III	4490.09	IV
3966.07	III	4127.62	IV	4248.22	IV	4494.57	III
3966.63	IV	4132.06	II	4250.13	III	4525.15	IV
3967.43	IV	4132.91	III	4250.79	II	4528.62	II
3967.97	IV	4134.68	IV	4258.39	I A	4531.16	II
3969.26	II	4137.00	IV	4260.49	III		
3970.39	IV	4139.94	II A	4266.97	IV		

PLATE X

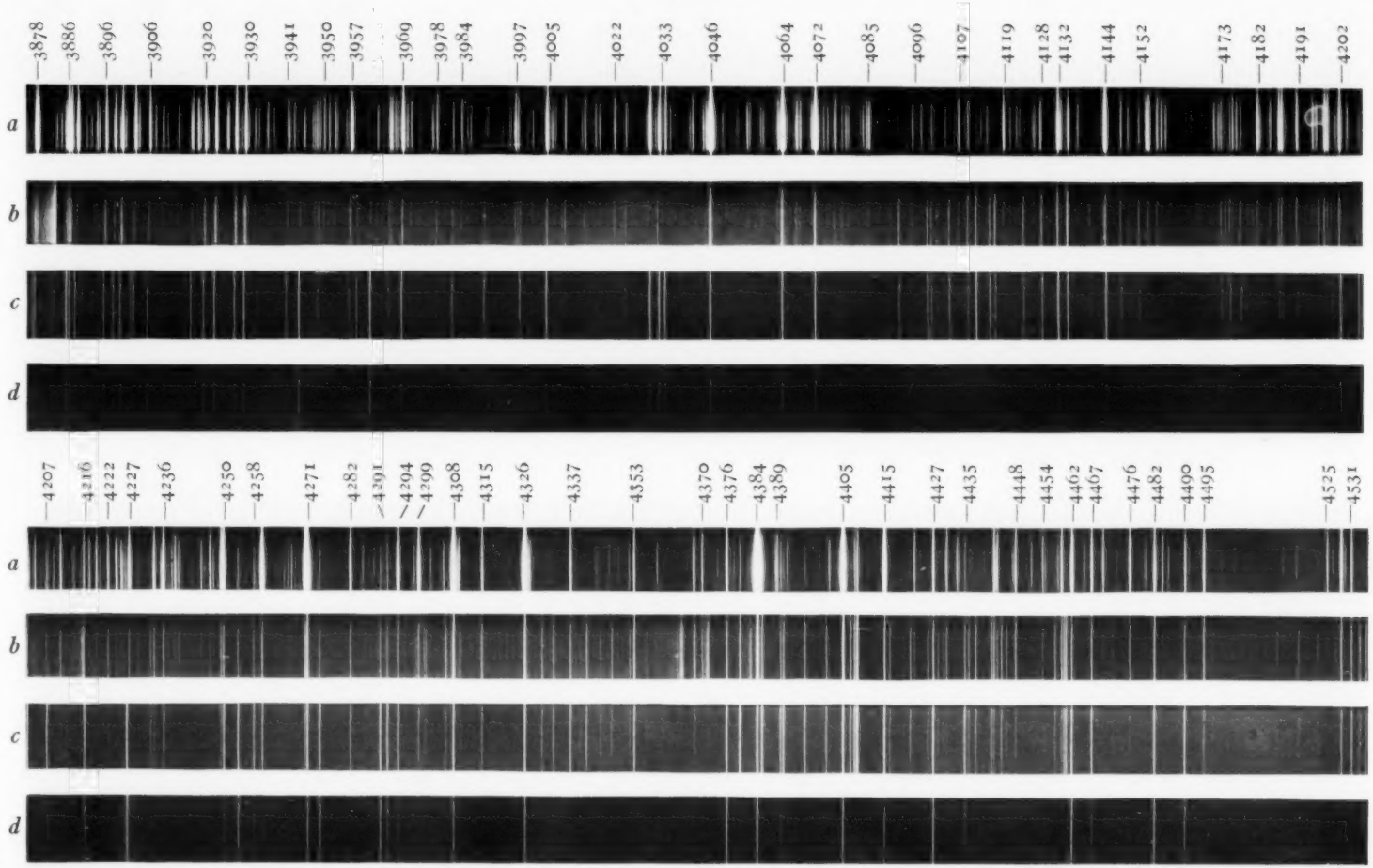

ARC AND FURNACE SPECTRA OF IRON IN VIOLET AND BLUE

a Arc spectrum; *b*, *c*, *d* Furnace spectra at 2600°, 2000°, 1650° C., respectively

classification of this kind, but most of the alterations result from the new low-temperature stage. A line may retain at 1800°–1900° an intensity sufficient to place it in class I if this were the low temperature selected; but a temperature drop of 200° may weaken it so that it clearly belongs in class II, possibly verging on class III. Naturally some lines still strong at 1600° may weaken rapidly below this, and the most pronounced low-temperature lines reduce to the small number in Table V (see p. 337) emitted at 1400°. The 1600°–1700° stage emits, however, a set of lines retaining fair intensity under as weak excitation as is ordinarily usable for the iron spectrum in the laboratory, and the high-temperature lines have had an opportunity to drop out in the range below 2000°.

As the gradation of intensities for the lines included in Table IV is shown in the 1913 paper, it was considered sufficient in this revision to print the classes only. Beyond λ 4600 into the red, the later photographs confirm the earlier so closely as to classes that it seems unnecessary to go over the ground.

Table IV is supplemented by a reproduction of this region in Plate X. Three furnace spectra for temperatures of 2600°, 2000°, and 1650°, respectively, are given with a strong arc spectrum, the latter just sufficing to show some of the more pronounced lines of the sort which are relatively stronger in the furnace than in the arc. The strong lines emitted in the furnace and not in the iron arc are due chiefly to titanium and vanadium. λ 4227 of calcium is strong in the medium- and low-temperature spectra.

ARC AND FURNACE SPECTRA OF IRON IN VIOLET AND BLUE

a Arc spectrum; *b*, *c*, *d* Furnace spectra at 2600°, 2000°, 1650° C., respectively

DISCUSSION OF RESULTS

a) Distinctive features of classes I, II, and III.—The difference between classes I and II is not as decided in the ultra-violet as in the visible region and for many purposes the two classes may perhaps be considered together as the low-temperature group. In segregating the lines in this paper, the absorption spectrum at low temperature has been of much service. It was considered that lines appearing in absorption at a temperature as low as 1600° were at least in class II, and those which maintained their intensity to the greatest extent were placed in class I. In the portion covered by the low-temperature emission spectrum, as far as λ 3440, the

appearance of the lines both in emission and absorption was considered. The experiments of Hemsalech[1] with the flame spectrum of iron showed that, of the stronger lines, a portion are emitted with relatively high intensity in the outer mantle of the flame, while others require the stronger excitation found on the boundary of the cone. The lines of these two classes correspond closely, in the region common to both investigations, with classes I and II, respectively, of the furnace lines. The susceptibility to reversal in either the high-temperature furnace or the arc often distinguishes between these two classes. Of the two emission lines having approximately the same width, one may show a wider reversal. In a low-temperature absorption spectrum it will be distinctly the stronger line. This indication that the line maintains its strength in the lower-temperature absorbing vapor distinguishes the class I line. The contrast between λ 3734.87 and λ 3737.14 illustrates this point. The first, having in the arc much greater brightness in proportion to its width, is given the higher intensity. In the low-temperature furnace, the second is much the stronger. In the visible region, the quartet of class I lines λλ 3920–3930 contrasts in the same way with the class II triplets having stronger lines at λ 4045 and λ 4384.

Class III lines, by reason of their absence from low-temperature vapors, do not show reversal in the furnace emission spectrum, and in the absorption spectrum, when the furnace is hot enough to absorb these wave-lengths, their weakness in comparison with lines of classes I and II is very pronounced. The rapid development of class III lines is the chief cause of the very different appearance of the low- and high-temperature spectra; while in the arc, the fact that the class III lines are often among the strongest in the spectrum and classes IV and V have become prominent makes the arc spectrum of iron very different from that of the furnace.

b) *Lines appearing at 1400° C.*—It may be of interest to record a list of the most persistent low-temperature lines of iron. By means of long exposure with a 1-meter concave grating spectrograph, the emission lines listed in Table V were obtained. The furnace temperature was held close to 1400° C. The film was of the Eastman portrait variety, showing little sensitiveness beyond the

[1] *Philosophical Magazine*, **33**, 1, 1917.

blue. The twenty-one lines which appear are all pronounced members of class I, except that a bare trace is visible of λ 4384, the strongest of the class II lines. The absence of the triplets to which λ 4384 and λ 4046 belong is one of the striking features of this very low-temperature emission. λ 4376 is under these conditions the strongest line of the spectrum.

TABLE V

PERSISTENT LOW-TEMPERATURE LINES OF IRON

λ	Intensity	λ	Intensity
3745.56	1	3920.26	8
3820.43	1	3922.92	8
3824.44	2	3927.94	8
3825.89	1	3930.30	8
3856.37	4	4216.18	2
3859.91	4	4375.93	10
3878.58	5	4383.55	tr
3886.29	6	4427.31	8
3895.65	5	4461.65	4
3899.70	5	4482.18	2
3906.47	2		

c) Lines relatively weaker in arc than in furnace.—In all of the furnace spectra thus far studied, attention has been drawn to this type. Such a line may be extremely weak in the arc and still strong in the furnace. The type may be found in any temperature class and its occurrence points to a difference, as yet obscure, between the arc and furnace excitations. These lines, designated by "A" after the class number, may reverse at high temperature, in which case they remain strong at low temperature and belong in class I A. Those which do not reverse are of two types. The type prevailing in the ultra-violet usually comes under class III A, becoming very faint at low temperature. The other type consists of I A lines, which are narrow at all temperatures, but remain strong at low temperature. These appear to be confined to the visible region, where λλ 4200, 4258, 4291, 5225, 5247, 5250.2, 5255 may be noted as conspicuous examples.

d) Relation to arc types.—It has been noted that lines appearing in the furnace spectrum are likely, in the arc spectrum, to show strongest in the region of the arc away from the poles. It was

possible to photograph the spectral region below λ 2800, covered in Table I, so as to show this change from center to pole, as the astigmatism of the concave grating is small for this part of the spectrum. Plate XI reproduces a section of this region, a high-temperature furnace absorption spectrum being placed between two arc spectra, the upper being the integrated spectrum of the central and polar vapors, and the lower taken with the axis of the arc along the slit. In the upper strip it may be seen that some lines relatively faint in the arc, such as λ 2750 and λ 2756 are distinct in the furnace, being radiated chiefly by the vapors away from the pole, while the adjacent strong lines λ 2749 and λ 2755, with major emission at the poles, are absent in the furnace. Strong furnace lines are wide and frequently reversed in the hood of vapor above the center of a vertical arc, and fade rapidly toward the lower pole, where polar conditions are more concentrated. Lines of the intermediate type, designated in Table I as "C–P," of about the same strength from center to pole, are usually present in the furnace, but relatively weaker than lines which are more closely confined to the center.

d) Probable relation to ionization phenomena.—The trend of recent investigations has been to show a parallelism between the excitation stages given by different temperatures and those produced by various voltages in studies of ionization potentials. As no work has been done with iron vapor as to the effect of different voltages, nothing definite can be said for this spectrum, but for metals which have been studied in both ways, there has as yet been no contradiction of the view that the two modes of excitation result, at corresponding points, in the same radiative processes. In other words, temperatures can be selected to bring out successive groups of lines in the same way that various voltages may be used, as in the recent work of Foote, Meggers, and Mohler.[1] On account of the high vaporization point of substances such as iron, the classification of many spectra can be carried out best by the furnace method, but the close connection of the critical voltages with the quantum theory, in the results obtained by the voltage method, makes desirable a study of the correspondence for those elements

[1] *Philosophical Magazine*, **42**, 1002, 1921; *Astrophysical Journal*, **55**, 145, 1922.

PLATE XI

PLATE XI

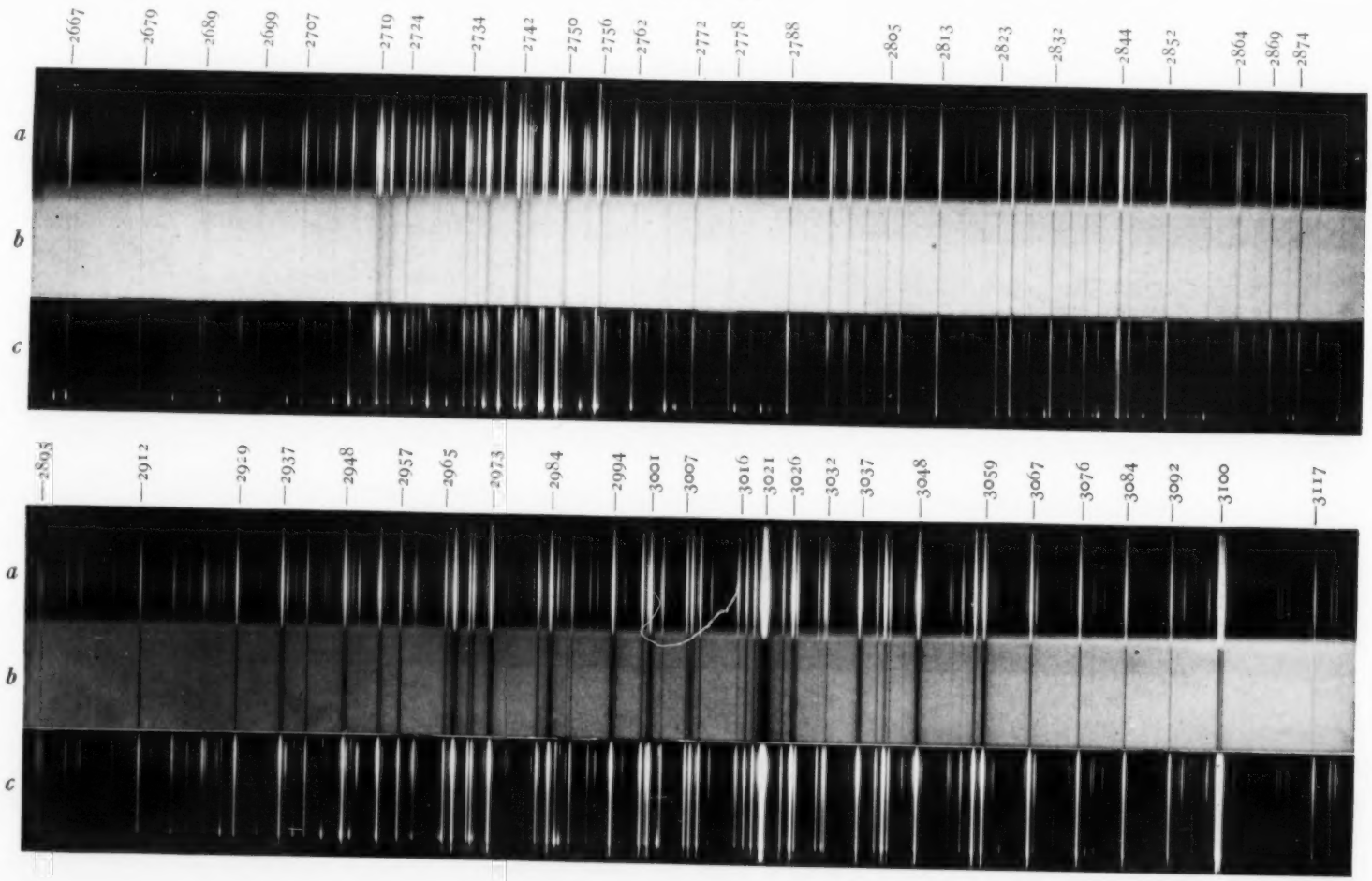

ARC AND FURNACE SPECTRA OF IRON

a Arc spectrum of combined central and polar vapors; *b* Absorption spectrum of high-temperature furnace; *c* Arc spectrum showing radiation by central vapor, and (below) in region close to positive pole

which may have their spectra excited in either way. The short extension into the ultra-violet of the furnace spectrum has prevented the observation of many important low-temperature lines as long as emission spectra only were employed. The methods here described for the production of the low-temperature absorption spectrum of iron can be applied with other elements to the grouping of their lines at various temperatures through the range from perhaps λ 2300 into the infra-red.

MOUNT WILSON OBSERVATORY
August 1922

CHANGES IN THE SPECTROGRAPHIC ELEMENTS OF Y SAGITTARII[1]

By JOHN C. DUNCAN

ABSTRACT

Changes in the spectrographic elements of Y Sagittarii.—A velocity curve of this Cepheid variable, derived from 17 single-prism spectrograms made at Mount Wilson and three triple-prism spectrograms made at Mount Hamilton in 1921, is compared with the curve derived from 26 single-prism spectrograms made at Mount Hamilton in 1908 (Fig. 1). Elliptic elements for both years are given. The velocity of the system is found to have changed from +3.6 to −5.9 km/sec., while the eccentricity in 1921 appears to be double its value in 1908. Other elements also seem to have changed, but less markedly.

Y Sagittarii is a well-known variable star of the δ Cephei class. The variability of its brightness was discovered by Sawyer in 1886, and that of its radial velocity by Curtiss in 1904. A preliminary velocity curve and elliptic elements, derived from observations made with the single-prism spectrograph of the Lick Observatory in 1908, were published by me in 1909.[2] Last winter my attention was called by Mr. Joy to the fact that observations made at Mount Wilson in 1918 gave a velocity some twenty kilometers below that shown by my curve of 1908, and I then undertook a new determination of the curve.

The star was placed by Mr. Adams on the observing list of the 60-inch and 100-inch reflectors, and in the spring and summer of 1921 seventeen one-prism spectrograms were secured. An approximate curve derived from these observations showed unmistakably a velocity of the system several kilometers less than that of 1908. This difference seemed too great to be due to the use of different spectrographs and methods of measurement, but that question was nevertheless referred to Director Campbell, who very kindly had three plates made with the three-prism spectrograph and measured at the Lick Observatory, the dates of the plates corresponding to salient points of the curve. These plates agree very well with

[1] *Contributions from the Mount Wilson Observatory*, No. 248. Read at the Swarthmore meeting of the American Astronomical Society, December, 1921.

[2] *Lick Observatory Bulletin*, 5, 82, 1909.

the Mount Wilson plates, and in the final determination of the elements were given additional weight on account of their high dispersion. Data concerning the 1921 plates, and also three plates made at Mount Wilson in 1918 and one in 1919, are given in Table I. Plates with numbers preceded by γ were made with the 60-inch telescope; by C, with the 100-inch. The phase (days since maximum brightness) is computed from the elements of Hellerich.[1]

TABLE I

Plate	Date, G.M.T.	J.D. 2420000+	Phase	Vel.	O.−C.	Wt.
γ 7145	1918 July $19^d 19^h 22^m$	1794.807	3.912	0.0	−12.1	.....
γ 7157	July 21 17 27	1796.727	0.059	−23.0	+ 0.1	.....
γ 7206	Aug. 17 16 20	1823.681	3.919	+ 2.2	−10.0	.....
γ 8710	1919 Sept. 13 15 00	2215.625	3.281	− 3.3	− 7.3	.....
γ 10002	1921 Mar. 17 01 10	2766.048	5.244	− 9.8	− 1.6	1
γ 10011	Mar. 18 01 05	2767.045	0.468	−28.4	− 5.9	1
C 952	Mar. 20 00 42	2769.029	2.452	− 0.9	+ 4.3	1
γ 10088	Apr. 17 00 19	2797.013	1.569	−10.0	+ 3.8	1
γ 10127	Apr. 25 23 26	2805.976	4.759	+18.7	+ 3.4	1
γ 10136	Apr. 27 23 53	2807.995	1.005	−19.9	− 1.2	1
γ 10165	May 25 19 57	2835.831	5.748	−14.4	+ 8.1	1
γ 10166	May 25 20 45	2835.865	5.782	−15.5	+ 7.3	1
γ 10178	May 26 22 28	2836.936	1.079	−25.9	− 7.8	1
γ 10204	June 15 22 07	2856.922	3.745	+ 9.3	− 0.6	1
γ 10207	June 16 21 11	2857.883	4.706	+19.8	+ 3.4	1
γ 10216	June 19 21 30	2860.896	1.946	−10.0	+ 0.2	1
γ 10221	June 20 19 45	2861.823	2.873	− 3.9	− 3.2	1
γ 10233	June 22 21 09	2863.881	4.931	0.0	− 9.1	1
C 1174	July 24 19 42	2895.821	2.232	−10.4	− 2.9	1
Lick	July 26 18 43	2897.780	4.191	+15.0	− 0.7	3
C 1185	July 26 18 54	2897.787	4.198	+11.0	− 4.8	1
γ 10337	July 26 19 07	2897.797	4.208	+12.8	− 3.1	1
Lick	Aug. 14 17 13	2916.717	0.035	−21.5	+ 1.4	3
Lick	Aug. 16 17 06	2918.712	2.030	− 8.6	+ 0.8	2

The velocity is in each case the mean result of measures by two or more observers. The residuals O.−C. are taken from the 1921 velocity curve shown in Figure 1.

Although the binary hypothesis of Cepheid variation is not universally accepted, the usual elliptic elements seem still to be the best means for numerically representing the observed variations in radial velocity; and I accordingly give these elements, leaving their interpretation on the pulsation and other hypotheses to the

[1] Inaugural Dissertation, Berlin, 1913.

reader. Corrections to the preliminary elements of 1908 (except the period) were computed by least squares. These corrections were in every case smaller than their probable errors. The period found from photometric observations by Hellerich was adopted. A

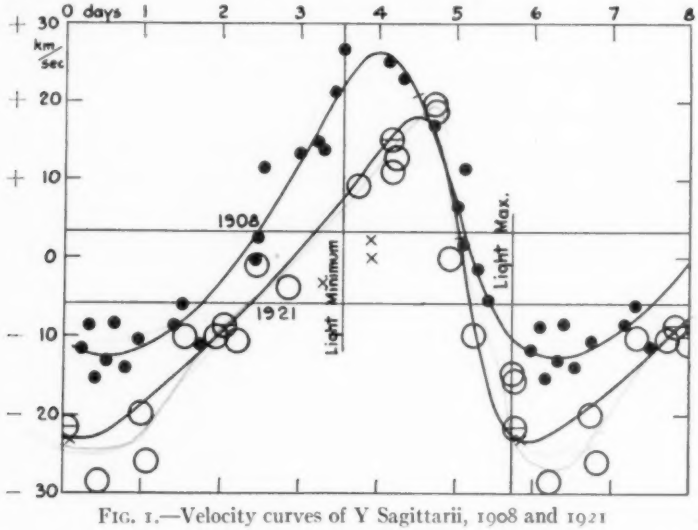

FIG. 1.—Velocity curves of Y Sagittarii, 1908 and 1921

least-squares solution was made for the elements of 1921, using the seventeen plates made at Mount Wilson and the three made at Mount Hamilton. The results are shown in Table II.

TABLE II

	1908	1921	Difference
P		5.773268 days (Hellerich)	
K	19.3± 0.8 km/sec.	20.6±0.8 km/sec.	+ 1.3± 1.2 km/sec.
γ	+3.6± 1.2 km/sec.	−5.9±1.5 km/sec.	− 9.6± 1.9 km/sec.
ω	43°.0±13°.8	74°.5±6°.2	+31°.5±15°.1
e	0.21± 0.04	0.42±0.04	+0.21± 0.06
T	4.51± 0.21	5.05±0.08	+0.54± 0.22
$a \sin i$	1 500 000 km	1 354 000 km	−146 000 km
$\frac{m_1^3 \sin^3 i}{(m+m_1)^2}$	0.004⊙	0.003⊙	
ϵ	±2.4 km/sec.	±3.1 km/sec.	

The time T of periastron passage is counted in days from the time of light-maximum. The interval from light-maximum to

velocity minimum was 0.64 days in 1908 and 0.19 days in 1921; the interval from light minimum to velocity maximum was 0.27 and 0.72, respectively—the former interval having diminished and the latter increased, each by 0.45 days. The observations, and the velocity curves representing the above elements, are plotted in Figure 1. The Lick observations of 1908 are indicated by filled circles; those of 1921 by barred rings; the Mount Wilson observations of 1921 by plain rings; and those of 1918 and 1919 by crosses.

The most important changes found are those in the velocity of the system and in the eccentricity, which are so large as to leave little doubt of their reality. From the large negative residuals of the observations made near light minimum in 1918 and 1919, one might infer that the curve has differed more from its position of 1908 at some intermediate epoch than in 1921. It seems evident that the star will repay further observation.

WHITIN OBSERVATORY
WELLESLEY, MASSACHUSETTS
February 1922

PREPARATION OF ABSTRACTS

Every article in the *Astrophysical Journal*, however short, is to be preceded by an abstract which should be submitted by the author with the manuscript. In order that the abstract may aid the reader by furnishing an index and brief summary of the contents of the article, and may also be suitable for reprinting in an abstract journal, it should be of the type of those which have been appearing in the *Astrophysical Journal* since 1920. It is requested that the abstracts be prepared in accordance with the following:

DIRECTIONS AND RULES

1. *Notes.*—Read the article carefully, taking rough notes covering all the new information reported, keeping a specially sharp lookout for new incidental results and suggestions not directly related to the main subject.

2. *Subtitles.*—Write, first, a title describing the group of results forming the main contribution of the article, including all that belong together. If there are in addition results which do not come under that title, gather them into as few groups as possible and formulate a complete and precise title for each. For examples of such subtitles see the italicized parts of the abstracts for 1920.

The subtitles should together form a complete index of the new information; that is, they should include every measurement, observation, method, suggestion, and theory which is presented as new and of value in itself. They should be complete in themselves and independent of the main title of the article.

3. *Text.*—Write a paragraph summarizing the main group of results and including the corresponding subtitle either all at the beginning or with parts scattered through the text; and then do likewise for the other groups.

The text should summarize the author's conclusions and should transcribe all numerical results of general interest, including all that might be looked for in a table of astronomical and physical constants, with an indication of the accuracy of each. It should give all the information that anyone, not a specialist in the particular field involved, might care to have in his notebook.

Complete sentences should be used except in the case of subtitles. The abstract should be made as readable as the necessary brevity will permit. Italicize subtitles but no other words or phrases.

4. *Final checking.*—Re-read the article so as to check the abstract and correct any omissions and mistakes; read the subtitles by themselves to see that they properly index the information; and read the abstract to see whether it cannot be condensed and its English be improved.

These rules, and the abstracts which have appeared up to this time, have been prepared by Dr. Gordon S. Fulcher, recently of the National Research Council, now of Corning, New York. The editors desire formally to express their obligation and that of all readers of the *Journal* to Dr. Fulcher for the patience and skill which he has shown in revising, according to the technical standards, the abstracts sent in by authors, and in many cases in writing entirely new abstracts where the authors had neglected our request for abstracts. It will in future be absolutely impossible for Dr. Fulcher to continue this labor of love. Meantime, authors are notified that their articles cannot be accepted unless accompanied by adequate abstracts, and if articles are sent without abstracts, otherwise acceptable for publication, they will not be forwarded to the printer for composition until the abstracts are received.